ERI/NRC 20-209

REVIEW OF ACCIDENT TOLERANT FUEL CONCEPTS WITH IMPLICATIONS TO SEVERE ACCIDENT PROGRESSION AND RADIOLOGICAL RELEASES

FINAL REPORT

Work Performed under the Auspices of the
United States Nuclear Regulatory Commission
Office of Nuclear Regulatory Research
Washington, D.C. 20555

ENERGYRESEARCHINC
P. O. Box 2034
Rockville, Maryland 20847

October 2020

Intentionally left blank

ERI/NRC 20-209

REVIEW OF ACCIDENT TOLERANT FUEL CONCEPTS WITH IMPLICATIONS TO SEVERE ACCIDENT PROGRESSION AND RADIOLOGICAL RELEASES

FINAL REPORT

October 2020

Mohsen Khatib-Rahbar, Alfred Krall, Zhe Yuan, and Michael Zavisca
Energy Research, Inc.
P.O. Box 2034
Rockville, Maryland 20847-2034

Work performed under the auspices of
United States Nuclear Regulatory Commission
Office of Nuclear Regulatory Research
Washington, D.C. 20555
Under Contract Number NRC-HQ-60-16-E-0002

Intentionally left blank

ABSTRACT

The U.S. Nuclear Regulatory Commission (NRC) is preparing for anticipated licensing applications and commercial use of accident tolerant fuel (ATF) in the United States commercial nuclear power reactors. This report documents the results of a literature survey of the various ATF concepts. The literature review covers consideration of ATF fuel and cladding designs, fuel enrichment, and fuel burnup. This review is aimed at identifying fuel/cladding behavior, degradation, and radiological release and transport phenomena that can potentially be impacted by ATF design, enrichment, and burnup, for application of severe accident models to these designs. This report is intended to serve as the basis for the development of a Phenomena Identification and Ranking Table (PIRT). It is found that the available literature is much more complete with respect to ATF design characteristics than with respect to the behavior of ATFs, fuel enrichment and burnup under severe accident conditions.

Intentionally left blank

EXECUTIVE SUMMARY

The United States (U.S.) Nuclear Regulatory Commission (NRC) is preparing for anticipated licensing applications and commercial use of accident tolerant fuel (ATF) in the U.S. commercial nuclear power reactors. Several fuel vendors, in coordination with the Department of Energy (DOE), have announced plans to develop and seek approval for various fuel designs with enhanced accident tolerance (e.g., fuels with longer coping times during loss of cooling conditions). Vendors have also expressed interest in increasing fuel burnup above the licensed limit (which varies by vendor, but roughly corresponds to 62 GWd/MTU rod-average), as well as increasing enrichment beyond 5%.

Austenitic stainless steel was used in commercial power reactors in the 1960s and 1970s until nuclear power plants started switching to fuel with Zircaloy (Zr) cladding. The decision to move away from stainless steel was based in large part on the superior mechanical performance of Zr, especially in BWRs, and particularly the neutron economy. Along with reduced Zr failure rates, changes in operations and increased performance under normal, reactivity-initiated accidents (RIA), and power-to-coolant mismatch scenarios allowed the industry to go to higher burnups and significantly increase plant capacity factors. Note that the power densities in Light Water Reactors (LWRs) can surpass 1 kW/cm^3 depending on the design.

Many ATF concepts have been considered, recently including Cr-coated claddings, Cr-doped UO_2 pellets, FeCrAl cladding, SiC cladding, UN pellets, and metallic fuels. It will be discussed later that of these concepts, the coated claddings, doped fuel pellets and steel cladding designs are considered to be nearer to commercial deployment. Silicon carbide cladding, uranium silicide fuel pellets and metallic fuels are considered for longer-term deployment. These ATF designs represent evolutions and deviations from the Zircaloy clad, uranium dioxide fuel forms.

In addition, the behavior of high burnup (HBU) and high assay low enriched fuel (HALEU) with less than 20 w/o% U-235 is also of interest to the NRC. In the present context, HALEU is to be viewed as increased fuel enrichment for use in Light Water Reactors (LWRs), and not as envisioned for non-LWRs. The LWR industry is anticipating fuel enrichments as high as 10% (but in reality it is expected that plants may request more modest enrichment increases in order to achieve the desired burnup and fuel cycle targets).

The introduction of ATF, high-burnup, and/or increased enrichment for UO_2 fuels and ATF may impact the progression of severe accidents as well as the release and transport of radionuclides, with implications on safety and regulatory requirements. Cladding-steam interactions, cladding failure, fuel microstructure, eutectic formations, release mechanisms, and other phenomena need to be assessed. In addition, fuel burnup and enrichment may also impact severe accident progression and radiological releases through changes such as decay heat load, isotopic inventories, fuel/cladding thermo-mechanical properties, and fuel microstructure.

The objective of this report is to document the results of a literature survey of the various ATF concepts, including experimental and analytic studies related to various ATF designs being considered by industry and research organizations. The literature review covers consideration of ATF fuel and cladding designs, fuel enrichment, and high burnup. This review is aimed at identifying fuel/cladding behavior, degradation, and radiological release and transport phenomena that can potentially be impacted by ATF design, fuel enrichment, and burnup, under severe accident conditions. This report is intended to serve as the basis for the development of a

Phenomena Identification and Ranking Table (PIRT). It is found that the available literature is much more complete with respect to ATF design characteristics than with respect to the behavior of ATFs, fuel enrichment and burnup under severe accident conditions.

The motivation of ATF claddings is to reduce the rate and total amount of heat generated from steam oxidation of cladding at elevated temperatures during accidents, which will in turn reduce the rate of temperature rise, reduce hydrogen generation, delay core degradation, and hence provide additional coping time for accident mitigation. Silicon carbide cladding has excellent resistance to steam oxidation; however, this technology is less well developed due to fabrication challenges and other issues, and it is considered as a candidate for longer-term deployment.

The near-term ATF designs with respect to the time of commercial deployment include:

- The use of Cr_2O_3 and Al_2O_3 dopants in uranium dioxide fuels,
- Conventional zirconium alloy cladding coated with chromium, and
- Advanced stainless steel (FeCrAl) cladding.

On the other hand, the longer-term ATF concepts being considered include:

- Silicon carbide cladding,
- High-density silicide fuels,
- High-density nitride fuels, and
- Metallic fuels (specifically, uranium-zirconium alloys with zirconium content near 50 weight percent).

Note, even though where available and for completeness, the review also includes some information on other advanced fuel concepts that are under development (e.g., Tristructural-isotropic [TRISO]); however, these fuels are not within the scope of the present activities.

Much of the motivation of new fuels considered for ATF designs is to compensate for poorer neutronic performance of ATF claddings. This is particularly true of FeCrAl claddings, where the option provided by this strong material to use thinner cladding only partly compensates for its higher neutron absorption. High-density fuels (e.g., U_3Si_2, UN, metallic fuels) are one way to compensate, as is higher enrichment. Some new fuels are not merely compensatory but have direct accident-tolerant benefits. For example, fuel dopants added to UO_2 fuel may improve fission product gas retention and to provide enhanced resistance to stress corrosion cracking due to the pellet-clad interaction; fuels of high thermal conductivity reduce the heat stored in the fuel; microencapsulated fuels improve the fuel/cladding interaction and/or improve fission product retention.

ATF claddings and fuels, including many more than those few mentioned in this summary, are described fairly completely in the literature, which is reviewed in the present report. Much less well covered by the literature is how the character of the fission product inventories and releases may change relative to that of conventional fuel, due to the changes entailed by ATF designs. This remark applies also to HBU and HALEU fuels. Hence the corresponding sections of this document are less complete than those that discuss the newly proposed cladding and fuel designs.

The review of the ATF-related severe accident simulation studies is limited to a summary of results of several representative analyses that are discussed throughout Sections 2.1 and 2.2. Within considerable variation, they tend to confirm a widely held impression that ATF designs typically afford a modest increase in coping time and a reduction of hydrogen generation, at least until very late times. The reviewed literature is focused on the early in-vessel phase of severe accidents and contains very limited insights into the late-phase behavior as well as radionuclide release and transport aspects of ATF designs during severe accidents.

On the basis of the literature review summarized in this report, as well as a review of the severe accident simulation models, a list has been prepared of candidate phenomena for consideration by the PIRT panel that will address severe accident modeling needs for ATF, high burnup and higher enrichment UO_2 fuel designs. The proposed list will be reviewed, revised, and ranked as part of the PIRT panel deliberations, the results of which will be documented in a separate report.

Intentionally left blank

TABLE OF CONTENTS

LIST OF TABLES

Intentionally left blank

LIST OF FIGURES

Intentionally left blank

LIST OF ACRONYMS

ADOPT	Advanced DOped Pellet Technology
ADU	Ammonium Diuranate
ANO-1	Arkansas Nuclear One Reactor
AOO	Anticipated Operational Occurrence
APMT	One of the FeCrAl alloys
AREVA NP	Corporation name (not an acronym)
ATF	Accident Tolerant Fuel
ATR	Advanced Test Reactor at Idaho National Laboratory
B136Y	One of the FeCrAl alloys
BDBA	Beyond Design Basis Accident (i.e., Severe Accident)
BISON	Computer code
BWR	Boiling Water Reactor
CASL	Consortium for Advanced Simulation of Light Water Reactors
CEA	French Alternative Energies and Atomic Energy Commission
CERMET	Ceramic / Metal
CHF	Critical Heat Flux
CORSOR	Computer code
Cr	Chromium
CVD	Chemical Vapor Deposition
CVI	Chemical Vapor Infiltrated
DBA	Design Basis Accident
DOE	Department of Energy
dpa	displacements per atom
ECCS	Emergency Core Cooling System
EFPD	Effective Full Power Day
EPR	European Pressurized Reactor
EPRI	Electric Power Research Institute
FAST	A fuel performance computer code
FCM	Fully Ceramic Microencapsulated
FeCrAl	Iron-Chromium-Aluminum Alloy (also, Advanced Stainless Steel)
FFRD	Fuel Fragmentation, Relocation, and Dispersal
FG	Fission Gas
FGR	Fission Gas Release
FLEX	Diverse and Flexible Coping Strategies
FP	Fission Product

FRAPCON	Fuel Performance Analysis computer code
FSCB	Fuel and Source Term Code Development Branch
GNF	Global Nuclear Fuel (company name)
GWd/MTU	Gigawatt-day per metric tonne of heavy metal (burn-up unit)
GRS	Gesellschaft für Anlagen- und Reaktorsicherheit
HALEU	High Assay Low Enriched Uranium fuel
HBS	High Burnup Structure
HBU	High Burnup
HTGR	High Temperature Gas Reactor
LBLOCA	Large-Break LOCA
LEU	Low Enriched Uranium fuel
LHGR	Linear Heat Generation Rate
LOCA	Loss of Cooling Accident
LUA	Lead Use Assembly
LWR	Light Water Reactor
M5	One of the proprietary formulations of Zircaloy
MAAP	Modular Accident Analysis Program computer code
MAX	Layered carbide/nitride phase material
MELCOR	Computer code name (not an acronym)
MCCI	Molten Core Concrete Interaction
MIT	Massachusetts Institute of Technology
MOX	Mixed Oxide
MPa	Mega-Pascal
MTR	Materials Test Reactor
MWd/kgU	Megawatt-day per kilogram of heavy metal [uranium] (burn-up unit)
NEA	OECD Nuclear Energy Agency
NITE	Nano-Infiltration and Transient Eutectic
NRC	U.S. Nuclear Regulatory Commission
NU	Natural Uranium
ODS	Oxide-Dispersion Strengthened
OPR-1000	South Korean 1000 MWe PWR
ORNL	Oak Ridge National Laboratory
Pa	Pascal
PCI	Pellet-Clad Interaction
PCMI	Pellet-Clad Mechanical Interaction
PCT	Peak Cladding Temperature
PDF	Portable Document Format

PIRT	Phenomena Identification and Ranking Table
ppm	parts per million
PRA	Probabilistic Risk Analysis
PVD	Physical Vapor Deposition
PWR	Pressurized Water Reactor
PyC	Pyrolytic Carbon
QUENCH	Tests facility at the Karlsruhe Institute of Technology
RCIC	Reactor Core Isolation Cooling
RCS	Reactor Cooling System
RELAP5-3D	Computer code
RG	Regulatory Guidance
RIA	Reactivity-Initiated Accident
SA	Severe Accident
SBLOCA	Small-Break LOCA
SBO	Station Blackout
SCC	Stress Corrosion Cracking
SiC	Silicon Carbide
SiC/SiC	Fiber-reinforced composite formulation of silicon carbide
SNL	Sandia National Laboratories
SWU	Separative Work Unit
TMI	Three Mile Island
TRACE	Computer code
TRISO	Tristructural-isotropic
TS	Technical Specifications
UC	Uranium Carbide
UN	Uranium Nitride
UO2	Uranium Dioxide
VERCORS	Radionuclide release test facility in France
VVER	Water-Water Energetic Reactor
WIMS	Winfrith Improved Multigroup Scheme computer code
ZIRLO	One of the proprietary formulations of Zircaloy

Intentionally left blank

ACKNOWLEDGEMENTS

The authors acknowledge the technical inputs and guidance provided by Drs. Shawn Campbell, Richard Lee, Hossein Esmaili, and others of the United States Nuclear Regulatory Commission, Office of Nuclear Regulatory Research throughout the course of this work.

In addition, the authors thank the valuable peer review comments on the draft version of this report, including access to additional literature publications, by Professor S. Bechta (Royal Institute of Technology, Sweden), Mr. C. Beyer (Consultant), Dr. J. Corson (NRC), Dr. E. Dickson (NRC), Dr. E. Fuller (Consultant), and Dr. T. Hollands (Gesellschaft für Anlagen-und Reaktorsicherheit, Germany). The authors also acknowledge additional comments provided by Drs. D. Powers (University of Wisconsin, Madison) and R. Hobbins (Consultant).

This work was performed under the auspices of the United States Nuclear Regulatory Commission, Office of Nuclear Regulatory Research, under contract number NRC-HQ-60-16-E-0002 (Technical Assistance in Severe Accident Research).

Intentionally left blank

1. BACKGROUND AND SCOPE

1.1 Background

The United States (U.S.) Nuclear Regulatory Commission (NRC) is preparing for anticipated licensing applications and commercial use of accident tolerant fuel (ATF) in the U.S. commercial nuclear power reactors. Several fuel vendors, in coordination with the Department of Energy (DOE), have announced plans to develop and seek approval for various fuel designs with enhanced accident tolerance (i.e., fuels with longer coping times during loss of cooling conditions). Vendors have also expressed interest in increasing fuel burnup above licensed limits (which varies by vendor, but roughly corresponds to 62 GWd/MTU rod-average), as well as increasing enrichment beyond 5%.

Austenitic stainless steel was used in the commercial power reactors in 1960s and 1970s until the nuclear power plants started switching to fuel with Zircaloy (Zr) cladding. The consideration to move away from stainless steel was based in large part due to superior mechanical performance of Zr, especially in BWRs, and particularly the neutron economy. Along with reduced Zr failure rates, changes in operations and increased performance under normal, reactivity-initiated accidents (RIA), and power-to-coolant mismatch scenarios allowed the industry to go to higher burnups and significantly increase plant capacity factors. Note that the power densities in Light Water Reactors (LWRs) can surpass 1 kW/cm^3 depending on the design.

The idea of ATF has seen many concepts, recently including Cr-coated claddings, Cr-doped UO_2 pellets, FeCrAl cladding, SiC cladding, UN pellets, and metallic fuels. Of these concepts, the coated claddings, doped fuel pellets and steel cladding designs are considered to be nearer with respect to the time to commercial deployment. Silicon carbide cladding, uranium silicide fuel pellets and metallic fuels are considered for longer-term deployment. These ATF designs represent evolutions and deviations from the Zircaloy clad, uranium dioxide fuel forms.

In addition, the behavior of high burnup (HBU) and high assay low enriched fuel (HALEU) with less than 20 w/o% U-235 is also of interest to the NRC. In the present context, HALEU is to be viewed as increased fuel enrichment for use in Light Water Reactors (LWRs), and not as envisioned for non-LWRs. The LWR industry is anticipating fuel enrichments as high as 10% (but in reality it is expected that plants may request more modest enrichment increases in order to achieve the desired burnup and fuel cycle targets).

The introduction of ATF, high-burnup, and/or increased enrichment for UO_2 fuels and ATF may impact the progression of severe accidents, release, and transport of radionuclides, with implications on safety and regulatory requirements. Phenomena such as cladding-steam interactions, cladding failure, fuel microstructure, eutectic formations, release mechanisms, among others need to be assessed. In addition, fuel burnup and enrichment may also impact severe accident progression and radiological releases through changes such as decay heat load, isotopic inventories, fuel/cladding thermo-mechanical properties, and fuel microstructure.

Many nuclear power plants within the U.S. have adopted the alternative source term guidance which is delineated in Regulatory Guidance (RG) 1.183. As a result, NRC approved changes to several technical specifications, including the deletion and relaxation of some requirements (e.g., deletion of operability and surveillance requirements of the auxiliary building filtration system from Technical Specifications [TS], relaxation of ventilation filter testing program acceptance criteria,

relaxation of technical specifications operability requirements for certain primary and secondary containment integrity during the movement of irradiated fuels and core alterations, etc.). However, the alternative source term is based on a Zr/UO_2 (cladding/fuel) combination and the fission product inventories are based on existing licensed burnup and enrichment limits. If a licensee were to change the cladding/fuel combination, increase the burnup, or increase the enrichment, it would require a reevaluation to determine if changes to technical specifications remain valid.

Outside of source term, through which severe accidents pose the majority of the public risk associated with the use of nuclear fuel, the relevance of severe accident phenomena (i.e., that phenomena which are only encountered when a postulated accident proceeds beyond those conditions that are designed against within a plant's safety analysis) to NRC's regulatory activities is several-fold. First, understanding of severe accident behavior is relevant to the understanding of uncertainties in design basis accident (DBA) and source term behavior (e.g., awareness of "cliff-edge" effects). Second, the severe accident behavior is central to the NRC's consideration of new requirements (e.g., the assessment of whether a new requirement meets the cost-justified safety enhancement aspects of the Backfit Rule, the assessment of a Petition for Rulemaking, etc.). Third, understanding of severe accident behavior is relevant to the NRC's incident response capabilities, in the event of a radiological emergency at a nuclear power plant. Fourth, severe accident behavior is fundamental to the modeling of postulated accidents in probabilistic risk analysis (PRA) studies, particularly with regard to establishing the surrogate criteria used to identify core damage and large early release.

1.2 Scope and Objectives

The objective of this report is to document the results of a literature survey of the various ATF concepts, including experimental and analytic studies related to various ATF designs being considered world-wide. The literature review covers consideration of ATF fuel and cladding designs, fuel enrichment, and high burnup [1-219][1]. This review is aimed at identifying fuel/cladding behavior, degradation, and radiological release and transport phenomena that can potentially be impacted by ATF design, fuel enrichment, and burnup, under severe accident conditions.

This report is intended to serve as the basis for the development of a Phenomena Identification and Ranking Table (PIRT) and elicitation of expert opinion, in order to enhance the knowledge-base of specific accident tolerant fuel concepts, impact of HBU and fuel enrichment, and the NRC's efforts to develop and review the required regulatory infrastructure to support accident tolerant fuels. In particular, NRC is seeking insights into the impact of ATF, HBU and fuel increased enrichment on severe accident behavior and resulting radiological releases.

The present review covers both near-term and longer-term ATF concepts. Specifically, the near-term ATF designs with respect to the time of commercial deployment include:

- The use of Cr_2O_3 and Al_2O_3 dopants in uranium dioxide fuels,

[1] A short bibliography [220 - 230] has been acquired that pertains to ATF development for VVER plants. The emphasis of this report is on conventional PWRs and BWRs, hence, the VVER-related literature is not discussed any further.

- Conventional zirconium alloy cladding coated with chromium, and
- Advanced stainless steel (FeCrAl) cladding.

On the other hand, the longer-term ATF concepts being considered include:

- Silicon carbide cladding,
- High-density silicide fuels,
- High-density nitride fuels, and
- Metallic fuels (specifically, uranium-zirconium alloys with zirconium content near 50 weight percent).

Even though where available and for completeness, the present review also includes some information on other advanced fuel concepts that are under development (e.g., Tristructural-isotropic [TRISO]); however, these fuels are not within the scope of the present activities.

Intentionally left blank

2. REVIEW OF LITERATURE RELATED TO ATF CONCEPTS APPLICABLE TO SEVERE ACCIDENTS

This section reviews the literature related to ATF concepts, consisting of the fuel (Section 2.1), cladding (Section 2.2), and fission product release issues (Section 2.3).

Information about the status of developing ATF designs is provided throughout Sections 2.1 and 2.2, as available and as appropriate. ATF concepts involving coated cladding, doped fuel pellets and steel cladding designs are considered to be nearer with respect to the time to commercial deployment. Silicon carbide cladding, uranium silicide fuel pellets, microencapsulated fuels, fuels other than uranium oxide, or any of several other advanced concepts are considered for longer-term deployment. These ATF designs represent evolutions and deviations from the Zircaloy clad, uranium dioxide fuel forms.

2.1 Fuel Designs

Design concepts of doped fuels, high-density fuels, and microencapsulated fuels are discussed respectively in Subsections 2.1.1, 2.1.2, and 2.1.3. Each subsection begins with some introductory remarks, broadly discussing the motivation for the corresponding fuel design. Next, most of the information gathered from the literature review is delineated in Subsections 2.1.1.1 and 2.1.1.2 for each of two types of doped fuel; 2.1.2.1 through 2.1.2.4 for each of four types of high-density fuel; and 2.1.3.1 through 2.1.3.3 for each of three types of encapsulated fuel. Review of any experiments, tests, and simulations studies is documented in Subsections 2.1.1.3 for doped fuels, and Section 2.1.2.5 for high density fuels. Note that there is no such subsection for microencapsulated fuels due to lack of data. Finally, each of Subsections 2.1.1 and 2.1.2 ends with comments on the status of the fuel designs that are being developed by several vendors. Subsection 2.1.4 reviews the material properties data available for several types of fuels considered in ATF concepts.

2.1.1 Doped Fuels Design Concepts

Among reviewed references, the motivation for adding dopants to UO_2 fuels is addressed best by Reference [1], which notes that Cr_2O_3 and Al_2O_3-$Cr2O_3$ dopants are expected to improve fission product gas retention and to provide enhanced resistance to stress corrosion cracking due to the pellet-clad interaction. Reference [2] notes that dopants create interstitial vacancies; the higher concentrations of vacancies may enhance some diffusion coefficients. Though Reference [2] is largely speculative, it states that the fission product release effects of Cr doping are expected to be small. The BISON code [3] is believed capable of predicting these effects, and some of its predictions are shown in Section 2.3 devoted to fission product release issues.

The information on doped fuels most important to this study are collected under this “Design Concepts” header. Almost all the material of the rest of Section 2.1.1 is drawn from Reference [1] which has the best information on doped fuel found by our literature review (but material properties of all fuel types, including doped fuels, appears in Section 2.1.4). Reference [1] divides ATF fuel concepts into three categories: “Improved UO_2,” “High density fuel,” and “Encapsulated fuel.” For the latter two categories, a review of Reference [1] is provided in later sections devoted to those fuel concepts. The following table shows how Reference [1] further subdivides the “Improved UO_2” category into two sub-categories, which are then even further sub-divided as listed in Table 2.1.

Table 2.1 Sub-categories of the "Improved UO_2" concept of [1] (pdf p. 195)

Improved UO_2	Doped UO_2		Cr_2O_3 doped UO_2
			Al_2O_3-Cr_2O_3 doped UO_2
			Ceramic Microcell UO_2
	High-thermal conductivity UO_2	Metallic additive	Metallic Microcell UO_2
			Ceramic / Metal ("CERMET")
			Mo-modified UO_2
		Ceramic additive	BeO-modified UO_2
			SiC/diamond modified UO_2

Thus one sub-category is doping, which in the view of Reference [1] may be by Cr_2O_3, or by a mixture of Al_2O3 and Cr_2O_3, or by the ceramic microcell approach. The other broad sub-category is high thermal conductivity UO_2, which according to Reference [1] can be arrived at by either of two ceramic additives, or again by any of three metallic additives, as listed by Table 2.1. The content of Reference [1] on ceramic microcell fuel is reviewed in Section 2.1.3 which is devoted to microencapsulated ATF fuels. Also in that section is the review of the content that pertains to the method of increasing the thermal conductivity by any of the three metallic additives, which constitute closely related approaches.

As noted by Reference [1], the desirable attributes for ATF pellets mainly include minimizing pellet-cladding interactions and enhancing the retention of fission products. Adding oxide dopants to UO_2 fuels uses existing infrastructure, experience, and expertise, and is considered to be an attractive technical and economical solution. According to the amount and type of the oxide dopant, one or the other of these desired attributes can be promoted. Doping with Cr_2O_3 or Al_2O_3-Cr_2O_3 aims at the first desired attribute by increasing grain size and enhancing the visco-plastic behavior. Doping with Si-based oxide ("ceramic microcell") aims at the second desired attribute. The first of these two approaches is discussed in the next paragraph, while the review of the second (ceramic microcell) is documented in Section 2.1.3.

2.1.1.1 Cr_2O_3 and Al_2O_3-Cr_2O_3 Doped UO_2

Modification of UO2 fuel by these dopants is considered mainly for the purposes of improvement of resistance to stress corrosion cracking (SCC) due to pellet-clad interaction (PCI), and also for improved fission gas retention [1, 4]. AREVA NP chose chromia (Cr_2O_3) as the relevant dopant to obtain the desired fuel large-grain microstructure and enhanced visco-plastic behavior [4]. Based on the parametric studies, chromia content is specified at an optimum value of 0.16 wt% corresponding to the solubility limit of the dopant in UO_2 at the applicable sintering conditions [5 - 7]. For a given optimized chromia content level, large grains favorably increase Cr_2O_3-doped fuel visco-plasticity. These features provide a lower stress-resistance capability of Cr_2O_3-doped fuel as compared to reference UO_2 fuel. This fuel is characterized by a homogenous large-grain microstructure, i.e., 50-60 μm, providing beneficial features for the fuel performance: dimensional stability, improved behavior in case of water/steam ingress, superior PCI and SCC-PCI resistance, and a higher fission gas retention capability, which could lead to lower fission gas release during accidents. Also, the crystalline growth enhances the fuel matrix densification. A large database is available with a maximum rod burn-up of approximately 75 GWd/MTU [1].

Westinghouse has developed UO_2 fuel containing Al_2O_3 and Cr_2O_3 (also referred to as Advanced DOped Pellet Technology (ADOPT)). The additives facilitate densification and diffusion during sintering, which results in about 0.5% higher density within a shorter sintering time and about five times larger grains than standard UO_2 fuel. Data show that Al_2O_3 enhances the grain size enlarging effect of Cr_2O_3. The properties of the Al_2O_3-Cr_2O_3-doped pellets are very similar to pellets doped only with Cr_2O_3; Al_2O_3 can be viewed as a way to lower the total amount of dopant [1].

Table 2.2, showing data collected from the tables of Appendix B of Reference [1], compares the behaviors among Cr_2O_3- or Al_2O_3-Cr_2O_3-doped UO_2 with undoped UO_2 under normal operation, AOOs, and DBAs or severe accidents. Excepting Reference [8], cited references are those indicated by Reference [1]. Added to the table is a reference to [8], not appearing in Reference [1], which provides a contrasting view from that of Reference [1] on the effect of doping on fission product release. Further discussion of this issue is provided in Section 2.3.1.

2.1.1.2 Conductivity-Enhancing Oxidic Additives to UO_2 Fuel

A review of the Reference [1] on the CERMET, Metallic Microcell, and Mo-modified UO_2 approaches to achieving high thermal conductivity is documented in Section 2.1.3, which is devoted to microencapsulated fuel designs. The ceramic additives discussed for this purpose by Reference [1] are BeO and SiC/diamond. Adding small fractions (e.g., 10% in volume) of a high conductivity solid phase can produce a two-phase fuel, characterized by a continuous minor phase at the grain boundaries in UO_2, as seen in microcell designs.

Reference [1] notes that UO_2-BeO fuel was studied by the U.S. Department of Energy (DOE) in the early 1960s but this research was not sustained. Reference [1] appears to cite Reference [9] for more recent laboratory-scale fabrication by two techniques ("SB" = slug bisque; "GG" = green granule) of samples of 10 vol% BeO doped into UO_2. The SB technique gave average grain size of 170 μm; the GG technique, 90 μm. The thermal conductivity is increased by over 40%. Reference [1] devotes several pages of discussion to UO_2-BeO fuel, citing many papers and collecting results on economic cost/benefit, irradiation tests (i.e., swelling or cracking was not detected), steady-state and transient fuel temperatures and internal gas pressure (significantly lower than for undoped UO_2), among other observations.

The thermal conductivity of pellets with added SiC or diamond has been measured and typically exceeds that of plain uranium dioxide pellets by 50% for UO_2-10vol% SiC to 500% for UO_2-10vol% diamond. Reference [1] cites References [10 - 11]. The high fuel thermal conductivity could potentially change the transient fuel behavior significantly[2]. With values as high as arise with SiC/diamond fuel (up to 5 times that of conventional fuel), could potentially trigger unfavorable differences in accidental progression, which worsen the severe accident progression. For example, earlier onset of critical heat flux with local steam blockage (at full power) and localized fuel melting would be a possibility, or cladding heat-up and oxidation could be affected.

Table 2.2 Comparison of behaviors among Cr_2O_3- or Al_2O_3-Cr_2O_3-doped UO_2 with undoped UO_2 under normal operation, AOOs, DBAs and severe accidents [1, 12]) (See also Table 2.6)

[2] T. Hollands pointed-out how the exceptionally high fuel conductivity could negatively affect accident conditions.

Phenomenon	Normal operation and AOOs	DBAs/Severe Accidents
Thermal-Mechanical Interaction		
Densification and swelling	High-dimensional and microstructural stability up to high burn-up [13]	
Deformation	Slightly faster that of standard UO_2	
Thermal behavior (unirradiated and irradiated)	Similar to that for UO2 due to low dopant amounts [14 - 16]	
Thermal conductivity (W/m·K)	No measurable differences or equivalent	
Specific heat (kJ/kg·K)		
Melting point (°C)		
Swelling and pellet-clad interaction		
Thermal expansion		
Thermal diffusivity		
PCI and SCC-PCI behaviors	Enhanced PCI resistance by enhanced creep deformation (References [4] and [17 - 18])	
Ballooning and burst		Decrease anticipated (no data available)
Chemical Compatibility & Stability		
Secondary degradation (oxidation and washout)	Corrosion and oxidation resistance enhanced [19 - 20]	
Resistance to steam oxidation	No measurable differences or equivalent	
Fission product behavior (including fission gas pressure and fission product retention)	Undecided: Reference [4] suggests improvements due to the increased intragranular fission gas retention capability of doped fuel (for burnup up to 55 GWd/MTU; but Reference [8] suggests no significant difference. See further discussion in Section 2.3.1.	Reference [4]: decrease anticipated (no data available)
Gas available for release at the grain boundaries and mesh-like cell structure	No measurable differences or equivalent	

2.1.1.3 Experiments, Tests and Simulation Studies

Information on doped fuels in the literature that is grounded closely in experiments, tests, or simulation studies, is discussed in this subsection. Reference [1] mentions some tests and simulations pertaining to enhanced conductivity fuels. Temperature calculations were performed with the EPR rod geometry for CERMETs fuels under irradiation in nominal conditions with the CEA thermal-mechanical METEOR V1.10 code modified with the properties of the composite fuels obtained with the CAST3M FE calculation code [21]. The calculated CERMET or microcell metallic fuel temperature improvements over standard UO_2 fuel reach several hundred degrees.

For LOCA conditions, an impact assessment of enhanced fuel thermal conductivity showed decreases in both the peak cladding temperature and the quench time of the fuel rod [22 - 26]. For UO_2-80%Mo composite fuel irradiated up to 125 GWd/MTU, then annealed at 350°C under vacuum for 3 hours, the composite fuel released less fission gas in transient than a standard UO_2 fuel (Reference [1] appears to cite no source for this result). This positive result should be confirmed for fuel with more representative lower Mo content [1].

Within the context of the severe accident simulations described in Reference [27], it was found that loss-of-coolant accident (LOCA) assessments have shown thermohydraulic improvements (e.g., lower peak cladding temperature) enabled by ATF designs that feature doped UO_2 pellets. The cause of these improvements, however, is not shown to be specifically the doping, as distinct from the co-effects of the ATF chromium coating added to the Zircaloy cladding that, being part of the complete modeled design, also is included in the simulations. Concerning doped fuel explicitly, this source considered that doped UO_2 fuel pellets may have a lower fuel thermal conductivity, and to account for this the simulations took a penalty in the form of higher prescribed pre-accident fuel temperatures, reflective of increased initial stored energy due to the assumed lower thermal conductivity attributed to the doping. Although Reference [27] noted that doped pellets have the potential to improve fission gas retention and thereby reduce end-of-life rod internal pressure and the possibility of rod rupture, this source considered these possibilities to be lower-order effects and therefore took no credit for them in the simulations. A typical thermohydraulic improvement found by Reference [27] is noted briefly for completeness, but as we have noted such results likely have more to do with the ATF cladding (Zr-alloy with a Cr coat) than with the Cr-doped UO_2 fuel. In a large LOCA scenario, the 95/95 Peak Cladding Temperature (PCT) for the ATF design found by Reference [27] is around 1990 °F, in comparison with 2180 °F for the baseline. (The baseline plant is assumed to have standard Zircalloy cladding with UO_2 pellets, including pre-transient corrosion of the Zircalloy cladding.)

According to Reference [28], AREVA is developing a Cr-doped-UO_2 fuel to be used with M5 cladding (M5 is one of the zirconium alloys) to which a Cr coating is added. Reference [28] further states that it is expected that this design entails no change to Regulatory Guide 1.183 for duration or fraction of gap or early in-vessel radiological releases.

Westinghouse is working to commercialize their advanced doped UO_2 fuel (ADOPT™ fuel) with Cr-coated cladding [29 - 31]. The Cr-coated cladding being developed by Westinghouse consists of ZIRLO® and Optimized ZIRLO™ claddings coated with chromium using a cold spray process. Application parameters for cold spray have been optimized to achieve dense and adherent coatings, while polishing processes have been developed to achieve the thickness and surface finish required for in-reactor performance and integration into current fuel designs, without a need for fuel assembly structure modifications [32]. The final coating thickness is between 20 and 30 microns. Westinghouse has performed in-reactor testing on Cr-coated cladding in the MIT reactor and the Halden reactor. Lead test rods of Cr-coated Zr with doped UO_2 fuel (also, U_3Si_2 fuel) were inserted for irradiation in the Byron Pressurized Water Reactor (PWR) in Spring 2019. Current plans are for lead test assemblies of SiC and Cr-coated Zr with doped UO_2 fuel (also, U_3Si_2 fuel) by 2022 and batch implementation by 2027 [29].

According to Reference [29], Framatome is currently working toward commercializing a near-term ATF design. This design includes chromium-coated zirconium alloy cladding (M5®) with Cr_2O_3 doped UO_2 fuel [33]. The chromium is applied using a physical vapor deposition (PVD) process.

The coating deposited is very dense and adherent. Additionally, the PVD technique is stated to not impact the underlying substrate microstructure since no heat treatment is applied on the tubes during deposition and the increase in temperature due to the incident Cr atoms is relatively small [33]. No additional processing steps following PVD deposition have been described by Framatome. The final coating thickness is between 8 and 22 microns. Framatome has performed in-reactor testing in Gösgen (Swiss PWR), Halden, and ATR. Lead test rods of Cr-coated Zr with Cr_2O_3 doped UO_2 fuel were inserted for irradiation in Vogtle and ANO-1 (both PWRs) [33] in, respectively, Spring 2019 and Fall 2019.

GNF has recently introduced aluminosilicate (SiO2-Al2O3) additive fuel pellets into GNF fuel products to increase fuel reliability and operational flexibility of nuclear fuel bundles and cores [34]. GNF provides data from steady-state and power ramp data from experimental test rigs as well as from Lead Use Assemblies (LUAs) from commercial reactors. No information on additive concentrations nor data from irradiations is provided in this non-proprietary document submitted to NRC and made available to the authors.

2.1.2 High-Density Fuel Design Concepts

This section gives at least some consideration to each of the following high-density fuels: uranium silicide, uranium nitride, metallic uranium, uranium/plutonium carbide, uranium/molybdenum. However, the most fully discussed high-density fuel compound is uranium silicide (U_3Si_2). Generally, the purpose of high-density fuels in ATF designs is to compensate for effects caused by proposed new ATF claddings. Most of the information is based on Reference [1], with additional information based on Reference [35], as indicated.

Reference [1] identifies the motivation for considering high-density fuels as being mainly a matter of compensating for penalties associated with newly proposed cladding materials; and it includes discussions of several high-density fuel compounds with respect to expected DBA and severe accident behavior as highlighted below.

2.1.2.1 Silicide Fuels

The information discussed here is extracted from Reference [1]. U_3Si_2 fuel has a larger margin to melting as compared to UO_2 fuel despite the fact that U_3Si_2 melts at 1665°C, whereas UO_2 melts at 2878°C. Using 0.82 cm diameter pellets with a surface temperature of 673K, the maximum linear heat generation rate (LHGR) before centerline melting occurs in UO_2 is ~750 W/cm. A comparably sized U_3Si_2 pellet can have an LHGR of 2300 W/cm before centerline melting occurs. This is due to the much higher thermal conductivity of this fuel when compared to UO_2. Additionally, it is beneficial that the thermal conductivity of U_3Si_2 increases with temperature. (e.g., suppose the peak linear power is being ramped up: the time to melting of the U_3Si_2 is increased, relative to what it would be absent this temperature dependence of fuel thermal conductivity.) Generally, the thermal properties and neutron economy properties for U_3Si_2 allows for a more advanced cladding to be used. Qualitatively, softer pellet-clad interactions (in relation to power ramps) and more exothermic fuel oxidation (in relation to clad failure) are expected when compared to UO_2 fuels, but this needs to be experimentally confirmed [1]. Reference [1] mentions this more exothermic oxidation of U_3Si_2 in the context of several transient types from normal operation to DBAs. During normal operations, the concern is pulverization of the silicide fuel form and substantial mass loss, i.e., the potential for dissolution of fuel pellets if exposed to the coolant

for long periods of time; see Reference [36] for further information. For information about oxidation of silicide fuel in a steam environment, see Reference [37].

Uranium silicide fuel is considered also by Reference [35], which remarks that this fuel type:

(a) Has low operating temperature due to high thermal conductivity;

(b) Does not decompose when in contact with hot water;

(c) Has low parasitic absorption of Si, no penalties on the uranium enrichment;

(d) Has only limited potential for increased cycle length given the current 5 wt% uranium enrichment limit.

2.1.2.2 Nitride Fuels

The first block of information in this subsection is based on Reference [1]. Accident conditions experienced by nitride fuel are very limited. Based on the understanding of the off-normal behavior of carbide and oxide fuel systems in fast breeder reactors, it is expected that the off-normal behavior of nitride fuel will mainly depend on the following:

- Accelerated swelling of the nitride fuel at high temperature could rapidly lead to pellet-cladding interaction failure mechanism;
- The (U, Pu) N fuel decomposition at T> 2000 K under He could lead to nitrogen release and thus to an over pressurization of the rods, this is not an issue with UN fuels since sintering temperatures of up to 2600 K have been used with no decomposition; and
- In case of cladding failure, nitride reaction with steam or water will generate hydrogen; however, the water resistance of UN can be improved by minimizing open porosity in conjunction with lowering the carbon content in the manufactured pellets [38 - 39].

Experimental data on these items are sparse. As a result, the assessment of these issues is quite difficult and requires further studies [1]. The Pu-related phenomena mentioned by Reference [1] appear to be considered as arising at the as-fabricated concentrations of Pu in (U, Pu) N fuels; they could be intensified by higher Pu concentrations that result from high burnup but authors have not identified any papers in the literature that discusses this possibility.

Uranium mononitride fuel is considered also by Reference [35], which remarks that this fuel type:

(a) Has low operating temperature due to high thermal conductivity;

(b) Requires demonstration of the process to waterproof the fuel;

(c) Needs about 35% to 50% more NU and 50% to 100% more SWU than a standard UO2 fuel producing the same energy, mainly because of the neutron absorption of natural nitrogen;

(d) Needs only about 10% to 15% more NU and SWU to produce the same energy, if run with 90 wt% 15N enriched nitrogen;

(e) Could admit extension of the cycle length to 24 months without exceeding the current 5 wt% uranium enrichment limit.

Experiments on UN fuel have been reported by Reference [40]. UN pellets of different densities were subjected to a superheated steam/argon mixture at atmospheric pressure to evaluate their resistance to hydrolysis. Complete degradation of pure UN pellets was obtained within an hour in 0.50 bar steam at 500 °C. The identified reaction products were uranium dioxide, ammonia, and hydrogen gas, with no detectable amounts of nitrogen oxides formed. The porosity of the pellets was identified as the most important factor determining reaction rates at 400–425 °C, and it is suggested that in dense pellets, cracking due to internal volume increase initiates a transition from slow surface corrosion to pellet disintegration [40].

Nitride fuel for LWRs is expected to be significantly enriched in N_{15} which has reduced thermal neutron absorption in comparison with the natural nitrogen isotopic mixture.

2.1.2.3 Carbide Fuels

Major challenging problems are expected during DBAs and severe accident conditions related to Pu evaporation from (U, Pu)C fuel when temperatures exceed T~1650°C; in case of high-temperature transients the accelerated fuel swelling may be a concern in design. Furthermore, the reactions of UC with steam could lead to products such as UO_2 and CH_4 or H_2 and gaseous carbon oxides which, for the most part, are explosively combustible in air, requiring that UC pellets be protected from steam at all times [1]. The Pu-related phenomena mentioned by Reference [1] appear to be considered as arising at the as-fabricated concentrations of Pu in (U, Pu) C fuels; they could be intensified by higher Pu concentrations that result from high burnup but the authors have not identified any papers in the literature that discuss this possibility.

Moderation by carbon in the fuel can affect reactivity feedback and Reactivity Initiated Accident (RIA) performance, as is remarked later in Section 2.3.3 in connection with the new cladding materials. The effect can be compensated by an increase of uranium enrichment.

2.1.2.4 Metallic Fuels

Using Metallic U-10% Zr and Metallic U-50% Zr, the irradiated U(-Pu)-Zr-alloy is easily oxidized resulting in generation of H_2. Accident conditions experienced by U-50wt%Zr are characterized as not reported by Reference [1]. One major concern is related to the high amount of zirconium, uranium, and other metals reacting with steam at very high temperatures with the risk of generating hydrogen during severe accidents. The low operating temperature and improved heat transfer, when the U-50wt%Zr fuel is metallurgically bounded to the cladding, should reduce the stored heat in the fuel during normal operation and hence facilitate decay heat removal and prevent rapid temperature increase at the very beginning of an accident. Therefore, increased time to restore cooling capability during DBA can be expected. However, a phase transition in the δ-phase alloy occurs from ~600°C that could result in swelling acceleration and detrimental pellet-clad mechanical interaction (PCMI). Therefore, in the absence of cooling over a long period, a worsening of the overall behavior in comparison with UO_2 fuel is anticipated. Additional drawbacks of the U-50wt%Zr fuel are its low melting temperature as well as its poor behavior in the event of contact with steam [1].

Uranium molybdenum fuel is considered by Reference [35], which states that this fuel type:

(a) Has low operating temperature due to high thermal conductivity;

(b) Requires demonstration of fabrication by extrusion at an industrial scale;

(c) Requires demonstration of the process to waterproof the fuel;

(d) Needs about 20% more NU and 30% more SWU than a standard UO2 fuel producing the same energy, mainly because of the neutron absorption of molybdenum – using depleted molybdenum would mitigate the impact on NU and SWU requirements;

(e) Could admit extension of the cycle length to about 23 months without exceeding the current 5 wt% uranium enrichment limit.

Reference [23] considers composites of UO_2 with UN and U_3Si_2 for compensation of ATF clad penalties. Several ATF pellet concepts are currently being suggested and evaluated around the world to mitigate the consequences of an accident. Desirable attributes for ATF pellets include enhancing the thermal conductivity and retention of fission products. A high uranium density fuel is also desired to compensate for the anticipated reduction of the fuel cycle length. For example, a ceramic composite cladding likely gives rise to a smaller volume of fuel pellets owing to the thick cladding wall and low thermal conductivity. Advanced non-Zr-alloy claddings, meanwhile, have a high neutron absorption cross section. To alleviate the cost penalty, therefore, it might be necessary to use high-density pellets in combination with the proposed ATF cladding materials. The exploration of UO_2/uranium mononitride (UN) and UO_2/uranium silicide (U_3Si_2) composite fuels is ongoing for long-term application. UN and U_3Si_2 are known to have many benefits, such as higher uranium density and thermal conductivity. The feasibility of composite fuel concepts in which the uranium nitride or uranium silicide particles are embedded in a UO_2 matrix is being evaluated. These concepts assume that a protective matrix of UO_2 would, for example, prohibit water corrosion of the nitride phase, or suppress irradiation swelling or chemical interaction of silicide at temperatures relevant to LWR operation [23].

With a particular focus on fuel thermal conductivity and the benefits of enhancing it, Reference [41] reviewed many composite fuels, including UO_2-BeO, UO_2-SiC, UO2-Mo, UO_2-Cr_2O_3, UO_2-Diamond, UO_2-Graphene, U_3S_{i2}, U_3Si_2/UN and FCM fuels, and some others. Reference [42] reported measurements of density and thermal conductivity of UO_2-SiC composites.

2.1.2.5 Experiments, Tests and Simulation Studies

Reference [43] presents the results of oxidation tests for UN, U_3Si_2, U_3Si_5 and a composite material composed of UN–U_3Si_2 as ATF materials. The spark plasma sintering method was used to fabricate UN and UN–U_3Si_2 to very high densities, to improve its resistance to oxidation. Using thermo-gravimetry in air, the oxidation behaviors of each material and the various microstructures of UN were assessed. All oxidation tests in this study were performed at temperatures below 1073 K, which is not representative of the conditions of severe accidents for the potential AFTs. The paper provides some thermo-physical properties which are reproduced in Section 2.1.4.

Reference [27] includes severe accident simulations of designs that include U_3Si_2 fuel. Table 2.3 gives some of the results for Peak Cladding Temperature (PCT). Based on preliminary available data and conservative estimates for high burnup performance, the model took credit for high U_3Si_2 thermal conductivity. The baseline plant is a 4-loop Westinghouse PWR, assumed to have standard Zircaloy cladding with UO_2 pellets, including pre-transient corrosion of the Zircaloy cladding. The scenario is a large LOCA. Very clearly, U_3Si_2 pellets reduce the PCT. The PCT benefit derives from the initial pellet temperature. The initial pellet temperature associated with

UO_2 fuel causes the cladding to heat up during the blowdown phase to around 1500 °F. The U_3Si_2 fuel, with its lower normal operating temperatures, heats the cladding only to 1000 °F. This difference during blowdown is, generally, retained throughout the duration of the transient, and ultimately at 1610 °F the PCT for the U_3Si_2 fuel is almost 400 °F less than that of the doped UO_2 fuel with the chromium-coated cladding (1990°F, quoted above in the doped fuels section), and smaller even still than the PCT of the baseline (2180°F).

Table 2.3 Predicted large LOCA peak cladding temperatures (PCT) for U_3Si_2 fuel versus current UO_2 fuel [27]

Case	**95/95 PCT (°F)**
Baseline (UO_2 fuel with Zircaloy cladding)	2180
U_3Si_2 fuel with Cr-coated Zircaloy cladding	1610

Reference [27] also has similar simulation results for U_3Si_2 fuel applying to other scenarios, to BWRs and PWRs of other design, and considers altered power peaking factors that might apply in ATF designs, among other factors.

Reference [27] also includes severe accident simulations of designs that include metallic fuel. (In the case the metallic fuel, the design is not described in detail in Reference [27], except that it includes U-Zr fuel and Zircaloy cladding.) A MAAP model of a 4-loop Westinghouse PWR was used to calculate the results reproduced in Table 2.4a under a short-term Station Blackout (SBO) condition. A BWR also was modeled and the relevant results for a short-term SBO are listed in Table 2.4b.

Table 2.4a PWR: predicted short-term SBO event timings (in hours) for various fuels [27]*

Parameter	**Zr / UO_2**	**FeCrAl/UO_2**	**Cr-Zr/UO_2**	**SiC/U_3Si_2**	**Metallic**
Cumulative generation of 10 kg of combustible gas	2.40	>4.64	2.55	3.13	2.37
Initial fission product release	2.03	2.10	2.90	2.11	2.51
First fuel melt	2.56	2.75	2.90	3.20	2.45
Hot leg creep rupture	>3.22	3.26	>4.15	3.32	3.16

* The > symbol indicates that the simulation ended with the considered event not having yet occurred.

Table 2.4b BWR: predicted short-term SBO event timings (in hours) for various fuels [27]

Parameter	**Zr / UO_2**	**FeCrAl/UO_2**	**Cr-Zr/UO_2**	**SiC/U_3Si_2**	**Metallic**
Cumulative generation of 10 kg of combustible gas	0.98	N/A	1.09	1.32	0.99
Initial fission product release	0.83	0.82	1.32	0.87	1.06
First melt	1.02	1.07	1.26	1.29	1.04

Reference [31] reports the results of simulations using the MAAP computer code for an SBO (including FLEX-type injection into the steam generators) for a typical PWR using, alternatively, conventional fuel/cladding or Westinghouse U_3Si_2 fuel. Depending on whether the cladding is Cr-coated Zircaloy versus silicon carbide, the coping time is increased by 0.35 versus 0.95 hours,

relative to the conventional fuel/cladding wherein the coping time is 2.54 hours. Mixed results are predicted for hydrogen generation (i.e., 27 kg for the conventional fuel design; 0 kg for Cr-coated Zircaloy cladding; 44 kg for SiC cladding).

Westinghouse is currently working toward commercializing two ATF designs that employ uranium silicide (U_3Si_2) fuel [29 - 31]. (Note, status of the Westinghouse design that uses doped UO_2 fuel is reported at the end of Section 2.1.1.) The first is silicon carbide (SiC) cladding with U_3Si_2 fuel [30 - 31]. The second is chromium-coated ZIRLO cladding with U_3Si_2 fuel [30 - 31]. It is expected [28] that the second design entails no change to Regulatory Guide 1.183 for duration or fraction of gap or early in-vessel radiological releases; note, though, that Reference [28] is not very detailed and further studies may be required. Westinghouse has performed in-reactor testing on Cr-coated cladding in the MIT and the Halden reactors [29 - 30]. Lead test rods of Cr-coated Zr with U_3Si2 fuel (also, doped UO_2 fuel) were inserted for irradiation in the Byron PWR in Spring 2019. Current plans are for lead test assemblies of SiC and Cr-coated Zr with U_3Si_2 fuel (also, doped UO_2 fuel) by 2022 and batch implementation by 2027 [32].

The "I^2S-LWR" reactor under development in the United Kingdom has a U_3Si_2 pellet of diameter 0.316" and FeCrAl cladding of thickness 0.016" (406.4 micron) [44]. Reference [44] is overall an analytic paper with, as a typical result, a calculation of criticality as a function of burnup by WIMS and SERPENT codes for burnups up to 50 GWd/MTU.

A design by Lightbridge uses metallic HEU fuel [28]. According to Reference [28], it is expected that this design requires a "Need to synthesize" updates of Regulatory Guide 1.183 for duration of early gap and in-vessel release, and requires "Needed data" on the associated release fractions of these releases.

2.1.3 Microencapsulated Fuel Design Concepts

Microencapsulated fuel designs discussed here consist of microcells and TRISO pellets.

The microcell fuels considered here consist of UO_2 plus an additive. In the case of microcells, a two-phase structure results, with granules of UO_2 surrounded by a thin continuous wall of the additive. The wall enhances the fuel thermal conductivity and/or improves the fuel/cladding interaction and/or improves fission product retention, with the relative importance among these benefits being determined by the chosen additive. Microcell fuels are sub-divided into metallic versus ceramic types.

Microcell UO_2 pellets are envisaged as having the potential to enhance the performance and safety of current LWR fuels under normal operating conditions as well as during transients/accidents. In the microcell UO_2 pellet concept, all UO_2 grains or granules are covered by thin cell walls. The cell walls are designed to provide multiple chemical traps or a physical barrier against the movement of volatile fission products, or to enhance the thermal conductivity of pellets [23].

Reference [23] includes the design details listed in Table 2.5 for metallic and ceramic microencapsulated UO_2 fuel concept.

Table 2.5 Specification of microcell fuel pellets irradiating in Halden reactor [23]

Cell Wall Materials	**Ceramic Microcell/UO_2**	**Metallic Microcell /UO_2**

	0.6 wt% Si-Ti-O (2 vol.%)	3.4 wt.% Cr (5 vol.%)
Averaged cell size (micron)	~80	~290
Pellet density (g/cm^3)	10.73 ± 0.03	10.45 ± 0.03
Pellet diameter (mm)	8.190 ± 0.002	8.196 ± 0.001
Pellet height (mm)	9.4 ± 0.2	9.12 ± 0.03
Pellet weight (g)	5.15 ± 0.10	4.93 ± 0.02
U235 enrichment	4.5%	4.5%

Carbon in fully ceramic microencapsulated (FCM) can reduce negative reactivity feedback in comparison with the conventional oxidic fuel. FCM fuel is considered also by Reference [35], which states that this fuel type:

(a) Could benefit from the excellent fission product retention of TRISO fuel particles if their performance under PWR operating conditions is shown to be satisfactory;

(b) Has low operating temperature due to high thermal conductivity;

(c) Needs modification of the uranium enrichment facilities to provide 19.9% enriched uranium;

(d) Makes challenging reaching an 18-month cycle length;

(e) Needs about 15% to 25% more NU (i.e., metric tonnes of Natural Uranium) and about 50% to 65% more SWU (i.e., Separative Work Units) than a standard UO2 fuel producing the same energy.

2.1.3.1 Metallic Microcell Pellets

The metallic microcell UO_2 pellet is a high thermal conductive pellet with a continuously connected metallic wall; 5 vol.% of either Mo or Cr phase. Cell sizes are ~290 microns. U-235 enrichment is 4.5% [23]. Metallic microcell pellet behavior under a high temperature steam environment needs to be evaluated because when the fuel rod is breached, high-temperature coolant penetrating through defects [45] may react with the Cr or Mo wall to form oxide phases [46]. The preliminary steam oxidation test at 500°C showed that the metallic microcell UO_2 pellets retained their structural integrity much longer compared with the standard UO_2 pellets. By contrast, a steam oxidation test at 1,100°C revealed that the Mo wall vanished owing to a formation and evaporation of the volatile oxide phase. In the case of pellets containing Cr, the formation of the Cr_2O_3 phase, of a low density, resulted in the swelling and cracking of the pellets. The authors report current modifications to the wall material by alloying with Al or Si. Formation of alumina or silica layers is expected to block, or at least retard, the growth of oxide layer in the metallic walls.

More insights on metallic microcell fuel designs are available from Reference [1]. Reference [1], a long review article, surveys the ATF subjects somewhat differently and some of its relevant aspects have already been discussed above under the heading of doped fuels (see Section 2.1.1). Reference [1] identifies three approaches for increasing the thermal conductivity of UO_2

according to the addition of any of three metallic additives: Ceramic / Metallic ("CERMET") fuels, the Metallic Microcell approach, and addition of molybdenum (see Table 2.1). In fact these approaches are closely related, since as discussed by Reference [23] the additive leading to metallic microcells can be Mo. Metal-doped UO_2 fuel is generally called a CERMET fuel ("CER" for ceramic UO_2; "MET" for metallic additive) [1]. Reference [1] notes that CERMET fuels were used in a commercial reactor as early as the early 1960s (i.e., at the Vallecitos BWR, where the additive was stainless steel). The following remark, in Reference [1] attributed to Reference [23], shows that some authors may draw a distinction between CERMETs and metallic microcell fuels: when granules of UO_2 are surrounded by a thin metal wall, Reference [23] and other sources refer to this concept as metallic microcell fuel.

During normal operations, the main benefit of Mo or Cr containing granules of UO_2 is an enhanced thermal conductivity [1, 47]. A high-thermal conductivity can provide a low fuel temperature and a large thermal safety margin during transients. A cold pellet with a reduced temperature gradient is expected to be beneficial in mitigating the fuel relocation (cracking) and reducing the release of fission products during normal operations. During loss-of-coolant accidents, an increase in thermal conductivity reduces both the peak cladding temperature and the quench time of the fuel rod [1].

As reported in Reference [1] in 2018, the UO_2-5vol% Cr microcell pellets were at that time being irradiated in the Halden Research Reactor. The peak burn-up achieved to that date was approximately 10.7 MWd/kgM. The UO_2-5vol% Cr rod showed a low centerline temperature, typically 15% lower than the reference UO_2 fuel rod. The temperature difference between the rods remains unchanged until now, indicating that the metallic network is intact [1].

Very low levels of fission gas release have been measured (< 0.4%) in UO_2-80vol%-Mo fuel pellets irradiated by CEA in an MTR up to 125 GWd/MTU [1].

2.1.3.2 Ceramic Microcell Pellets

The main purpose of the ceramic microcell UO_2 pellet is to minimize the release of fission products contained in the pellet structure by providing a microcell structure with oxide additives [48]. The main benefit of ceramic microcell UO_2 pellets is an enhanced retention capability of the volatile fission products, such as Cs [23]. The ceramic microcell UO_2 pellet was obtained by mixing 0.6 wt.% of SiO_2TiO_2 oxides mixture with ADU-UO_2 powder. The sintered pellet density for these pellets is 10.73 g/cm^3. Cell sizes (average grain size) are ~80 microns. U-235 enrichment is 4.5%. In the case of ceramic microcell UO_2 pellets, the impact on fuel cycle was found to be negligible because the wall volume is smaller than that in metallic microcell pellets, and the neutron absorption due to Si is very small [23].

Reference [1] adds to the above account (quoted there from Reference [23]) the following information about ceramic microcell UO_2 pellets. The fabrication feasibility of ceramic microcell UO_2 pellets has been demonstrated [47]. The conventional liquid phase sintering technique has been applied. Less than 1 wt% of SiO_2-based oxide additives was blended into UO_2 powder and then the powder mixture was sintered at around 1700°C for several hours in a dry hydrogen atmosphere. This manufacturing process is exactly the same as for standard fuel, which is an advantage in terms of infrastructure availability and economics. An improvement in fission product retention capability leads to a reduction of the inner surface cladding corrosion caused by fission products as well as the internal pressure of the fuel rod. A soft, thin wall facilitates the fast creep deformation of the pellets, thereby reducing the mechanical loading of the cladding under

operational transients. It has been speculated that a mesh-like rigid wall structure may prevent the massive fragmentation of pellets during a severe accident [1]. However, data are needed to confirm this speculation, because a contrasting view is that the fragmentation of fuel is a result of thermal cycling during normal operations, and that in severe accidents fuel pellets actually get welded together by high temperature sintering, as indicated by residual rods from the Phébus experiments[3].

The chemical affinity of the wall to cesium may have a large impact on the retention capability of fission products [1]. Ceramic microcell UO_2 fuel is characterized by a homogenous large-grain (~100 micron) and cell structure, speculated to provide beneficial features for the fuel performance (dimensional stability, improved behavior in case of water/steam ingress, superior PCI and SCC-PCI resistance and a higher FPs retention capability). Testing is required to confirm this speculation,

Table 2.6, showing data reproduced from Appendix B of Reference [1], compares the behaviors among ceramic microcell UO_2 fuel with conventional UO_2 fuel under normal operation, AOOs, and DBAs or severe accidents.

2.1.3.3 TRISO-SiC-Composite Pellets

Tristructural-isotropic (TRISO) fuel particles, originally developed for use in High Temperature Gas Reactors (HTGRs), is also being considered for LWRs [1]. TRISO fuel is a type of micro fuel particle. It consists of a fuel kernel composed of UOX (sometimes UC or UCO) in the center, coated with four layers of three isotropic materials deposited through fluidized Chemical Vapor Deposition (CVD). The four layers are a porous buffer layer made of carbon that absorbs fission product recoils, followed by a dense inner layer of protective pyrolytic carbon (PyC), followed by a ceramic layer of SiC to retain fission products at elevated temperatures and to give the TRISO particle more structural integrity, followed by a dense outer layer of PyC. TRISO particles are then encapsulated into cylindrical or spherical graphite pellets. TRISO fuel particles are designed not to crack due to the stresses from processes (such as differential thermal expansion or fission gas pressure) at temperatures up to 1600 °C, and therefore can maintain the fuel integrity during severe accidents. This is due to a combination of multiple barriers to fission product release and slow kinetics of the SiC reaction with high-temperature steam, which can provide larger margins of safety under DBAs and severe accidents. CVD-SiC exhibits exceptional oxidation resistance in high-temperature steam environments [49 - 51]. The SiC matrix of Fully Ceramic Microencapsulated (FCM) fuel exhibits similar behavior and is quite resistant to steam oxidation [52]. Furthermore, the SiC coating layer in the TRISO particles, in addition to being a robust barrier to transport of most radionuclides, is also an effective layer to inhibit steam ingress into the coated fuel particles. Exceptional steam oxidation resistance of SiC-based materials, coupled with the discrete nature of fuel particles and their inherent protective layer (the SiC coating shell), designates FCM fuel as a robust ATF technology.

[3] Comment by D. Powers.

Table 2.6 Comparison of behaviors among ceramic Microcell UO_2 pellets with undoped UO_2 under normal operation, AOOs, and DBAs/severe accidents [1] (See also Table 2.2)

Property	**Ceramic Microcell UO_2 Pellets, Compared to UO_2**	
	Normal operation and AOOs	**DBAs/Severe Accidents**
Thermal-mechanical interaction		
Densification and swelling		
Deformation	Faster than that of standard UO_2 pellet (i.e. a reduction of cladding strain)	
Thermal behavior (unirradiated and irradiated)		
Thermal Conductivity (W/m·K)	Unexamined	
Specific heat (kJ/kg·K)		
Melting point (°C)		
Swelling and Pellet-clad interaction		
Thermal expansion	Similar to those of a standard UO_2 pellet	
Thermal diffusivity		
PCI and SCC-PCI behaviors		
Ballooning and burst		Decrease is speculated (no data available)
Chemical compatibility, stability		
Secondary degradation (oxidation and washout)	Washout rate of the ceramic microcell UO2 reduced	
Resistance to steam oxidation	Enhanced	
Fission product behavior (including fission gas pressure and fission product retention)	Enhanced retention capability of the volatile FPs (e.g. Cs)	
Gas available for release at the grain boundaries and mesh-like cell structure		Decrease anticipated (no data available)

Improved performance using an optimized TRISO-SiC fuel assembly design (FCM+FeCrAl rod) in a Korean OPT-100 design has been noted under large LOCA conditions (i.e., reduced peak cladding temperature and the quench time of the fuel rod). However, very limited data exist with respect to the fuel behavior and failure mechanism of TRISO-SiC fuel under postulated severe accident conditions. Calculation results carried out for OPR-1000 showed that the FCM+FeCrAl core allows longer coping time under the SBO and LB-LOCA without safety injection when compared with those of a reference UO_2 core. Fission product releases from TRISO pellets as functions of burnup are reported on by Reference [53], which discusses both experiments

(performed in the High Flux Reactor in Petten, The Netherlands in 2006) and predictions by the MFPR computer code.

Moderation by carbon in TRISO fuel can affect reactivity feedback and RIA performance, as is remarked in Section 2.3.3 in connection with the new cladding materials.

2.1.4 Summary of Available Property Data for ATF

Reference [3] presents a list of the models available for predicting the properties of Cr_2O_3-doped UO_2 (and also U_3Si_2 fuel) including the range of applicability of the models and an estimation of the associated uncertainties. The models were validated against experimental data – the references are given in Reference [3] but are not reproduced here. The described properties include thermal properties (thermal conductivity and specific heat), thermal expansion, fission gas behavior, elasticity, and cracking, among others. The actual models/formulas are available in Reference [3]. Table 2.7 lists properties and the page numbers in Reference [3] where they can be found. The effect on the prediction for fuel performance metrics of interest such as fission gas release, fuel temperature, fuel elongation, and rod internal pressure was also identified Reference [3].

Reference [3] also presents a list of the models available for predicting the properties of U_3Si_2 fuel, similarly, listed in Table 2.7. Reference [54] is another source for information on the material properties of U_3Si_2 fuel, including specific heat, thermal conductivity, thermal expansion, and elastic properties. Reference [54] also points out that U_3Si_2 can oxidize, although only air-oxidation is mentioned and no data are provided on the reaction rates; a reference is given for the reduction of air-oxidation of U_3Si_2 fuel that results when the fuel contains some aluminum.

Table 2.7 Cr_2O_3-doped UO_2 and U_3Si_2 properties [3]

Physical property	**PDF Reference Page**	
	Cr_2O_3	**U_3Si_2**
Thermal conductivity	7 of 52	17 of 52
Specific heat and range	8 of 52	19 of 52
Elasticity and range	14 of 52	22 of 52
Thermal expansion and range	9 of 52	49 of 52
Thermal and irradiation creep and range	-	22 of 52
Grain size and range	10 of 52	-
Fission gas behavior	11 of 52	25 of 52
Atomistic model for diffusivity and range	13 of 52	28 of 52
Gaseous swelling	13 of 52	-
Solid swelling and range	13 of 52	29 of 52
Densification and range	14 of 52	30 of 52

Table 2.8, reproduced from Reference [35], shows thermo-physical properties (thermal conductivity, heat capacity, melting temperature and U density) for several high-density fuels.

Table 2.8 Thermo-physical properties of several fuels [35]

Physical property	**UO_2**	**FCM**	**UN**	**U_3Si_2**
Thermal conductivity (W/m·K)	4	19 (UN fuel kernel)	20	15
Heat capacity at 500°C (J/kg·K)	300	230 (UN fuel kernel)	230	250
Melting temperature (°C)	2840	2400 (SiC) 2762 (UN fuel kernel)	2762	1665
U density* (g/cm^3)	9.6	~1 to 2	13.5	11.3

* Partial density of uranium within the mixture

Table 2.9 lists the thermal conductivity and melting point as reported in Reference [43] (devoted overall to oxidation tests), also for several high-density fuels.

Table 2.9 Thermo-physical properties of several high-density fuels [43]

Physical property	**UO_2**	**UN**	**U_3S_2**	**U_3Si_5**	**UN-U_3Si_2(10%)**
Thermal conductivity (W/m·K) 600-1400 K	6.0-2.5	19-25	15-27.5	8-16	Unassessed, assumed mixture of UN and U_3Si_2
Melting point (K)	3130	3120	1938	2043	1938

Figure 3 in Reference [23] shows the thermal conductivity of metallic microencapsulated UO_2 fuel. The conductivity of Mo- and Cr-containing microcells is given in the form of a factor that applies to UO_2 conductivity, where the effective thermal conductivity of pellet is additionally a function of pellet shape as shown in the cited figure.

Reference [23] reports that thermal diffusivity and thermal expansion test results showed that the thermal properties of ceramic microcell UO_2 pellets are similar to those of a standard UO_2 pellet. By contrast, concerning mechanical properties, the compressive-creep deformation of ceramic microcell pellets at high temperature was faster than that of a standard UO_2 pellet. Fast creep deformation is beneficial since it implies that the ceramic microcell pellets can reduce the cladding strain during a transient or accident, as well as during normal operation.

2.2 Cladding Design

During severe accidents, core cooling is often not available and the core temperature escalates due to the decay heat in the fuel. As the core becomes uncovered, the core temperatures rise further, and the fuel elements start to experience physical and chemical degradation. Physical degradation occurs first at about 700-1000°C, involving ballooning and burst of the thin-walled cladding tube. Chemical degradation by steam oxidation of Zr metal, which generates excessive amounts of heat and hydrogen gas, becomes increasingly important as the temperature increases beyond 850°C. For this reason alternatives to Zircaloy are being considered.

The motivation therefore for potential accident tolerant fuel (ATF) claddings is to reduce the rate and total amount of heat generated from cladding oxidation at elevated steam temperatures during severe accidents, which will in turn reduce the rate of temperature rise, reduce hydrogen

generation, and delay core degradation, and hence provide additional coping time for accident mitigation.

The identification of potential candidates for the ATF by vendors is guided by the desire to identify performance criteria for cladding materials applicable to normal operation, DBAs and severe accidents. Reference [1] identifies the following performance criteria for ATF and associated cladding:

During normal operation:

- Reduced corrosion
- Equivalent or superior physical and mechanical properties (including creep and stress relaxation, resistance to pellet-clad mechanical interaction [PCMI] and stress corrosion cracking due to pellet-clad interaction [SCC-PCI])
- Equivalent or superior low neutron absorption
- Interface stable under neutron irradiation
- Good adherence
- High thermal conductivity to limit fuel centerline temperature
- High critical heat flux

During DBAs and severe accidents:

- Significantly reduced high temperature steam oxidation
- Higher mechanical strength at high temperature to maintain coolable geometry
- Good adherence and very limited cracking after significant clad creep/ballooning
- High thermal conductivity to limit fuel centerline temperature
- High Zr and coating material (e.g., Cr) eutectic temperature

To these attributes defined by Reference [1] can be added: adequate ductility in normal operation; and reduced fragmentation and dispersal in DBAs and severe accidents.

For a severe accident scenario such as a station blackout, the cladding temperatures could reach much higher than 1200°C. Resistance to high temperature steam oxidation depends on the formation of an oxide film. The oxidation rates for chromia, alumina, and silica are about two orders lower than those of the oxides associated with traditional Zr alloy-based cladding or with 304 stainless steel. The reduction in oxidation rate directly results in the reduction in the rate of heat and hydrogen generation under accident conditions. The oxide films need to be stable physically and chemically and also act as effective resistance against the transport of the oxidized species to reach the underlying materials. Although zirconia exhibits good thermodynamic stability in steam and excellent adherence to the underlying metal at high temperature, it is a fast conductor of oxygen and does not protect the underlying Zr metal, while chromia, alumina, and silica, on the other hand, exhibit acceptable stability in steam, and can act as effective resistances for diffusion of oxidizing species and reaction products. There may be a trade-off, however, for in contrast to the better protective character of these oxides compared to zirconia, the lower melting temperature of the underlying metallic phase of some proposed ATF claddings could lead to

cladding failure and loss of protection. Especially for coated claddings, such a failure could lead to oxidation of pure metal and the attendant severe effects.

The following subsections provide a review of three ATF cladding technologies, namely coated Zr-based cladding, advanced steel (FeCrAl) cladding, and SiC/SiC composites cladding, including their development status, technical challenges, and future work for these cladding technologies. Very few studies were found for the refractory metals (lined Mo-alloy cladding used for its high strength) and therefore these are not discussed in this review. The end of this section also includes a collection of the data for the physical and mechanical properties, and parabolic oxidation rate constants for various ATF cladding concepts. The physical properties include thermal conductivity; specific heat capacity/enthalpy; density, melting temperature, thermal expansion coefficient; and eutectic temperature for multi-layer cladding.

2.2.1 Coated and Improved Zr-based ATF Cladding

A protective coating on the surface of Zr-based alloys becomes an obvious approach to ATF cladding [55], because thin coatings are expected to have a minimal effect on the thermal-mechanical behavior of Zr-based cladding while they have the potential to enhance their corrosion resistance and high-temperature steam oxidation resistance during severe accidents. Therefore, the thickness of the coating plays a major role in maintaining the zirconium substrate properties and behavior. In general, for coatings below 20 μm, the neutronic impact on the fuel cycle cost or cycle length of all investigated coating types (Cr, Cr-Al, CrN, FeCrAl, MAX phase) is small and can be easily compensated by very slight design modifications [1]. Since coating materials usually have a higher thermal neutron absorption cross-section than Zr-based alloys, a thick coating will increase the fuel cycle cost and economics.

The coating technologies applicable to Zr-based alloys consist of metallic coatings and ceramic coatings in the form of nitrides or MAX phases. In the acronym MAX, M stands for an early transition metal, A is one of a group of 13–16 elements, and X is C and/or N, representing a family of layered ternary carbides and nitrides. The MAX phases are considered due to their unique combination of metallic and ceramic properties. The most widely explored coating technologies on Zr-based alloys are the ones that form chromia, specifically, Cr metal, CrAl, and CrN coatings [56 - 61]. The materials that contain Al and Si also produce a protective oxide film. Other materials without Cr, Al and Si coatings cannot form a protective oxide film and are not discussed here.

In the case of a metallic coating (Cr, CrAl and FeCrAl), the thicknesses usually varies in a range of 2 to 30 μm [57, 62 - 69]. In a case with thickness of 80 μm [23], the steam temperatures in the reported tests were up to 1310 °C, which is within the severe accident conditions. The results show that chromia formed under high steam temperature conditions protects the oxidation of underlying Zr alloy [63, 70], and reduces the cladding ballooning during LOCA testing [63, 71]. Cr coatings of 2 to 10 μm on Zircaloy-4 resulted in a ~50 times reduction in oxidation rate over Zircaloy-4 in a 1310°C steam environment [68].

Resistance to corrosion in LWR coolant was also evaluated in References [23, 57, 62, 72]. The Cr coating exhibited a significantly reduced corrosion rate (ten times smaller) and consequently, a reduction of hydrogen generation by the steam oxidation of cladding. On the other hand, corrosion tests on FeCrAl-coatings in BWR normal water chemistry at 288°C showed somewhat increased weight gain compared to uncoated Zircaloy-2 samples. This requires further investigation to determine the behavior of FeCrAl coatings in LWR operating environment.

Good adhesion to the metallic substrate at steam temperature as high as 1200 °C was also observed [67]. It is reported that a thin ceramic coating thickness (less than 10 to 30 µm) is needed to limit the neutronic penalty. In addition, Cr metal exhibits its geometrical stability during neutron irradiation at LWR temperatures as expected; namely, no degradation of the Cr-Zr interface was observed [73 - 74]. Furthermore, the strength and ductility of Cr coating on Zr alloy was investigated [23], which used a surface modification technique called partial Oxide Dispersion Strengthened (ODS). Application of the technique with zirconium alloy and a relatively thick Cr coating of ~80 µm was investigated. The results showed an increased strength but reduced ductility. Eutectic formation between the coating material and the underlying zirconium substrate at temperature beyond 1200 °C was also presented in this paper. The eutectic temperature increased with a Cr-Al coating, but very little data were found for the eutectic behavior with the different investigated coating materials.

In the case of nitrides ceramic coating on the surface of Zr-based cladding, the behavior is strongly dependent on the Al content of the coating because Al_2O_3 is unstable and dissolves in water in LWR environments. As expected, TiAlN and CrAlN coatings show poor corrosion behavior, while TiN and CrN exhibit significantly increased corrosion resistance as compared to uncoated Zr alloys (see References [60, 75 - 79]). The limited results show an excellent stability of a thin (<5 µm) CrN coating under prototypical fuel irradiation conditions, while the TiAlN and CrAlN coatings disappeared from the fuel rod surface after irradiation [79].

Integral LOCA testing of unirradiated CrN-coated cladding at 1000-1100°C steam also exhibited excellent coating adherence even with some cracking after burst testing [60]. However, no improvement was observed under high temperature steam oxidation condition. In comparison, TiAlN and CrAlN coatings showed significant cracking and degradation and allowed zirconium oxidation to occur.

In the case of MAX phase coatings, alumina and silica coatings are two potential ATF candidates, of which Ti_2AlC [80 - 83], TiAlN [75 - 76], Cr_2AlC [83 - 84], $(TiNb)_2AlC$ [83], and Ti_3SiC_2 [85] have been investigated.

Oxidation of single-phase Ti_2AlC coatings was studied with or without a 500 nm TiC diffusion barrier deposited on Zircaloy-4 in steam temperatures between 800 °C and 1200 °C. The coatings with the TiC barrier showed that a triple layered scale grew on the coatings at 800 °C, as compared to a duplex scale without the TiC barrier. The TiC barrier suppresses the rapid diffusion of Al into the substrate, thereby contributing to better oxidation performance and longer life of Ti_2AlC/TiC coatings. But both coatings demonstrated low protection effect at 1000 °C in steam. Similar results were also observed where a much thicker oxide and significant TiO_2 were formed for Ti_2AlC at 1200 °C [86 - 87]. The main reason is that TiO2 is not stable beyond 800°C, resulting in the degradation of the coating. Therefore, Ti_2AlC may be challenging to form as a cladding or a coating for high-temperature application beyond 1000 °C.

Si-coated Zr cladding was investigated for its high temperature oxidation behavior in 1200°C steam for 2000 seconds [64]. It was found that the Si coating layer successfully acted as a corrosion barrier layer to resist the high temperature oxidation of the zirconium-based alloy, but adhesion property of the coating prepared via a plasma spray method was insufficient for the high-temperature application.

There is a significant lack of data concerning the corrosion behavior of MAX phases in normal LWR environments, also a lack of a complete assessment of MAX-phase coating performance under normal operation, DBA, and severe accident conditions. Further investigations on MAX-phase coatings are needed.

The performances of Cr coating on Zr-based cladding as a promising ATF concept under severe accident conditions were also evaluated by using several accident analysis codes [27, 88 - 90]. Material properties for the Cr coating obtained from the literature were introduced into these codes by alteration of the thermal properties and oxidation kinetics models of the materials of the fuel and cladding.

The peak cladding temperature (PCT) was simulated for a typical LBLOCA for a Westinghouse PWR using the WCOBRA/TRACTF2 (WCT-TF2) code associated with the Westinghouse FULL SPECTRUM™ LOCA (2FSLOCA™) evaluation model [27]. The results showed that the PCT for Cr-coated cladding and doped UO_2 pellets reduced to 1088°C as compared to 1193°C for uncoated standard Zr-alloy cladding with UO_2 pellets, which indicates a margin gain in coping time for the investigated large LOCA scenario by applying Cr-coated cladding and doped UO_2.

The coping time to start of core damage and hydrogen generation was also evaluated for Cr-coated Zr cladding using RELAP5-3D code [88 - 89]. The small LOCA scenarios for a generic Westinghouse PWR were simulated with eight sub-variants depending on the ECCS and other systems [88]; the average gain in coping time is about 4 minutes for Cr-coated Zr cladding compared to uncoated Zr cladding and the average hydrogen production at the time of core damage with Cr-coated cladding was 36.9% of that with uncoated Zircaloy. In comparison, the simulated average gain in coping time, for ten SBO scenarios for a generic Westinghouse PWR, is 7 minutes for Cr-coated (20 μm) Zr cladding compared to uncoated Zr cladding, and average total hydrogen generation production at the start of core damage with Cr-coated cladding was about 10% of that with uncoated Zircaloy [89].

The coping time to start of core damage (melting) and hydrogen generation was also simulated for Cr-coated Zr cladding using the TRACE code [90]. Short- and long-term SBOs with or without RCIC for the Peach Bottom BWR plant were investigated. TRACE simulations estimated only marginal increase of the coping times (1-22 min) with Cr-coated Zr ATF claddings. However, the hydrogen productions from Cr-coating are one to two orders of magnitude less that those from Zircaloy cladding at the time when clad melting is expected.

In summary, the simulations performed for DBAs (SBO, SBLOCA and LBLOCA) up to the time of start of core damage using various codes showed some benefit in terms of start of core damage and cladding oxidation. The introduction of Cr-coated cladding results in only marginal increases of coping time, but Cr-coated cladding showed improved performance in the reduction of hydrogen generation at the time of core damage.

A summary of the coating performance characteristics of reviewed ATF cladding materials is tabulated in Table 2.10.

Table 2.10 Summary of coating performance characteristics of reviewed ATF cladding materials(1) (majority of the data are reproduced from Table 2 of Reference [91] and Table 10.1 of Reference [1])

Condition	Metallic Coatings			Ceramic Coating							
				Nitrides				MAX Phase			
	Cr [*]	CrAl [**]	FeCrAl, CrAlC [***]	CrN [+]	TiN [++]	TiAlN [+++]	CrAlN [++++]	Ti_2AlC [#]	Ti_3SiC_2 [# #]	Cr_2AlC	Zr_2AlC/ Zr_2SiC
Normal operation											
Resistant to corrosion in LWR coolant	Y	U (2)	U (2)	Y	Y	N	N	U	U		
Stable under neutron irradiation	Y		Y	Y	U	U	U	N	N		
Good adherence	Y	Y,U	Y	Y		N		U			
DBA and Severe Accident											
Significantly reduced steam oxidation	Y(3)	U (2)	U (2)	Y&N(4)	U	Y&N	U	Y&N	N	Y	
Strengthening high temperature effects: 1. good adhesion 2. reduced creep/ballooning 3. limited cracking	Y	Y,U	Y	Y&N(4)		N	N		N		

(1) Y: yes, N: No, U: Unknown, Y&N: Some studies show improved performances but others show little or even worse performance.

(2) In these instances, negligible or contradicted effects on corrosion and high temperature steam oxidation were observed, but the tests conducted at UIUC used CrAl and FeCrAl coating thicknesses of only 1 µm.

(3) But benefit may be limited to temperatures below the Zr / Cr eutectic.

(4) For no significant oxidation benefit of CrN relative to uncoated cladding, see Reference [91]. Reviewed sources agree on good adhesion of CrN coatings under various conditions, probably including DBAs and/or severe accidents. Less than favorable comments are interpreted to mean that CrN is likely no better than uncoated cladding, and such comments were reported for creep/ballooning (Reference [1] p. 129) and cracking (Reference [1] p. 128; Reference [60]).

For Cr: Reference [*] [56 - 58, 62 - 66, 73, 92 - 93]
For CrAl: Reference [**] [57, 64 - 66]
For FeCrAl/CrAlC: References [***] = [84, 86, 94]
For CrN: References [+] [60 - 61, 79, 95]
For TiN: References [++] [75 - 76]
For TiAlN: References [+++] [75 - 76, 78, 96]
For CrAlN: References [++++] [59, 78]
For Ti_2AlC: References [#] [80 - 82, 86, 97]
For Ti_3SiC_2: References [# #] [48, 85 - 86, , 97]

The most widely explored coating technologies for Zr-based alloys to date are the ones that form chromia, specifically, Cr metal, CrAl, and CrN coatings.

The limited information listed in Table 2.10 appear to indicate that Cr metal coating is the most promising technology for further development. The same protective oxide films that protect Cr-, Al-, and Si-bearing coatings (TiAlN and Ti_2AlC) at high temperatures may also form in the aqueous environment of the LWR coolant, but only chromia is stable in this environment, while silica and alumina tend to dissolve rapidly as silicic acid and aluminum oxy-hydroxide. Incorporation of Ti, which forms a stable oxide (similar to Zr), into these coatings can mitigate dissolution (e.g., TiN/TiAlN); however, similar to Zr, Ti undergoes rapid oxidation at elevated temperatures and its prevalence in the coating will likely compromise the protective nature of alumina/silica. Integral LOCA testing of unirradiated CrN-coated cladding exhibited excellent coating adherence but showed little or no improvement in oxidation or burst behavior as compared with uncoated cladding [91]. The FeCrAl coating, although adequate for normal operating conditions, forms a eutectic with Zr at temperatures less than 1200°C and is not considered as a useful ATF coating.

Under LOCA conditions, given the large quantity of Zr metal in LWRs, rod ballooning and rupture may occur at temperatures as low as 700°C, even though the outer cladding surface may be protected by the coating. This is still challenging due to high heat and hydrogen generated from Zr oxidation on the interior surface of cladding once steam enters this region after the rod burst.

Another challenge is eutectic formation for metallic coatings between the coating material and the underlying zirconium substrate [1]. For example, the Cr-Zr eutectic occurs at 1330°C. (The Cr-Zr phase diagram is available as Figure 4-1 in Reference [29], where it has been reproduced from the original source which is Reference [98].) A Cr-Al coating increases the eutectic temperature between the coating and the zirconium substrate. Incorporation of a thin barrier layer between the coating and the substrate such as with molybdenum or other refractory metals might be a solution, since it may prevent the eutectic formation. Nonetheless little data exist concerning the eutectic behavior for the different investigated coating materials, and the behavior of the coating beyond the eutectic point has to be investigated. If the coating is too thick, the coating-substrate interaction will be much higher and might therefore lead to significant degradation of cladding because of eutectic formation. Consequently, a compromise has to be determined between the minimum thickness necessary to provide significant benefits in high-temperature steam oxidation and a maximum thickness allowing a reduction of the potential detrimental consequences of eutectic formation.

Except for a few studies [94, 99 - 100], none of the research has exceeded the temperature limit of the design basis LOCA scenario (1204°C) during steam oxidation tests. In Reference [100], the oxidation performance and quench behavior of cold spraying Cr coated Zircaloy-2 tubes were investigated from 1100°C up to 1500°C in steam using the single-rod quench facility QUENCH-SR. When the temperature exceeds the Cr-Zr eutectic temperature (~1330°C), formation of liquid phase contributed to failure of the coatings at about 1500°C [100]. A much faster oxidation rate compared to uncoated reference sample was detected at temperatures above ~1450°C [100]. The coating on Zr-based cladding technology is deemed adequate for normal, anticipated operational occurrences and DBA scenarios. However, severe accident testing must be further conducted on ATF cladding technologies to show their improvements in cladding performance. Alternatively, the impact of the coating technology on the performance of the severe accident behavior of LWRs should be assessed by severe accident analysis codes; however, to do this,

the codes should be improved in the parts of the properties, data, and models describing core performance and severe accident behavior affected by the cladding.

2.2.2. Advanced Steel Cladding

This section provides a review of the behaviors and performances of advanced stainless steel cladding material (i.e., FeCrAl and its variants) for uranium dioxide (UO_2) fuel pellets.

The ATF technology by definition is expected to perform at least equivalently to current Zircaloy-UO_2 fuel systems under normal operational conditions, and better than the current Zircaloy-UO_2 fuel systems under accident conditions.

FeCrAl was designed to provide excellent mechanical behavior at high-temperature severe accident conditions. Exceptional steam oxidation resistance was observed for FeCrAl at a temperature near its melting point [101 - 104], resulting in a significant reduction in heat and hydrogen generation during accident conditions [105]. Therefore, compared to Zr-alloy cladding, the FeCrAl cladding designs increase reactor coping time, enhance the ability to maintain a coolable geometry, enhance fission products retention, reduce coolant oxidation reaction kinetics [86], and increase allowable peak cladding temperatures during operational and accident conditions. FeCrAl-clad fuel rods (with UO_2 as fuel) apparently exhibit the properties that meet or exceed current fuel design technical requirements while providing increased safety benefit during normal operation, DBAs, and severe accident conditions.

The excellent high temperature oxidation resistance of FeCrAl alloys relies on the formation of a protective alumina scale, which may be challenged during fast transients [106 - 107]. In addition, high temperature oxidation resistance also comes with a penalty of the higher neutron absorption of steel, although the higher absorption may be mitigated by the use of thinner cladding and increased fuel pellet radius or increased fuel enrichment [35, 69].

To form effective protective chromia films, a high Cr content in the FeCrAl cladding is desired. However, if the Cr content in the FeCrAl cladding is above the α precipitation [108 - 111], it can cause embrittlement of FeCrAl cladding after irradiation at LWR-relevant temperatures [112 - 113]. The investigations on commercial FeCrAl alloys ((≤13 wt% Cr, ≤4 wt% Al) and their variants found that the commercial FeCrAl alloy was resistant to oxidation in air but had poor resistance to high-temperature steam [101]. B136Y alloy (Fe-13Cr-6Al wt%), a variant of FeCrAl alloy developed at Oak Ridge National Laboratory, showed five-fold higher oxidation as compared to APMT FeCrAl alloy (Fe-21Cr-5Al-3Mo wt%) [114]. Other studies were performed for suitable Cr and Al contents in the FeCrAl alloy such that it could have adequate steam oxidation resistance up to ~1500°C [102, 104, 115 - 117] and avoid embrittlement or cracking [86] by minimized susceptibility to irradiation-assisted α formation. In addition, the effects of alloy contents on the melting point and oxidation beyond the melting point have been evaluated [103, 118].

In order to produce the same fission energy density, the use of FeCrAl cladding can require increased fuel enrichments compared to those used with current Zr-based claddings because of the higher neutron absorption of steel [35]. This penalty on uranium enrichment could be mitigated by the use of thin cladding (thinner than current Zircaloy cladding). For instance, in a PWR, the same neutronic performance could be achieved by thinning the cladding to 350 μm and slightly increasing the UO_2 enrichment to 5.06% (as compared to 571.5 μm cladding and 4.9 %

enrichment in a standard Zr cladding design) [119]; or by employing cladding thinner than 300 µm; or increasing fuel enrichment by up to 1.74% [69].

Mechanical and thermal properties (to be provided and discussed in Section 2.2.4) and other behaviors of FeCrAl alloys for the ATF cladding application were examined and provided by References [22, 29, 120 - 127]. FeCrAl alloys have mechanical strength similar or superior to that of Zircaloy, with plastic yielding (ballooning) and perforation characteristics similar or better than Zircaloy [128]. To achieve comparable or better performance of ductility than Zr-based alloys, FeCrAl alloys may be improved by controlling alloy composition and microstructure [128 - 129]. Sufficient ductility of FeCrAl alloys after neutron irradiation could still be retained [108 - 109]. Similar to unirradiated Zr-based cladding, FeCrAl cladding exhibits abundant ductility during rapid pellet cladding mechanical interaction (PCMI) tests [130]. However, additional tests for ductility, including post-LOCA quench tests, are needed for better understanding. Corrosion behavior of the FeCrAl alloys under LWR coolant environments were superior [131]; resistance to the cracking of the FeCrAl alloys under LWR coolant environments is far superior to 304SS/X-750 (materials used in the nuclear power industry) [1]; and performance of FeCrAl alloys did not exhibit a notable dependence on alloy composition [132 - 135].

References [123, 132] reported that no substantial eutectics would form by reaction of the FeCrAl cladding with various reactor-internals materials (SS304H, Inconel718, B_4C) at temperatures below 1500°C [123], or with UO_2 below 1400°C [132]. Reference [107], however, reported interaction between AISI-304 thermocouples and FeCrAl cladding above 1400° C. The contrast of this result with those of Reference [123] may indicate that suppression of eutectic interaction between FeCrAl and stainless steel depends on an oxide layer (present on the cladding of Reference [123] but absent on the thermocouples of Reference [107]); in any case it merits further investigation.

Normal-operation thermal and mechanical behavior of the FeCrAl cladding is expected to be much better than that of current Zr-based cladding; moreover FeCrAl exhibits enhanced oxidation resistance during post critical heat flux (CHF) events and the higher CHF conditions [91, 136 - 137] occurring under heating rates relevant to reactivity-initiated accidents [137].

In comparison, there have not been extensive experimental or even analytic investigations of the performance and behavior of FeCrAl-clad UO_2 pellets fuels under severe accident conditions in which temperatures greatly exceed the 1204°C limit [125, 138 - 139]. LOCA simulation tests on low-strength wrought alloys indicate burst behavior comparable to that of Zr-based cladding [140], while loss of post-quench ductility was not observed [141 - 142]. Adoption of oxide dispersion strengthened FeCrAl variants with higher strength and high-temperature creep resistance [129, 143], due to the dispersion of fine oxide particles [144], is expected to greatly enhance burst margins while preserving oxidation resistance to near its melting point. However, as pointed out in Reference [145], when the melting point of the FeCrAl (~1500°C) is approached (well below the melting temperature of Zr-O alloy (1850°C)), the rate of steam oxidation increases dramatically. Similar behavior with FeCrAl claddings was reported by Reference [107]: melting was observed in the integral test QUENCH-19 around 1500 °C and hydrogen generation also was affected. The products of the steam oxidation of FeCrAl alloys (e.g., Al_2O_3 and Cr_2O_3) will form a solution and have a foamy structure on the surface of the steel compared to the solid and uniform structures of oxide products of steam oxidation of Zr-alloys [145]. In addition, the FeCrAl alloy cladding may drain from the fuel as soon as it melts. This leads to the likelihood of collapse of fuel pellet stacks, a core degradation sequence that differs from that of Zr-alloy cladding [28, 145].

The performance of FeCrAl cladded-UO_2 fuel pellets as an ATF under severe accident conditions was evaluated using accident analysis codes in References [22, 88 - 90, 122, 146 - 148]. Material properties for the FeCrAl obtained from the literature were introduced into these codes by alteration of the thermal properties and oxidation kinetics models of cladding materials.

The cladding temperature and evolution of hydrogen generation due to steam oxidation at temperatures up to 1720 K were simulated using the MAAP code with B136Y alloy (Fe-13Cr-6Al wt%), a variant of FeCrAl alloy [146]. The simulation results are in reasonable agreement with the test results performed at QUENCH-19 test facility. There were also simulations of QUENCH-19 performed [54] that showed inadequacies in the modeling of the oxidation behavior of FeCrAl. Reference [146] also shows that some assumptions are necessary to predict the hydrogen generation observed in the experiment correctly. Both references show the need for further experiments and modeling efforts to minimize uncertainties and enhance the predictability of simulation models, because the oxidation of FeCrAl is strongly dependent on the composition and the progression of the scenario to form oxides[4]. QUENCH-19 has additionally been simulated using AC^2 [149 - 150] and SOCRAT [151] computer codes.

The time to start of core damage and cumulative hydrogen generation were evaluated for FeCrAl cladding using RELAP5-3D [88 - 89] and TRACE [90] codes. A small-LOCA scenario for a typical Westinghouse PWR was simulated with seven sub-variants that differ with respect to the use of various ECCS and other systems [88]. The average time to core damage is about 340 minutes; the average gain in time to core damage is 16 minutes; the average hydrogen generation at the time of core damage is 6.4% (16 minute gain with FeCrAl compared to Zircaloy; H_2 generation with FeCrAl 6.4% of that obtained with Zircaloy) [88]. In comparison, these same figures of merit were predicted as 20 minutes and about 3.7%, respectively, as compared to that with Zircaloy cladding, for ten SBO scenarios for a generic Westinghouse PWR; here the average time to core damage is about 460 minutes [89]. TRACE simulations performed for a short-term- and long-term-SBO, with or without RCIC for the Peach Bottom BWR, estimated marginal increases of the coping times (5-12 minutes), but substantial reduction in the amounts of hydrogen production compared to those with Zircaloy cladding at the time of clad melting [90].

Accident response during SBO conditions in typical LWRs using FeCrAl cladding was also investigated utilizing the MELCOR computer code [22, 105, 122, 147 - 148]. Simulated results showed that the accident progression was slower [122, 147]; the amount of hydrogen generation was reduced [22, 147] due to slower oxidation kinetics with FeCrAl cladding; and the additional time available to restore core cooling and mitigate the accident is on the order of an hour to a few hours [22, 105]. In the simulation of the TMI accident with the actual Zircaloy cladding replaced by FeCrAl cladding of the same thickness (670 µm) [148], the simulation of the modified plant, with much uncertainty in the models, led to a PCT slightly below 1870 K compared to a PCT of ~2500K for Zircaloy, due to oxidation heat being much suppressed by the slower FeCrAl oxidation kinetics.

In addition, the influence of uncertainties in the FeCrAl material properties on the outputs of interest (including fuel centerline temperature, cladding temperature, and fission products release) with FeCrAl cladding was investigated using the BISON code [152]. The results showed that, under normal operation and LOCA conditions, the influence was minimal.

[4] Comments provided by T. Hollands of GRS.

Based on the literature review, a summary of properties, behaviors, and performances of FeCrAl-alloy cladding, as compared to Zr-alloy cladding, is provided in Table 2.11.

Table 2.11 Summary of properties, behaviors and performances of FeCrAl-alloy cladding as compared to Zircoloy-alloy cladding*

Phenomenon/Property	**FeCrAl alloys / APMT (1)**		
	Normal operation & AOOs	**DBAs**	**Severe Accidents**
Thermal-hydraulic Response - Relative heat flux - Average fuel temperature - Coolant temperature	Very similar		
Mechanical strength & ductility			Excellent (designed for high temperature)
- Without irradiation	Superior		
- Under/post- irradiation	Decreased ductility (anticipated) [111, 153]	Unavailable	Unavailable (but no issue anticipated)
- Post- quench		Unavailable	Unavailable
Thermal Properties			
- Thermal Conductivity (W/m·K)	Comparable 11-21 (50-600°C)	10-40 (~70-1500°C) [22]	29 (1200°C) [154]
- Specific heat (kJ/kg·K)	Higher 0.48-0.71 (20-600°C)	0.45-0.8 (~70-1500°C) [22]	0.7 (1220°C) [154]
- Density (kg/m^3)		8000-7300 (~70-1500°C) [22]	
- Melting point (°C)	Lower(2) 1500	Temperature for DBA < 1500°C (melting point)	
- Swelling and Pellet-clad interaction (PCI)		Unavailable	Tests ongoing (as reported in Reference [1] in 2018)
Neutronic behavior - Peaking factors and power levels	Similar		
Chemical compatibility			
- Corrosion			Superior [131]
- Resistance to steam oxidation	Superior	Resistant if T<1500°C	Lost above 1500 °C (melting temperature); critical amounts of Cr and Al needed to establish a protective alumina scale.

Phenomenon/Property	FeCrAl alloys / APMT (1)		
	Normal operation & AOOs	**DBAs**	**Severe Accidents**
- Reduction in Hydrogen generation at the time of core damage		Significant due to highly resistant of FeCrAl to reaction with steam [+](4)	Significant due to much lower kinetics of steam oxidation [105], [+](4)
- Gain in coping time to core damage	N/A	Marginal [+](4)	Marginal [+](4)
- Eutectics formation		No stable eutectics formed by reaction of FeCrAl cladding with the fuel [132]	
Fission product behavior - Fission gas pressure - Fission product retention within cladding	Same except a potential higher concentration of tritium in the coolant (3)	Similar since same fuel material	Expected to be similar since same fuel material(5), but no data available

* Information obtained mainly from [1] unless otherwise noted.

(1) APMT: a commercial FeCrAl, (Fe-21Cr-5Al-3Mo wt%) [114]
(2) Although the melting temperature of FeCrAl alloy (1500°C) is lower than that of a zirconium-based alloy (1849°C), zirconium-based alloys incur autocatalytic oxidation at temperatures above 1200°C, a temperature which is much lower than the melting of FeCrAl cladding.
(3) The use of FeCrAl cladding has a potential risk to result in a higher concentration of tritium in the coolant. However, the tritium release may be minimized by pre-oxidation of the cladding at 1200°C for two hours to form a continuous layer of alpha alumina on the surface. An alumina layer may reduce the hydrogen permeation rate by more than three orders of magnitude [12]. Further studies are needed in this area.
(4) References [22, 88 - 89, 122, 147 - 148]
(5) Also, any expectation of similarity ends for temperatures above 1500° C (FeCrAl melting temperature), for if the FeCrAl cladding melts and drains away, the fuel may very well collapse much earlier than for the case of Zircaloy cladding, possibly leading to substantially different core degradation progression and fission product release.

In summary, the computer simulations performed for severe accidents (SBO and SBLOCA) have shown that the introduction of FeCrAl cladding results in marginal to a few hours of benefit in coping time; however, a significant reduction in hydrogen generation has been reported.

There are two challenges for a FeCrAl alloy cladding system. The first is the increased thermal neutron absorption cross-section of ~4-6% in the FeCrAl alloy cladding relative to ~1% in the current Zr-based cladding, resulting in a reduction in total exposure. To compensate for this absorption, it may require an increase in the pellet enrichment and/or a reduction of cladding thickness and an increase of pellet radius, for cycle lengths comparable to those of the current fuel systems in LWRs.

The second challenge is a potential increase in tritium release into the reactor coolant, as a result of ternary fission in the fuel. Similar to a zirconium-based alloy, FeCrAl does not react with hydrogen to form stable hydrides, resulting in higher permeability of tritium through the cladding to the reactor coolant. Mitigation technologies may be required to minimize this concern and the full impact of increased release needs to be understood.

Although UO_2-FeCrAl cladding has been studied extensively as part of the ATF program, with the aim of quantifying the gains in margins of safety and coping time during severe accident conditions, additional work, including integral fuel bundle oxidation tests up to and beyond its melting point, is necessary.

Some seeming contradictions among the entries of Table 2.11 disappear on closer consideration, or can be dismissed as basically definitional. Therefore, the entry for DBA steam oxidation resistance is not meant to imply that DBAs include such high temperatures. Likewise, refer to the severe accident entries for oxidation resistance versus hydrogen generation and consider that the superior resistance of FeCrAl to steam oxidation may be lost at sufficiently high temperatures because critical amounts of Cr and Al are needed to establish a protective alumina scale; yet at the time of core damage (defined, for example, as a certain amount of core uncovery), significantly less hydrogen may have been generated in the cases of FeCrAl versus Zircaloy cladding.

2.2.3 Silicon Carbide (SiC) and SiC/SiC Composites

High-purity silicon carbide-based ceramics (SiC) and SiC fiber-reinforced SiC matrix composites (SiC/SiC) possess excellent high-temperature strength and exceptional oxidation resistance to high-temperature steam both in DBAs and severe accidents, and low neutron absorption cross-section relative to the Zr-alloys, among other superior physical/chemical properties.

The behavior, properties, and performances of silicon carbide (SiC) and SiC/SiC composites as ATF cladding under normal operation, DBAs, and severe accidents are reviewed in this section. Table 2.12 provides a summary of thermal properties and behaviors of silicon carbide (SiC) and SiC/SiC composites alloys as compared to current Zircoloy-based cladding.

There are two main distinct production paths for SiC/SiC cladding currently being considered. The first is the isothermal chemical vapor infiltrated (CVI) methodology, which results in a silicon carbide matrix that is highly pure, highly crystalline, and therefore highly radiation-stable; with relatively low density (~10-25% porosity) [155 - 157]. The SiC-composite claddings are based on multi-layered structures in all SiC/SiC-composite layers, combined with monolithic chemical vapor deposition (CVD)-SiC layer(s) or a metallic layer. Specifically, they consist of three layers: an inner monolithic layer of SiC, a central composite layer of SiC fibers infiltrated with SiC, and an outer SiC coating. The inner monolith provides strength and hermeticity for the tube, the composite layer adds strength to the monolith while providing a pseudo-ductile failure mode in the hoop direction, and the outer SiC coating protects against corrosion [23, 158]. Total thickness of cladding is about ~690 µm [23].

Table 2.12 Summary of properties, behaviors and performances of SiC/SiC composites cladding as compared to Zircoloy-alloy cladding*

Phenomenon/Property	Silicon carbide (SiC) and SiC/SiC composites	
	Normal operation and AOOs	**DBA & Severe Accidents**
Thermal-hydraulic response - Critical heat flux	Higher [159]	
Mechanical Strength & Ductility		Equivalent or marginal decrease at temperature up to 1500°C [155, 160 - 163]
- Quenching in water up to 2000°C		Maintain their coolable geometry [164 - 165]
- Ductility	Low pseudo-ductility should be assessed	To be investigated
Thermal Properties		
- Thermal Conductivity (W/m·K)	Low and decreases under neutron irradiation	
- Specific heat (kJ/kg·K)		
- Density (kg/m^3)	Low 2.58 (vs. 6.56 for Zr cladding) [119]	
- Melting point (K)	1870 (silica melts) ~3000 (SiC sublimates)	
- Swelling and Pellet-clad interaction (PCI)		
- Irradiation-induced swelling	Increases [162, 166]	
Neutronic behavior - Peaking factors and power levels	Improved	
- Neutron absorption cross-section	Lower compared to Zr-cladding	
Irradiation resistance	Excellent [23]	
Chemical compatibility		
- Corrosion of irradiated due to cracking	To be investigated [23, 167 - 168]	To be investigated
- Resistance to high temperature steam oxidation		Outstanding [25]
- Reduction in Hydrogen generation		2-3 orders lower at 1800°C [169]
- Gain in coping time to core damage		Significant (Days to hours) [169]
- Margin to melting		Favorable over Zr-based claddings
Fission product behavior - Fission product retention within cladding	To be investigated [23, 167 - 168]	To be investigated

* Information obtained mainly from Ref. [1] unless otherwise noted

The second path for production of SiC/SiC cladding involves the nano-infiltration and transient eutectic phase (NITE) process with utilization of hot pressing for production of cladding. This

methodology results in a dense material and therefore, improved mechanical properties and a better hermeticity to fission gas within the elastic deformation domain [170]. A combination of the CVI and NITE techniques for nuclear-grade SiC/SiC production has also been reported [171].

The SiC/SiC-composite layer improves mechanical properties in increasing the tolerance to damage and in preventing a catastrophic failure of the cladding tube. One of the efforts of the studies of SiC/SiC composites is focused on understanding and quantifying the mechanical behavior of SiC/SiC composite tube structures [155, 158, 160 - 161, 163, 172].

Neutron irradiation tests showed that the mechanical behavior, including irradiated swelling, thermal conductivity, elastic modulus, and strength of the high purity SiC ceramics and SiC/SiC composite, do not degrade at LWR-relevant temperatures of 300-800°C within the irradiation level of 30–40 displacement per atom (dpa) applicable for LWR cladding applications [155, 163]. Also, material mechanical properties are also almost time independent, and water quench tests from 1000°C up to 1500°C result in only a small decrease in mechanical properties [23, 161], while hoop stress tests irradiated at PWR coolant and neutronic conditions revealed a 10% to 60% reduction in strength due to mismatched physical properties among the three layers, and corrosion [158].

Chemical compatibility tests indicated no notable interaction between SiC and uranium dioxide below 1200°C [172]. In case of a severe accident, the margin to melting places the SiC/SiC composites in a more favorable position than the zirconium-based alloys claddings, as demonstrated by the tests with SiC where the first liquid phase appeared within the temperature range of 1850-1950 K [172]. Note, the sublimation temperature of SiC is about 3000K, but the melting temperature of silica (i.e., oxide layer present on the surface of the SiC) cladding is about 1870K.

The leak-tightness is an important issue in SiC/SiC design. A fully ceramic SiC-cladding design cannot prevent the micro-cracking of the matrix beyond the elastic limit to the composite, while a metal/ceramic multi-layer SiC/SiC composite cladding, due to the fair ductility of the metal, withstands the strain imposed by the deformation of the composite to improve the leak-tightness. Nevertheless, due to potential mechanical stresses caused by relatively poor thermal conductivity under neutron irradiation in the LWRs normal operating range, early micro-cracking may still occur [1]. Reference [173] investigated techniques to ensure hermeticity in SiC/SiC designs, finding that SiC-based cladding tubes composed of an inner SiC/SiC composite layer coated by an outer SiC overcoat and sealed with a SiC end plug and a SiC-based joint can show robust behavior and survive different loading conditions while maintaining hermeticity.

At high temperature under severe accidents, SiC cladding will rapidly oxidize in steam to form silicon dioxide (SiO_2), combustible gases of H_2 and CO, and other gases (e.g., SiO and $Si(OH)_4$). These gases could contribute to vaporization of the layer of SiO_2 from the surface of SiC and accelerate the kinetics of steam oxidation with the carbide [174 - 177]. In addition, the SiO_2 layer on the inner surface would also attack the fuel at the grain boundaries and lead to fuel liquefaction much as that for Zr-cladding fuel below a temperature sufficient to melt the SiC cladding [174]. SiO_2 cladding may also lead to release of gaseous iodine, relative to iodine in particulate form, to the containment (which will be discussed in Section 2.3.3) [174].

A number of high-temperature steam oxidation and quench tests have been conducted on SiC-based materials to evaluate their performance under severe accident scenarios [167, 169 - 170,

178]. The oxidation tests with SiC specimens prepared by chemical vapor deposition (CVD-SiC) and NITE-SiC showed that at 1700°C steam atmosphere, even though the silica film on the surface is molten at this temperature, oxidation progresses far more slowly than in metallic cladding materials [167]. The oxidation rates of SiC/SiC claddings in steam up to ~1500°C showed ~3 orders of magnitude lower than that for Zircaloy cladding [178]. SiC/SiC claddings can give an additional safety margin, maintaining coolability in steam atmosphere for up to three days at 1600°C and several hours at 1700-1800°C [169].

These tests indicate that due to the superior performance of SiC/SiC composite (coolability, low steam oxidation and consequently low hydrogen generation) under high temperature conditions, SiC-based cladding would significantly increase the fuel margin during LOCAs and provide additional margin for severe accident conditions, and is a promising ATF technology for mitigating severe accidents in LWRs. In addition, using silicon carbide cladding, there is no penalty on uranium enrichment.

Simulations performed for the TMI accident with the actual Zircaloy cladding replaced by SiC cladding of the same thickness (670 µm) showed a PCT slightly below 1830 K, less than the melting temperature of the protective silica scale (~1873 K) [148]. The corrosion of SiC with the control of dissolved hydrogen under PWR-simulating water conditions showed a reduction, by slow formation of the surface oxide layer [23].

Reference [179] is an analytical paper treating PWR cores with silicon carbide cladding. There is little or no emphasis on accidents; instead, the study assesses the neutronic and thermal-hydraulic feasibility of achieving higher power levels and burnups than presently allowed with zirconium-based cladding, via the use of silicon carbide cladding. The thermo-mechanical behavior of the SiC-clad fuel rods was estimated using FRAPCON, a steady-state fuel performance analysis computer code developed by the Pacific Northwest National Laboratory under NRC-sponsorship. For 18-month cycles, the use of SiC clad cores reduces fuel cost due primarily to reduced neutron capture in the carbide compared to zirconium-based alloy. As the number of assemblies loaded is reduced to achieve higher discharge burnups, this advantage increases, reaching almost twelve million dollars per cycle (about ten percent) when assemblies are loaded so as to achieve a discharge burnup of about 80 MWd/kgU. This burnup level is projected to be quite feasible with SiC. Furthermore, the savings is large enough so it would not be offset by any reasonable fabrication cost increase due to use of silicon carbide [179].

There are two key feasibility issues that need to be addressed for the LWR application [1, 91, 180 - 181]. One is hydrothermal corrosion of SiC (SiC dissolution in aqueous environments). The other is fuel cladding failure due to micro-cracking during normal operating conditions and the resulting diminished fission products retention capability of ceramic composites. Different fuel/cladding differential thermal expansion of ATF/SiC-clad combinations, relative to UO_2/Zr, and lower SiC ductility, likely increase the cracking challenge to SiC, relative to Zr, in normal operations and in transients[5]. These issues require further examination in the course of the technology development.

2.2.4 Thermophysical Properties, Oxidation Rate Constants and Mechanical Properties for Cr, FeCrAl and SiC Cladding Material

[5] Comment by T. Hollands of GRS.

The data obtained for thermal physical properties, parabolic oxidation rate kinetics and mechanical properties for Cr (used as a coating on the surface of Zr-based claddings), FeCrAl (used as a ATF cladding) and SiC (used as SiC fiber-reinforced SiC matrix composites) materials are summarized in this section.

2.2.4.1 Coated and Improved Zr-Based Cladding

Except for the limited results summarized below, the present literature review did not identify any data and/or correlations for coated and improved Zr-based cladding applicable to severe accidents. The only correlations that were identified relate to the thermal conductivity, specific heat, thermal expansion coefficient and thermal creep as functions of temperature over the temperature range of 300K to 1300K [120], which does not cover the severe accident range.

A datum narrowly considerable as belonging to the severe accident temperature range is the Cr/Zr eutectic temperature, 1603K [98].

A phenomenon belonging to the severe accident temperature range is the marked increase in the rate of steam oxidation, observed, for example, by Reference [100] beginning above ~1670K during a LOCA test. This burst is probably in accord with the oxidation rate correlation given by Reference [90]. Reference [90] provides the oxidation reaction rate k(T) for Cr-coated cladding that is of the form:

$$k\,(T) = 2Ae^{-c/T} \tag{1}$$

Here T is the temperature in Kelvin, and the unit of k is kg^2_metal/(m^4·s). This oxidation rate coefficient is defined in terms of the cumulative mass per unit surface area of metal consumed during the accrued time of the reaction. (MELCOR, for example, uses this definition and this unit.) Alternatively, the factor 2*A* can be replaced by a factor *a* via this relation:

$$a = 2A \times \left(\frac{MW_{clad}}{MW_{O2}} \times \frac{1}{\rho_{clad}}\right)^2 \tag{2}$$

to yield a rate coefficient defined in terms of the thickness of the layer that has undergone reaction (here the unit of k is m^2·/s). Also, for either form, different authors make different choices for kg vs. g and m vs. cm, and some authors consider the square root of k. Table 2.13 provides the constants for various cladding materials. Note, 2*A*, *a*, and c are as defined by Equations (1) and (2). Numerical data in Table 2.13 are as appear in Reference [90]. The various original data sources appear in the table's bottom row, and also are as given by Reference [90]. The step changes defined (in the case of Cr coating) to occur at 1600K for both *c* and either of 2*A* or *a* result in a ~100-fold increase of the oxidation rate as the temperature increases through that value.

In addition, Reference [89] provides the steam oxidation rate constants for Cr-coated cladding in the form of Arrhenius (see Figure 1 of Reference [89]). In contrast to the correlation of Reference [90], it shows no notable feature at 1000/1600 = 0.625. References [182 - 183] provide more information on steam oxidation of Cr-coated zirconium alloys.

Table 2.13 Oxidation models used for Zircaloy, FeCrAl and Cr-coated cladding material [90]

Property/Parameter	Cladding Type			
	Zircaloy	**FeCrAl (ORNL) Alloy B136Y**	**FeCrAl (MIT) Alloy B136Y**	**Cr-Coating**
Density (kg/m^3)	6500	6860	6860	7190
Molar mass (g/mol)	91.224	52.540	52.540	51.996
Activation energy of Oxidation (kJ/mol)	150	334	334	280
$a\left(\frac{m^2 \cdot metal}{s}\right)$	6.9889E-06	6.5883E - 05, T < 1773 K 138.6411, T > 1773 K	5.5113E-17, T < 1473 K 8.6996E-05, 1473 K < T < 1648 K 138.6411, T > 1648 K	1.50776E-04 T < 1600 K 3.4944E-06, T > 1600 K
-c (K)	-20100.7	-41375.9923, T < 1773 K -42400.0, T > 1773 K	0.0, T < 1473 K -41376.0, 1473 K < T < 1648 K -42400.0, T > 1648 K	-33678.1, T < 1600 K -20100.7, T > 1600 K
$2A\left(\frac{g^2 \cdot metal}{cm^4 \cdot s}\right)$	0.3633	11.5012, T < 1773 K 2.4202E + 07, T > 1773 K	9.6210E-12, T < 1473 K 15.1816, 1473 K < T < 1648 K 2.4202E+7, T > 1648 K	29.5223, T < 1600 K 0.6842, T > 1600 K
Heat of oxidation reaction (MJ/kg)	6.45	12.47	12.47	12.47, T < 1600 K 9.46, T > 1600 K
Failure temperature (K)	2800	1804	2800	2800
Oxidation model source	Cathcart-Pawel model [184 - 185]	Empirical model [86, 101, 114]	Empirical model developed by MIT [186]	Kim Hyun Gil's data [24]

The only relevant mechanical property that was identified is the yield stress of chromium, provided by Reference [120] as a correlation in temperature over the range of 300 K to 1500 K.

2.2.4.2 Advanced Steel Cladding Material

Table 2.14 lists the thermophysical properties of FeCrAl cladding material from various sources. Note that some of values provided in the references do not include the applicable temperature or range of temperatures.

Reference [120] provides the thermal conductivity, specific heat, thermal expansion, and thermal creep as functions of temperature for FeCrAl, applicable over a temperature range of 300 K to 1500 K. Reference [125] provides the thermal and irradiation creep for FeCrAl as follows :

$$\epsilon = 2.89 \times 10^{-36}\sigma^{5.5} exp\left(-\frac{29709}{T}\right) \text{ for T} < 873.15 \text{ K} \quad (3)$$

Table 2.14 Thermal physical properties of FeCrAl

Thermophysical Properties	**FeCrAl [22]**	**FeCrAl Oxide [22]**	**FeCrAl (75 Fe, 20 Cr, 5 Al, wt%) [119]**	**FeCrAl [122]**	**FeCrAl Oxide [122]**	**FeCrAl (Fe with 0-16wt% Cr and 5-8wt% Al) [125]**	**FeCrAl [145]**
Thermal conductivity (W/m·K)	10-40 (at 70-1500 °C)				4	29 (at 1473 K)	
Specific heat (kJ/kg·K)	0.45-0.8 (at 70-1500 °C)				0.9	0.7 (at 1493 K)	
Density (kg/m^3)	8000-7300 (at 70-1500 °C)		7100		5180		
Melting point (K)	1773.0	1870		1804		1798-1813	
Latent heat fusion(kJ/kg)	268	598		275	664		
Eutectic temperature (K)							~2123 for Al_2O_3-UO_2

While for T> 873.15 K, the following correlation proposed by [187] is noted:

$$\epsilon = 5.96 \times 10^{-27}\sigma^{5.5} exp\left(-\frac{47136}{T}\right) \quad (4)$$

Where ε is the creep rate in s^{-1}, σ the effective (Mises) stress in Pa, and *T* is the temperature in K. An irradiation creep law suggested by [188] is considered applicable to all FeCrAl alloys. The coefficient recommended for irradiation creep is 5 x 10^{-6} per MPa per dpa. Utilizing the following conversion factor: 1×10^{25} n/m^2 = 0.9 dpa as suggested by [108], a correlation for irradiation creep can be derived:

$$\epsilon = 4.5 \times 10^{-31}\sigma\phi \quad (5)$$

Where σ is the effective stress in MPa and ϕ is the fast neutron flux in n/m^2-s.

The thermo-physical properties as function of temperature (density, specific heat, thermal conductivity, volumetric heat, thermal expansion) and melting temperature for FeCrAl, along with several other materials, are shown in Figure 2-1 of Reference [22].

Thermo-physical properties (enthalpy, specific heat, thermal conductivity, and density as functions of temperature, and melting temperature, latent heat of fusion) for both FeCrAl and FeCrAl Oxide are shown in Figures 13 through 18 of Reference [147].

Additional material properties can be found in Reference [125] for FeCrAl cladding material, including the parabolic rate constants.

Reference [90] provides two alternative correlations ("FeCrAl (ORNL)" and "FeCrAl (MIT)", with FeCrAl (MIT) being a conservative model and FeCrAl-ORNL being a non-conservative model) for the oxidation coefficient of FeCrAl, see Table 2.13. Both are stated to apply to the FeCrAl alloy known as B136Y [90]. Note again the relation between the constants "2A" and "a":

$$\mathrm{a} = 2\mathrm{A} \times \left(\frac{\mathrm{MW_{clad}}}{\mathrm{MW_{O2}}} \times \frac{1}{\rho_{\mathrm{clad}}}\right)^2 \tag{6}$$

The molecular weight and density of the cladding, required in Equation (6), are listed in Table 2.13 in Section 2.2.4.1, as reproduced from Reference [90].

References [122 - 123] provide for the FeCrAl alloy known as APMT another correlation for the oxidation rate constant K(T) with respect to the metal reacted (kg^2 /(m^4 s)):

$$K(T) = \left(230.0\,\frac{kg^2 metal}{m^4 s}\right) \times exp\left(\frac{-41376.0\ K}{T}\right) \qquad T < 1773\ K \tag{7}$$

$$K(T) = \left(2.42\ x\ 10^9\,\frac{kg^2 metal}{m^4 s}\right) \times exp\left(\frac{-42400\ K}{T}\right) \qquad T \geq 1773\ K \tag{8}$$

Equation (8) is identical to the parabolic coefficient for steam oxidation of stainless steel as defined in MELCOR for use at all temperatures. Recent versions of MELCOR include FeCrAl and also treat its oxidation according to Equation (8) for the stated temperatures, while for T < 1748K an equation similar to Equation (7) is applied: the leading factor is 4360.0 kg^2/(m^4 s) while the factor in the exponent is -41376.0K as in Equation (7). References [122 - 123] are published by ORNL, but the "ORNL model" defined by Reference [90] (Table 2.13) does not agree[6] with Equation (7). The reason is not known.

Reference [148] provides one more parabolic rate coefficient for steam reaction with FeCrAl:

$$K(T) = (0.5213\ kg^2\text{-FeCrAl} / m^4\text{-s})\ exp[(-260\ kJ/mol)/RT] \tag{9}$$

Note that the form of the correlation given by Reference [148], relative to ones quoted above, has a factor of the universal gas constant inserted into the denominator of the exponential. After discussing an ambiguity concerning the heat of reaction, [148] defines the reaction heat on the assumption that the heat of steam oxidation of the three metals should be added with the mole

[6] But for T>1773 K, the "ORNL model" of Reference [90] is the same as Eq. (8) which is given by Reference [123]. By either correlation, the oxidation rate is much slower for T<1773 K than for T>1773 K.

fraction weights of the alloy. Reference [148], considering the alloy of FeCrAl referred to as AMPT (i.e., 69% Fe, 21.6% Cr, 4.9% Al), thus obtains a value of 1.278 MJ/(kg-FeCrAl), at 298 K.

Reference [54] is also a source for information on the oxidation of FeCrAl, but the temperature dependence of the rate coefficient is not addressed.

Figure 2 of Reference [91] shows the oxidation rates as functions of temperature for the oxides of various materials considered for cladding, including FeCrAl and Al_2O_3. For the original measurements, Reference [91] cites the data of References [86, 184, 189]. It is noted that the curve in that figure for FeCrAl agrees with Eq. (8) within ~20%.

Correlations for oxidation rates have been quoted in this report without indication of their ranges of validity, as these ranges have generally not been given by the cited sources. Possibly Figure 2 of Reference [91] implies these validity ranges via the ranges over which the various curves are shown, but this issue has not been examined critically. For example, for the FeCrAl correlation, the cited figure would indicate an upper temperature of about 1750K.

2.2.4.3 Silicon Carbide (SiC) and SiC/SiC Composites

The figure appearing as Figure 2.1 in Reference [22] provides several SiC properties, including density, specific heat, thermal conductivity, and melting temperature. The thermal diffusivity as function of temperature of SiC is shown in Figure 7 of Reference [173]. Figure 2 of Reference [91] shows the parabolic oxidation rate constant as function of temperature for SiC and various other cladding materials. Reference [54] is another source for information on the steam oxidation of SiC, including an account of how the oxide layer undergoes further reaction with the steam. The only mechanical property that was identified is for ultimate hoop stress as listed in Reference [23] for SiC as 282 MPa without a corresponding temperature at which it was measured.

As with other continuous fiber-reinforced ceramic matrix composites, SiC/SiC is considered a damage-tolerant ceramic material [190]. This damage tolerance feature is enabled by the deflection and branching of microcracks at the fiber/matrix interfaces and the frictional energy dissipation at the de-bonded interfaces while the reinforcing fibers are bridging the matrix cracks. Hence, microcracking is the mechanism for damage tolerance in ceramic matrix composites, and the primary failure mode for the ceramic fuel cladding incorporating SiC/SiC is the progressive and interconnected microcracking leading to release of gaseous fission products. This leads to a probabilistic treatment of cladding failure. Reference [190] gives correlations for the associated probability distributions.

2.3 Fission Product Release Characteristics of ATF Concepts

2.3 1 Fission Product Release Aspects of Doped Fuel

The effects of Cr doping of UO_2 fuel on fission product (FP) release may be small enough to neglect in the first approximation. This appears to be the suggestion of Reference [2]. Reference [1] has some remarks about doping with BeO and Mo, and the resulting effects on FP release. Concerning doping with BeO, Reference [1] reported that the BeO dopant has no significant influence on the fission gas release under a range of burn-ups (Reference [1] cites [191]). Concerning doping with Mo, Reference [1] reported that very low levels of fission gas release

were measured (< 0.4%) in UO_2-80vol%.-Mo fuel pellets irradiated by CEA in an MTR for up to 125 GWd/MTU.

See Table 2.2 where, citing Reference [4], Reference [1] considered it established that, at least in normal operation and in AOOs, the fission product behavior (including fission gas pressure and fission product retention) of UO_2 fuel is improved by Cr_2O_3- or Al_2O_3-Cr_2O_3 doping, due to the increased intragranular fission gas retention capability of doped fuel [4]. In DBAs and DBDAs, Reference [1] conjectured a fission gas release (FGR) decrease but noted the lack of data. Reference [8] advocates the contrasting view that differences between the fission product release character of doped- versus un-doped UO_2 fuels are likely insignificant[7]. The irradiation test in Halden reactor suggest that for steady-state power conditions (wherein the powers remain nearly unchanged for several days at a time), the release is similar for doped and standard UO_2 fuels at similar measured fuel temperatures [8, 192]. The Halden Reactor Project has irradiated Al_2O_3-Cr_2O_3 doped UO_2 in two test rods (Rods 1 and 5) and a UO_2 test rod (Rod 6) in the same experimental rig at similar operating powers to provide differences in behavior for these two fuel types. The rod powers remained between 35 to 45 kW/m with most of the FGR occurring above 40 kW/m based on the continuous rod pressure measurements during the test irradiation. The rod puncture data for Rods 5 and 6 demonstrated that the FGR of Rod 5 (doped; 16%) was slightly lower than that of Rod 6 (standard UO_2 ; 19%). However, the measured maximum fuel temperatures were slightly higher (30 to 50°C) in Rod 6 than Rod 5 when release was experienced which may explain the small difference in FGR. The situation may be different in the case of power-ramped and bumped rods. Fission gas release data under these conditions at ~30 GWd/MTU burnup [193] suggest that FGR is 30% to 50% lower for doped fuel than for standard UO_2 fuel, but again uncertainties arise because the hold times for the power ramps were significantly less for the doped fuel (7.7 hours) versus the standard UO_2 fuel (12 hours). FGR increases with increasing hold time at the terminal power (particularly for hold times less than 12 hours) such that the FGR difference between the two fuel types would be less if the hold times were the same. Power ramps are more typical of what can be experienced during AOO events. Additional power-ramped FGR data provided by Reference [4] demonstrate that doped fuel has reduced FGR relative to standard UO_2, such that at higher ramped powers (~50 kW/m) there is a 50% reduction in FGR at moderate burnups. No details such as hold times or other information were provided for the data of Reference [4].

Based on the above findings it is seen that there is conflicting evidence about the effect of doping on the FGR behavior. The conflicts may arise in the different FGR mechanisms that apply in steady-state operation versus during power/temperature transients (AOOs), with the former being due to diffusion and the latter mainly due to release from grain boundaries. The fission gas diffusion coefficient is known to be higher for doped fuel but the diffusion length to the grain boundary is longer, such that these two mechanisms counterbalance each other resulting in similar release for steady-state conditions as observed in the Halden tests [8, 192]. The release due to power/temperature transients is believed to be from the gas on the grain boundaries, with large-grain doped fuel having less grain boundary area per unit volume of fuel than standard UO_2 , such that less gas exists on grain boundaries in doped fuel.

Finally it should be noted that the above discussion applies only to burnups up to 55 GWd/MTU. The FGR behavior may not be the same at higher burnups because the fuel matrix can hold only

[7] Comment by C. Beyer.

a limited amount of gas such that it does not increase with increasing burnup: beyond some point, additional gas either goes to the intra-grain bubbles, the grain boundaries, or is released. This is one of the reasons why FGR is observed to increase with increasing burnup at a constant fuel temperature. Therefore, FGR data are needed for doped fuel up to the future high burnup levels, for normal operation, AOOs, DBAs, and severe accidents.

A paper published under the auspices of CASL [3] advocates the BISON fuel performance code as sufficiently sophisticated and benchmarked to predict FP release of ATFs. (CASL – the Consortium for Advanced Simulation of Light Water Reactors – is a DOE organization. The paper states that in 2018, CASL took over further ATF work in BISON in support of the NRC engagement.) The BISON model has been used to calculate the fission gas transport from within the fuel grains to the grain boundaries in the case of Cr_2O_3-doped UO_2 fuel (see Reference [3], PDF page 11 of 52). Although the given results appear to be more in the nature of a model status report than a definitive study, the model itself is described in some detail. This quote mentions some of the physics: “The BISON model was originally developed for pure UO_2 and has been extended to account for the specificities of Cr_2O_3-doped UO_2 in the present work. Specificities include (1) the effect of a larger grain size and (2) an enhanced diffusivity of gas atoms in the lattice due to the dopant. The grain size affects the fission gas behavior in two ways, i.e., (i) increasing the average diffusion distance for gas atoms in the grains, which reduces the rate of gas transport to the grain boundaries and ultimately FGR and (ii) reducing the grain surface to volume ratio, hence the capacity of the grain faces to store fission gas. Both of these effects are considered naturally in the BISON fission gas model, as it directly describes the grain radius dependent intra-granular and grain-boundary processes. To this end, in BISON the fission gas behavior model is coupled to the grain growth model.” Among the provided results, the one reproduced in Figure 2.1 is typical.

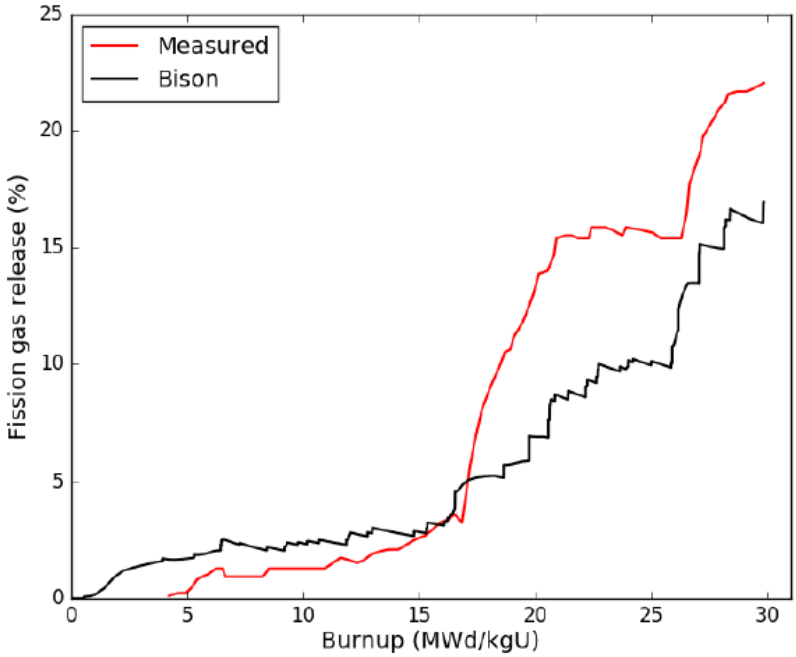

Figure 2.1 BISON-predicted and measured FP gas release [3]

Figure 2.1 pertains to a fuel rod containing UO_2 doped to 900 ppm of Cr_2O_3 and 200 ppm of Al_2O_3. It reflects normal operations at fairly low burnup, showing approximate equivalence of doped vs.

undoped fuel. However, there is an expectation of lower fission gas release during normal operations and power ramps for doped fuel at burnups past 30 MWd/kgU[8]. Other results apply to another five rods of various but similar design. Actual rods were irradiated in a Halden test, leading to Figure 2.1 which shows the BISON predictions as compared to the measurements.

2.3 2 Fission Product Release Aspects of High-Density Fuel

The BISON code, mentioned in Section 2.3.1, has also been used to predict FP release from U_3Si_2 fuel (see Reference [3], PDF page 25 of 52). The authors remark that "these simulations are to the authors' knowledge, the first validation of U_3Si_2 fuel performance models. The experiments were designed to investigate the low-burnup behavior." Reference [194] is cited for the experimental work. The fuel is U_3Si_2 fuel enriched to 5.44wt% U-235. The reported results are less detailed than those like the one reproduced above for doped UO_2. In two experiments, the burnup was 17.1 MWd/kgU in one case and 19.6 MWd/kgU in the other; the experimental fission gas release was 0.06% in both cases. The BISON prediction is consistent with the experiment, but the error bands (± 2 σ uncertainty analysis) are very broad, being 0 to 1.4% in one case or 0 to 0.9% in another case (these cases being distinguished by alternative treatments in the model).

2.3.3 Impact of the ATF Cladding on Fission Product Release:

There have not been extensive experimental and analytic studies of the impact of ATF cladding on the fission product release under severe accident conditions. The very limited studies indicated that for the case of FeCrAl alloy cladding with UO_2 pellets fuels, there is a potential risk to result in a higher concentration of tritium in the coolant. FeCrAl does not react with hydrogen to form stable hydrides similarly to a zirconium-based alloy, resulting in higher permeability of tritium through the cladding to the reactor coolant [1, 91]. The tritium release may be minimized by pre-oxidation of the cladding at 1200°C for two hours, which will form a continuous layer of alpha alumina on the surface. An alumina layer may reduce the hydrogen permeation rate by more than three orders of magnitude [12]. A study of FeCrAl oxidation in air indicated that an alumina barrier layer on the cladding's inner surface, thickness of oxides 0-50 nm, formed only after 100 hours exposures at 300-600°C; crystalline alumina formed only at the highest temperature [195]. Mitigation technologies may be required to minimize this concern and further studies are needed in this area.

Another presumed issue for FeCrAl cladding is unoxidized aluminum in the core debris produced by the degradation of FeCrAl clad during severe accidents, leading to sub-stoichiometric composition of the uranium fuel, which could affect the chemistry of fission products and the stratification of the phases of molten core debris [145].

This literature review yielded no significant information on the question of any fission product release characteristics that may be attributable specifically to the coating of coated-Zircaloy cladding designs.
In the case of SiC/SiC composites cladding, there is a key feasibility issue among others that need to be addressed for the LWR application. The SiC-composite claddings are based on multi-layered structures in all SiC/SiC-composite layers, combined with monolithic chemical vapor deposition (CVD)-SiC layer(s) or a metallic layer. Because the isothermal chemical vapor infiltrated (CVI)-processed SiC/SiC-composite does not have enough gas hermeticity, the

[8] Comment by J. Corson.

monolithic CVD-SiC or metallic layer provides a primary retention of fission products [1]. In the case of fuel cladding failure due to micro-cracking during normal operating conditions, this results in diminished fission products retention capability of ceramic composites. This issue requires further examination in the course of the technology development.

In addition to the oxidation and cracking of the outside of the cladding, there will be internal oxidation of the cladding at the elevated temperatures under severe accident conditions. An oxygen partial pressure develops over the uranium dioxide fuel made hyper-stoichiometric by the fission process. This oxygen partial pressure will be sufficient to react with the inner surface of the cladding to form a silicon dioxide layer. Molten silicon dioxide is not miscible with uranium dioxide. Reactions with metal oxide fission products will lead to the formation of silicates on the inner surface which will attack fuel at grain boundaries and lead to fuel liquefaction much as that for zirconium-clad fuel, well before the external oxidation penetrates the cladding and before temperatures sufficient to melt the silicon carbide cladding are reached. Silicon dioxide formed on the inner surfaces of the cladding will be quite a good absorber of fission products such as cesium, rubidium, strontium, and barium [174].

During a severe accident, the silicon dioxide product of clad oxidation will trap at least temporarily fission products such as cesium and barium. It will not react strongly with iodine. Silicon carbide cladding may lead to an accident source term to the containment. Boric acid from steam oxidation of boron carbide may tie up the cesium and other metal oxides or hydroxides so that there is nothing to bind with iodine. Consequently, a very large fraction of the iodine released to the containment may be in gaseous form rather than in the form of aerosol particles. Thus we would expect a weaker interaction of the silicon dioxide with tellurium released from the fuel. Without more quantitative analysis, it is hard to estimate how silicon carbide cladding might affect the late in-vessel source term. Cesium may be trapped as a cesium silicate (probably $Cs_2Si_4O_9$) and can further decompose to CsOH in continued steam flow. Similar arguments can be made for barium revaporization from the silicate. One expects less effect on the revaporization of tellurium deposited in the reactor coolant system. Little retention in the RCS of released iodine is expected because it will not be able to react to form particulate species such as CsI. It will be released and remain largely in gaseous form until it reaches the reactor containment [174].

Reference [196] is an analytical paper devoted to modeling the behavior of SiC cladding during severe accidents, including fission product release. For mechanical rupture of the SiC tube, the Larsen-Miller approach is reviewed and an attempt is made to evaluate the parameters applicable to SiC, but the lack of experimental data prevents a very definitive conclusion. For fission product release, the diffusion of a fission product atom through the intact cladding wall is calculated, with consideration of thinning of the wall at high temperatures. As an example, at 2500 K the fraction of Cs released through a 0.25 mm thick SiC wall is calculated to reach 3% at 2×10^5 seconds.

The new cladding materials of ATF designs may have an impact on reactivity and on RIAs[9]. ATF cladding materials will yield different neutronic characteristics than the present zirconium-based cladding alloys, due to different cladding material properties, reactor physics, and thermal hydraulics characteristics [197]. Differences in reactor physics are driven by the fundamental properties (e.g., neutron absorption cross section in iron for an iron-based cladding) and also by design modifications necessitated by the candidate cladding materials (e.g., a larger fuel pellet to

[9] RIAs per se are beyond the scope of this review; however, some discussions are included for completeness and any potential implications under severe accidents.

compensate for parasitic absorption). Reference [197] reports simulations of a RIA in a representative PWR with both FeCrAl and SiC/SiC cladding materials. The study shows similar RIA neutronic behavior for SiC/SiC cladding configurations versus reference Zircaloy cladding. However, the FeCrAl cladding response indicates similar energy deposition but with shorter pulses of higher magnitude. This is due to the shorter neutron generation time of the core models based on FeCrAl cladding. The FeCrAl-based cases exhibit a more rapid fuel thermal expansion rate than other cases, and the resultant pellet-cladding interaction may occur more rapidly. (Material freely quoted from Reference [197]).

2.4 Summary

This literature review has collected a body of information that can be applied to identifying the phenomena likely to influence the behavior of ATF designs during severe accidents. It is to be noted, though, that such applications must be predominately inferential. That is, little or none of the literature refers in any essential way directly to severe accidents. Therefore, to varying degrees the application of the collected information will involve going beyond the stated subject matters. It can be remarked that the collected literature is especially lacking in experimental studies indicating how severe accident fission product releases from ATFs may differ from those of conventional LWR fuels. Nonetheless, substantial studies have been performed over the last several years that provide considerable information on the thermophysical aspects of ATF concepts that may be utilized for performance of sensitivity studies, using severe accident codes (e.g., MELCOR) to identify the most important phenomenological issues that will be listed as part of the PIRT development process in Section 4, which may have a marked influence on cladding behavior, core damage progression, and radionuclide release behavior.

ATF concepts involving coated cladding, doped fuel pellets and steel cladding designs are considered to be nearer with respect to the time to commercial deployment. Silicon carbide cladding, uranium silicide fuel pellets, microencapsulated fuels, fuels other than uranium oxide, or any of several other advanced concepts are considered for longer-term deployment. These ATF designs represent evolutions and deviations from the Zircaloy clad, uranium dioxide fuel forms.

The results of several severe accident simulations have been quoted throughout Sections 2.1 and 2.2. Within considerable variation, they tend to confirm a widely held impression that ATF designs typically afford a modest increase in coping time, and a substantial reduction of hydrogen generation, at least until very late times. However, the available literature do not any significant studies addressing fuel damage progression and fission product release characteristics as compared with existing fuel and cladding designs.

3. REVIEW OF LITERATURE RELATED TO THE IMPACT OF FUEL ENRICHMENT AND BURNUP APPLICABLE TO SEVERE ACCIDENTS

The literature search resulted in 24 documents/paper related to fuel high enrichment (including HALEU) and/or burnup. Of these 24 documents/reports, 18 were found to be not relevant for the purposes of this study. Moreover, none of the 24 documents/papers bear significantly on the impact of fuel enrichment on severe accidents. Rather than extend the literature search at this time, it is decided to review the few applicable papers that are available while accepting the indication that, with respect to the impacts on severe accidents, the literature on high fuel enrichment and burnup is indeed very terse.

3.1 Impact of Enrichment

Among the identified papers/documents in the literature on HALEU, the topics that are typically covered relate to how HALEU will be supplied for research and development (e.g., by repossessing spent fuel from the Experimental Breeder Reactor II [198]; how it will be supplied commercially (e.g., by a new generation of centrifuge plants [199]); economic projections of future demand for HALEU [200], among other aspects. Therefore, at this time, the search has been limited to the available literature, even though, it is possible that other relevant studies may have been performed that have not been published in the open literature.

3.2 Impact of Burnup

The formation of the so-called high burnup structure (HBS) [201 - 203] is the only specific phenomenon identified by this literature search that, peculiar to fuels irradiated to high burnups, appears to induce different severe accident behaviors between future high-burnup fuels versus the traditional fuel burnup levels at the operating plants. As is discussed further below, HBS formation requires local burnup greater than ~55 GWd/MTU and irradiation temperature less than ~1100 °C. The HBS occurs around the rim of the UO_2 pellet, being an annular ring of typical thickness of 100–200 μm, characterized by fine subdivision of the grains and redistribution of fission gases into micron-sized closed pores [201]. It is expected that a much greater contingent of the loadings of future high-burnup fuels will be affected by HBS.

The authors of Reference [204] subjected irradiated and unirradiated rods to simulated LOCA conditions. The irradiated rods were taken from the Limerick BWR where they had been burned to a pellet-average burnup of 56 GWd/MTU. The direct comparison of the behavior under severe accident conditions of highly irradiated versus unirradiated fuel is particularly helpful for the present purpose, though of course the best comparison would be between burnups typical of the end of cycles of traditional versus future fuel designs. The authors of Reference [204] do not refer to HBS, but the burnup condition for HBS formation was most likely attained. (That is, local burnups likely exceeded ~55 GWd/MTU since the local burnup at the relatively cold outer rim of the fuel pellet, which is where the HBS forms, is 2–3 times higher than the average pellet burnup [201]. This result from Reference [201] does depend, however, on the burnup.) The paper provides information on the mechanical failure of the rods; on oxidation; but not on release of fission products.

The differences found by Reference [204] between the behaviors of irradiated versus unirradiated rods do not appear very striking. In the simulation of the LOCA, which included holding the rods

at 1204 °C for five minutes, then quenching them, irradiated and unirradiated rods burst at similar temperatures (730 to 790 °C). Both types showed two-sided oxidation in the ballooned and burst region. A difference was found for the shape of the burst: oval for irradiated rods, “dog bone” for unirradiated rods. The major post-LOCA difference observed between high-burnup rods and unirradiated rods was the degree and location of secondary hydriding in the balloon neck region. For nonirradiated specimens, the hydrogen pickup was low in the burst region but high elsewhere, 70-90 mm above and below the burst mid-plane. For high-burnup fuel cladding, the hydrogen peak was toward the burst mid-plane.

Three other papers reviewed here specifically discuss HBS. They give some information on fission product release, but emphasis on severe accidents is mostly or totally lacking. Reference [201] describes ~25 years of research on HBS. A conclusion of this paper is that the HBS likely will not compromise the safety of nuclear fuel during the normal operations of the longer cycles that are now being considered. However, since the paper does not consider severe accidents, any role played in severe accidents by HBS is not made completely clear by these conclusions. In fact, there are concerns about HBS in some DBAs. It has been posited that the HBS could fracture during RIAs, leading to significant transient fission gas release that could increase the probability of fuel rod failure and increase the source term in the event of rod failure. It is for this reason that NRC added a transient FGR table to the draft update to RG 1.183 to be used for RIA source term calculations. There is also the potential for the HBS to fracture in other scenarios where significant stresses or temperature changes may occur (e.g., following a LOCA)[10]. NUREG-2121 provides some information about the relationship between the rim structure and fuel fragmentation Reference [205]. Moreover, it is important to distinguish possible negative impacts of high burnup from those of HBS: the findings of Reference [201] that HBS will be un-problematic need not mean that all other aspects of high burnup are without issue. Thus, the authors write “measurements of fission gas release both in-pile and after fuel rod discharge do indicate an increase of the fraction of gas released with increasing burnup. However, it is now generally agreed that this release does not originate from the HBS, but rather from higher temperature regions towards the axial center of the fuel pellet, where temperature effects allow interconnection among intergranular fission gas bubbles and the opening of pathways for fission gas release along the grain boundaries." Any increase of fission gas, or unfavorable change of its chemical and isotopic composition, with increasing burnup beyond the current license limit, whether related to HBS or not, needs further study for the present purposes; however, the subject is not well-represented in the literature.

The following discussions freely paraphrase or quote from the relatively recent paper [201]. From the earlier papers [202 - 203] a few graphs are reproduced herein.

HBS “is characterized by grain subdivision and redistribution of fission gases and extended defects. The original grains, with a typical size of around 10 μm, subdivide by a factor of ~10^4 into sub-micron grains with a size of about 0.1–0.3 μm. The fission gas is removed from the fuel matrix and is retained in a high concentration of micron-sized intergranular closed pores; reported values for the porosity fraction in the HBS can exceed 20%. The microstructure of the subdivided grains appears free of extended defects.” The removal of fission gas from the fuel matrix, and its retention in the micron-sized intergranular closed pores that are part of the HBS, appears to be viewed by the authors as beneficial. Thus the paper states “the restructuring process does not cause the release of the fission gas out of the fuel pellet. From the operational point of view, this

[10] Comment and information provided by J. Corson.

is clearly a positive feature of the HBS." Another benefit is that HBS enhances the fuel rod thermal conductivity by removing crystal defects. The pressure inside the pores is calculated to be as high as 45 MPa, but this seems to be regarded as not a problem, i.e., by Reference [201] and the other cited papers in consideration of conditions not too different from those of normal operations.

Note that this view may change when severe accident conditions are considered. Significant release is possible for DBAs and severe accidents when HBS is raised significantly above the low irradiation temperatures of the HBS during normal operation. The gas releases begin anywhere from 200 to 400K above normal operational temperatures as demonstrated in the literature, as further discussed below. As Reference [201] has noted, it has also been observed that the bubbles/porosity in the restructured HBS are under very high pressure that may cause fuel fracturing when heated above the normal low in-reactor temperatures of the HBS. This phenomenon has been observed by experimenters heating irradiated discs with the HBS above the irradiation temperature in the measurement of thermal conductivity at various temperatures. The experimenters have described the HBS conductivity disc samples as exploding into pieces making it difficult to retrieve the fractured sample pieces. This could be a mechanism for fuel dispersal during DBAs and severe accidents when the HBS achieves temperatures 200 to 400K above the HBS normal irradiation temperatures[11]. This fuel fragmentation and dispersal has been observed in Reference [206].

Figure 11 of Reference [201] shows the normalized Krypton release in the case of a high local burnup (90 to 96 GWd/MTU), as a function of annealing temperature, with different curves for different irradiation temperatures. It appears that the authors consider that the low irradiation temperature results show HBS effects that are beneficial from a safety viewpoint, because they indicate the greater inventory of gas that, relative to fuel un-affected by HBS, under normal operating conditions, remains locked in the fuel (i.e., in the HBS pores) instead of being released into the fuel/cladding gap. (In the measurement – as opposed to normal operations – this HBS-retained gas is released at lower annealing temperature, as the cited figure shows. In essence, the figure proves that gas is retained in the HBS pores, until attainment of conditions that arise in the measurement but not in normal operation.) The high irradiation temperature results, wherein due to excessive temperature there was no HBS formation, are less favored in that, not being retained in the pores (which in this case are interconnected rather than isolated), gas may more easily leave the fuel matrix and accumulate in the gap.

Figure 7 of Reference [202] reproduces from Reference [207] (the original source) shows the normalized release of other gasses. Note that this short informal article from 2010 includes a useful and extensive bibliography of 73 papers that survey the HBS literature as of 2010. Figure 10 of Reference [202] reproduces from Reference [208] (the original source) shows the increase in thermal conductivity that accompanies HBS formation. The increase in thermal conductivity after HBS formation is due to the fission gas (Xe and Kr) atoms precipitating out of the matrix as bubbles in a restructuring process [209]. The Xe and Kr atoms are quite large atoms that cause large strain perturbations in the lattice, reducing the phonon heat transfer. When these atoms precipitate out of the UO_2 lattice as gas-filled bubbles/porosity, they reduce the lattice strains thus increasing thermal conductivity [209].

Figure 3.1 shows the fission gas release, and Figure 3.2 shows the pellet swelling, both as functions of burnup, reproduced from Reference [203]. The irradiation temperature, on which

[11] Comment and information provided by C. Beyer.

these quantities may depend, is not identified in Reference [203]. References [210 - 212] provide additional information of fission product release at high burnups.

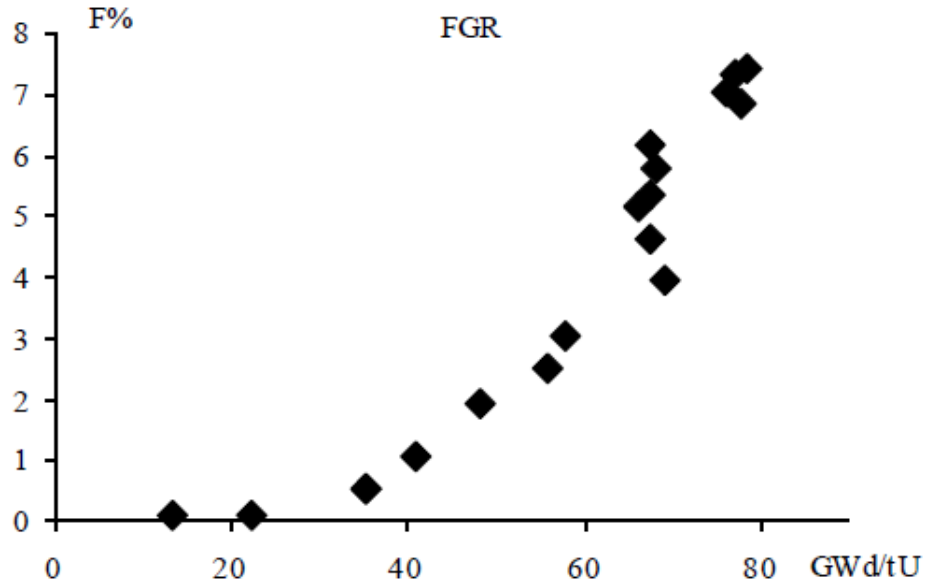

Figure 3.1 Fission gas release at high burnups [203]

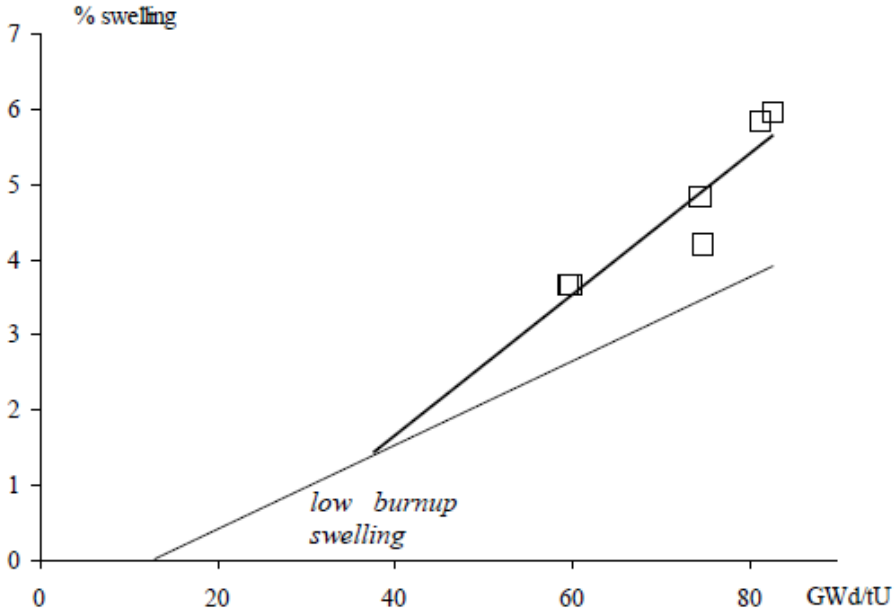

Figure 3.2 Fuel swelling at high burnups [203]

Reference [213] identified several phenomena whose character depends on the extent of burnup (see Table 3.1). That research showed that most current design limits could be retained if supported with data at the targeted burnup levels. Reference [213] stated that criteria relating to the response of fuel to reactivity initiated accidents or to loss of coolant accidents require a more

complex evaluation, and that these criteria were to be deferred to two separate topical reports on RIA and LOCA issues, to be published also by EPRI, the publishers of Reference [213] (Note Reference [213] was published in 2006). However, the EPRI topical reports on burnup and LOCA and/or RIA issues are not referred to in Reference [213] and the authors were not able to locate these references.

Notwithstanding the lack of an accident context in Reference [213], the consideration of the burnup effect on numerous phenomena is valuable. As examples, the following lightly edited extracts from [213] retain its Q and A format:

> Does burnup have an effect on {cladding stress}?
>
> Yes – Burnup does affect the factors that contribute (or control) the stress loads. These factors include rod internal pressure, cladding wall thickness, pellet-cladding gap thickness, pellet and cladding mechanical properties, amount of rod axial growth, and grid spring relaxation.
>
> Does burnup have an effect on {strain}?
>
> Yes – Burnup does affect the factors that contribute to the cladding material ductility. The key parameter affecting cladding strain is the cladding material ductility. These factors include the amount of, fast neutron fluence, cladding oxidation, hydrogen content, zirconium hydride distribution and orientation, and the condition of the cladding oxidation layer including non-uniformities and local loss of oxide.
>
> Does burnup have an effect on {strain fatigue}?
>
> Yes – Burnup has an effect on the strain amplitude and the number of cycles experienced by the cladding. The key parameters for strain fatigue are the strain (or stress) amplitude and the number of cycles. Several factors that depend on burnup can influence the strain amplitude, including fuel pellet swelling, rod internal pressure, fuel pellet thermal conductivity, and cladding oxidation. Operating to higher burnup levels may increase the residence time of the fuel, thus increasing the number of strain cycles experienced by the cladding.
>
> Does burnup have an effect on {fretting wear}?
>
> No – The key parameter for fretting wear is the cladding wall thinning due to material loss caused by cladding-grid contact during fuel rod vibration. Relaxation of the fuel rod-to-spacer grid contact force to a minimum saturation level occurs during the first or second cycle of operation. Extended burnup operation will not cause additional contact force relaxation.

And so on with consideration of oxidation, hydriding, crud formation, structural bowing, irradiation growth, internal pressure, overheating, ballooning, among others. As in the above-quoted discussions, the analysis is more qualitative than quantitative. Table 1-2 of Reference [213] shows the full scope of the analysis.

Reference [214] is a year 2000 conference proceeding that includes many papers related to high burnup, experimental and analytical work on fission gas release, clad modeling, MOX fuel modeling, code development, and high burnup fuel modeling. However, the old papers documented in this conference proceeding do not contained any material useful to the present investigation.

In 2001 and 2002, NRC formed a review panel to examine the applicability of NUREG–1465 to reactors using a high-burnup (HBU), low-enriched uranium (LEU) fuel and to reactors using mixed oxide (MOX) fuel (i.e., mixed uranium and plutonium). The panel proposed changes to the NUREG–1465 source term for such applications. In addition, the review panel drew attention to

changes in understanding LEU fuel fission product release behavior that have emerged after NUREG–1465 was issued.

Since the publication of NUREG–1465, the NRC has sponsored the development and incorporation of improved models into the MELCOR computer code for use in severe accident and source term studies. These models were assessed using limited available experimental data including those from France and Japan—that encompassed the effects of fuel burnup up to 60 GWd/MTU for UO_2 and MOX fuels. Based on the recommendations of the 2002 panel review, the NRC commissioned Sandia National Laboratories (SNL) to use MELCOR and determine a more defensible basis for source term estimates applicable to LWRs operating with HBU and MOX fuel.

It became apparent during the course of the SNL work that advances in modeling the progression of severe accidents would result in source terms for low-enriched fuel significantly different from those found in NUREG–1465. This program also observed that changes between the NUREG–1465 source terms and those generated for the HBU and MOX fuels resulted primarily from advances in modeling and not from differences in fuel types or burnup [215].

Some of the experimental and analytic bases of Reference [215] are from Reference [216] and the references contained therein. In particular, the VERCORS data reported in Reference [216] show higher fission product diffusivities at higher burnup (based on a pellet irradiated to 72 GWd/MTU) compared to lower burnup. Nevertheless, the MELCOR calculations by SNL demonstrated that this does not make much difference in releases between high versus low burnup fuel because at high temperatures, the difference in diffusivity observed at more modest temperatures disappears.

A peer review performed in 2011 [217] of the SNL studies [215] concluded that there were ample justifications for changing the source terms in NUREG–1465; the proposed source terms in the SNL studies were found by Reference [217] to be technically justified and appropriate. In addition, the peer reviewers stated that even though the revised source terms were based on the state-of-the-art; however, the estimates were based on limited experimental data. It was further stated that the assumed magnitude of release of gaseous iodine into the containment that is referenced in the SNL report (i.e., 5 percent) was considered as highly uncertain.

The 2011 peer review documented in Reference [217] recommended that the source terms in the SNL reports be modified to eliminate the gap-release phase; and consider any available information from the Fukushima Dai-ichi accident, when available, to determine if the results of the SNL studies are reasonable.

There was no specific context of ATF designs in SNL studies; moreover, at ~62 GWd/MTU, the high burnup considered by the SNL studies are not as high as those that may arise in ATF designs.

The open literature information that has been examined as part of the present review did not identify any information, especially, experimental measurements that can be used to assess the significance of high burn-up ATF on radionuclide releases, beyond those already discussed earlier in this section.

4. PROPOSED PHENOMENA OF SIGNIFICANCE TO SEVERE ACCIDENTS

On the basis of the literature review summarized in Sections 2 and 3 of this report, as well as a review of the models contained in the core, radionuclide release and transport, and other relevant packages in the MELCOR severe accident simulation code, a list has been prepared of candidate phenomena for consideration in the Phenomena Identification and Ranking Table (PIRT) for severe accidents (see Table 4.1). The proposed list of candidate phenomena and assignment of ranks is expected to be completed as part of the PIRT panel deliberations, which will be documented in a separate report.

The importance and state-of-knowledge levels may vary for different accident-tolerant fuel designs; hence, in theory the PIRT needs to be evaluated for each of the different design concepts (i.e., for each contemplated combination of new fuel and cladding material). In general, all of the fuel-related phenomena need to be considered separately for near-term ATF designs:

- Cr_2O_3 and Al_2O_3 dopants in uranium dioxide fuels,

Similarly, for other (longer-term) ATF concepts:

- High-density silicide fuels,
- High-density nitride fuels, and
- Metallic fuels (specifically, uranium-zirconium alloys with zirconium content near 50 weight percent).

Note that carbide fuels and all types of microcell fuels, though discussed in Section 2 where the whole of the ATF literature has been reviewed, are omitted here. The reason is that U.S. vendors have not proposed any of these designs at this time, and hence the PIRT panel will not consider these in the process of phenomena identification, importance and ranking.

In addition, all of the cladding-related phenomena need to be considered for each of the following design concepts:

- Conventional zirconium alloy cladding coated with chromium
- Advanced stainless steel (FeCrAl) cladding; and
- SiC and SiC-composite cladding.

However, where appropriate, Table 4.1 notes certain phenomena of exclusive or particular significance to certain fuel design concepts. Note that some phenomena, such as eutectic formation, depend not just on the fuel design or the cladding design but on the two in combination with each other.

4.1 Thermophysical Properties

Severe accident simulation codes rely on tables and/or formulas for various thermophysical properties of materials in the reactor core. In MELCOR, these properties are assumed to be either constant or functions of temperature, and it is assumed that the fuel is UO_2 while the cladding is Zircaloy. It is noted that thermophysical properties for FeCrAl have recently been added to the code. In the case of accident-tolerant fuel designs employing novel materials, the MELCOR property tables will need to be replaced or augmented with data adequately derived from or

validated by experiment. Among the thermophysical properties required for the fuel and cladding, in general, are:

- Mass density;
- Thermal conductivity;
- Specific heat;
- Melting point;
- Heat of fusion; and
- Surface emissivity.

To analyze phenomena such as melt spreading, fragmentation, etc., thermophysical properties of the melt during in- and ex-vessel accident progression including viscosity, surface tension, solidus, liquidus, and eutectic may be important.

4.2 Oxidation Behavior

Cladding oxidation and hydrogen generation are important aspects of severe accident progression that must be modeled in severe accident simulation codes. MELCOR relies on formulas for oxidation kinetics, the parameters of which are validated for high-temperature oxidation of Zircaloy cladding. New cladding materials will require adequately supported new oxidation kinetics parameters or models. In addition, the heat of oxidation for new cladding materials must be known with accuracy. In the case of coated Zircaloy cladding, the interaction of coating materials with the cladding, including possible eutectic formation, becomes an issue relevant to oxidation since it could lead to melting of the coating and bring about pure Zr oxidation. In the case of steel alloys, an open issue is the extent to which each of the metal constituents (e.g., iron, chromium, and aluminum) contributes to the reaction. In the case of silicon carbide cladding, the continuing reaction of the oxide with steam is a phenomenon to which there is no analog in Zircaloy cladding oxidation. It should be considered, in the case of metallic fuels, whether an oxidation model for the fuel pellets should be implemented as well as the cladding.

In addition to the cladding, it should be considered in the case of BWRs whether potential new channel box or control rod materials will impact oxidation and hydrogen generation.

Hydrogen and oxygen production by radiolysis in steam and water may of greater significance for some ATF designs as compared to conventional UO_2 fuels with Zircaloy cladding.

4.3 Fission Product Release and Transport Behavior

In general, the fission gas inventories and pressure in the fuel-cladding gap for accident-tolerant fuels may differ from those in conventional UO_2/Zircaloy fuels. These inventories must be known with adequate accuracy and input to the severe accident code appropriately.

Fission product retention of and release from UO_2-based fuels, as modeled in MELCOR, is a time- and temperature-dependent process simulated by an empirical Booth diffusion model. This model, or the parameters contained therein, must be adequately validated against any new accident-tolerant fuel designs. In addition, aspects of new cladding design which may result in increased or decreased cladding retention must be considered.
In fuel designs with Zircaloy cladding, it is understood that radioactive Tellurium releases from the fuel may be held up by the cladding until a certain level of oxidation has been achieved

(recognizing that sequestration of Te by cladding does not appear to be supported by recent knowledge; nonetheless, it remains an issue that needs to be considered). This behavior may be qualitatively or quantitatively different for various fuel or cladding designs, and it needs to be considered during severe accidents, and represented appropriately as part of the fission product release models.

For fuel designs incorporating SiC cladding, in particular, it is believed that the partitioning between aerosolized and gaseous Iodine release might be significantly different from that in conventional fuels. Although MELCOR does not model this phenomenon with any real fidelity (i.e., Iodine combines stoichiometrically with Cesium into CsI aerosols, and any incidental excess over a given time interval becomes gas), it may be considered as an area for improvement if the state of knowledge for new fuels is such that this may differ sufficiently.

It should also be considered whether the material mix of the corium resulting from accident-tolerant fuels may affect the rate or magnitude of fission product release during the ex-vessel phase of core-concrete interactions.

Tritium releases and transport in water and steam need to be considered, particularly for FeCrAl-clad fuel pellet designs. Tritium may need to be added to the model as a radionuclide and tracked from the point of release from the fuel matrix to transport into the environment during severe accidents.

4.4 Mechanical and Relocation-Related Behavior

The phenomena of fuel and cladding densification and swelling; pellet-cladding interaction and stress-corrosion cracking; and clad ballooning and burst are not mechanistically treated in a severe accident simulation code such as MELCOR, even though they have been remarked upon in Sections 2 and 3 of this report. Nevertheless, it is worth considering whether any new consideration is due to these phenomena given the different behavior of new accident-tolerant fuels.

ATF design impacts on all phenomena related to fuel and cladding material interactions with water during flooded conditions need to be reconsidered.

The present PIRT is focused on severe accidents, not DBA LOCAs or RIAs. However, any transient that results in a large depressurization (including LOCAs) may result in fuel fragmentation, relocation, and dispersal (FFRD). Fuel and cladding fragmentation and fuel dispersal (e.g., as consequences of ballooning) have been considered by References [206] and [218] under LOCA conditions and by Reference [219] for RIA conditions. These references consider conventional UO_2 fuel/zirconium alloy cladding designs; re-consideration of their findings for ATF designs is required[12]. If ATF designs can reduce ballooning and burst strains, that may reduce fuel dispersal. Also, lower gas retention on grain boundaries may reduce fuel fragmentation because high fuel temperatures can fracture fuel at grain boundaries due to the high gas pressures at boundaries [206]. Similar DBA and severe accident testing is needed for future extended burnup levels.

[12] Comment provided by C. Beyer.

Relocation of fuel and cladding in MELCOR is largely modeled as a logical process[13] rather than a detailed mechanistic one, with specified criteria for fuel failure temperature, cladding failure temperature, and cladding oxide thickness for molten material holdup. Not only must these criteria be re-evaluated for new fuel and cladding materials, but it should be considered whether they remain fundamentally valid for the new designs. For example, it has been remarked upon previously in this report that FeCrAl cladding may potentially drain more suddenly on reaching its melting point, leading to simultaneous collapse of the fuel pellet stacks.

In ATF designs for BWRs, channel boxes may be made of a new material. Modeling of channel box deformation and relocation may require review with respect to how these processes manifest differently in box versus fuel, as may the effect of the new materials. Similarly, the topics of control rod material deformation and relocation need to be included.

Severe accident progression in LWRs and associated radionuclide releases can be strongly affected by the specific combination of ATF fuel and cladding with neutron absorber and control rod/blade cladding. For example, different combinations of materials considered for fuel, cladding, and control rod in a contemplated ATF design may lead to significant variation of the time window during which in-vessel flooding can result in re-criticality. Molten pool behavior in the lower head, including stratification, element partitioning, natural convection, phenomena during water flooding on top of the melt, melt oxidation including crust effects, etc., may be different for different ATF designs[14].

The eutectics formation characteristics of new fuel and cladding materials must be considered in their quantitative aspects (i.e., eutectic pair temperatures and ratios), but whether they demand a more adequately functioning eutectics model than currently included in codes such as MELCOR remains an open question.

4.5 Core Debris Properties

Several aspects of debris or molten material behavior are noted which need to be reconsidered in light of new fuel material compositions, to determine whether any quantitative or qualitative change in the severe accident simulation models is called for. These include solid debris particle size and debris porosity; melting and crystallization behavior of corium of different compositions; and dynamics of molten material candling, and radial relocation. Note that the latter, as currently modeled in MELCOR, are largely logical processes rather than based on detailed mechanistic models (e.g., characteristics such as the molten material viscosity are irrelevant). Nevertheless, it should be evaluated whether the models in MELCOR are sufficient in this regard, with respect to corium melt properties such as viscosity, surface tension, stratification, element partitioning, natural convection, melt oxidation, crust formation and growth, and convective heat transfer to overlying water.

[13] For our purposes, we can define a logical process as a set of step-by-step explicit assumptions based on experimental observations for a physical process rather than a theoretical/mechanistic approach.

[14] Comment provided by S. Bechta.

Table 4.1 Candidate Severe Accident PIRT Template for ATF

Phenomenon	Component(s)	Importance Rank*	State-of-Knowledge Rank*	Severe Accident Modeling Capability
Thermophysical Properties				
Mass Density	Fuel			
Mass Density	Cladding			
Thermal Conductivity	Fuel			
Thermal Conductivity	Cladding			
Specific Heat	Fuel			
Specific Heat	Cladding			
Melting Point	Fuel			
Melting Point	Cladding			
Heat of Fusion	Fuel			
Heat of Fusion	Cladding			
Coefficient of Thermal Expansion	Fuel			
Coefficient of Thermal Expansion	Cladding			
Surface Emissivity	Cladding			
Viscosity	In- and Ex-Vessel Molten Configurations			
Surface Tension				
Phase Equilibria				
Heat Transfer, including Critical Heat Flux**	Cladding			

* Each rank should include a short discussion and supporting technical basis

** As it may be affected by surface roughness or material properties

Phenomenon	Component(s)	Importance Rank*	State-of-Knowledge Rank*	Severe Accident Modeling Capability
Oxidation Behavior				
Oxidation Kinetics	Cladding, Channel Boxes, and Control Rod Materials			
Oxidation Kinetics	Fuel[1]			
Heat of Oxidation	Cladding, Channel Boxes, and Control Rod Materials			
Heat of Oxidation	Fuel[1]			
Hydrogen and Oxygen Generation by Radiolysis	Coolant			
Fission Product Release and Transport Behavior				
Gap Inventories and Pressure	Fuel			
Fission Gas Retention in/Release from Fuel	Fuel			
Fission Product Retention by Cladding	Cladding			
Tellurium Holdup	Cladding			
Iodine Aerosolization[2]	Fuel[2]			
Ex-Vessel Release during MCCI	Fuel and Cladding			
Tritium Release and Transport	Fuel			
Fission Product Leaching with Water	Cavity			
Mechanical and Relocation-Related Behavior				
Densification and Swelling	Fuel and Cladding			

Phenomenon	Component(s)	Importance Rank*	State-of-Knowledge Rank*	Severe Accident Modeling Capability
Pellet-Cladding Interactions and Stress Corrosion Cracking	Fuel and Cladding			
Coating Adhesion at the Contacts with Spacer Grids and Top/Bottom Fuel Assembly Structures	Coated Cladding			
Ballooning and Burst	Cladding			
Fuel and Cladding Fragmentation, and Fuel Dispersal	Fuel and Cladding			
High-Temperature Deformation and Relocation	Fuel			
High-Temperature Deformation and Relocation	Cladding and Channel Boxes			
Eutectic Formation	Fuel and Cladding			
Specific Phenomena during Reactivity Initiated Accidents (RIA) Leading to Severe Accidents	Vessel Internals			
Re-criticality – In- and Ex-Vessel (e.g. after reflood)	Fuel, Cladding, Control Rods			
Molten Pool Behavior in the Lower Head, Including Stratification, Element Partitioning, Natural Convection, Overlying Water, Oxidation, and Crust Effects	Late Phase Melt Behavior			
Other Qualitative Aspects of Relocation Behavior	Fuel and Cladding			
Core Debris Properties				
Solid Debris Particle Size and Porosity	Fuel and Cladding			
Molten or Sublimated Material Transport	Fuel and Cladding			

Phenomenon	Component(s)	Importance Rank*	State-of-Knowledge Rank*	Severe Accident Modeling Capability
Melting and Crystallization Behavior of Corium of Different Compositions	Melt			
RPV Thermomechanical Failure or Melting Through or Phenomena during In-Vessel Melt Retention	RPV			
Melt Interactions with Water, Melt Fragmentation	Fuel and Cladding (in-vessel) Cavity (ex-vessel)			
Spreading of Molten Material Under Dry and Flooded Conditions				
MCCI	Cavity			
Long-term Corium Behavior and Coolability				

[1] For metallic fuels.

5. REFERENCES

1. NEA,"State-of-the-Art Report on Light Water Reactor Accident-Tolerant Fuels," Nuclear Energy Agency, Organization for Economic Co-operation and Development, Report No. 7317, 2018.

2. Powers, D. A., "Views on Cr-doped UO2 Fuel," E-mail to R. Lee (NRC), November 5, 2018.

3. Gamble, K. A. et al., "ATF Material Model Development and Validation for Priority Fuel Concepts, L3:FMC.FUEL.P19.06" Department of Energy Report, CASL-U-2019-1870-000, Rev. 0, July 30, 2019.

4. Delafoy, C. and Arimescu, I., "Developments in Fuel Design and Manufacturing in Order to Enhance the PCI Performance of AREVA NP's Fuel," Proceedings of the NEA Workshop on PCI in Water-Cooled Reactors. Lucca (Italy), 22-24 June 2016.

5. Riglet-Martial, Ch. et al., "Thermodynamics of Chromium in UO2 Fuel: A solubility model" Journal of Nuclear Materials, Volume 447, Issues 1-3, 63-72, April 2014.

6. Cardinaels, T. et al., "Chromia Doped UO2 fuel: Investigation of the Lattice Parameter," Journal of Nuclear Materials, Volume 424, Issues 1-3, 252-260, May 2012.

7. Leenaers, A. et al., "On the Solubility of Chromium Sesquioxide in Uranium Dioxide Fuel," Journal of Nuclear Materials, Vol. 317, 62-68, 2003.

8. Josek, R. and Blair, P., "Evaluation of the Large Grain Size Fuel Tests IFA-676.1 and IFA-677.1 Using STAV7", Paper 2.3 at Enlarged Halden Program Group Meeting, 2013.

9. Zhou, W.Z. and Liu, R., "Fabrication Methods and Thermal Hydraulics Analysis of Enhanced Thermal Conductivity UO2-BeO fuel in LWRs," Annals of Nuclear Energy, Vol. 81, 240-248, 2015.

10. Tulenko, J., "Development of Innovative Accident Tolerant High Thermal Conductivity UO2-diamond Composite Fuel Pellets," Project No. 12-4037, NEUP Final Progress Report, January 2016.

11. Yeo, S. et al., "Enhanced thermal conductivity of uranium dioxide-silicon carbide composite fuel pellets prepared by Spark Plasma Sintering (SPS)," Journal of Nuclear Materials, Vol. 433, 66-73, 2013.

12. Levchuk, D. et al., "Al-Cr–O thin films as an efficient hydrogen barrier," Surf. Coatings Technol., Vol. 202, 5043-5047, 2008.

13. Joseph, R., "The High Initial Rating Test IFA-677, Final report on in-pile results," OECD Halden Reactor Project, 2008.

14. Arborelius, J. et al., "Advanced Doped UO2 Pellets in LWR Applications," Water Reactor Fuel Performance Meeting, Kyoto, 2005.

15. Muller, E. et al., “Thermal Behavior of Advanced UO2 Fuel at High Burnup,” Proceedings of the LWR Fuel Performance Meeting, 2007.

16. Valin, S. et al., “Synthesis of the Advanced UO2 Microstructures Program in the TANOX Device,” IAEA Technical Committee Meeting on Advanced Fuel Pellet Materials and Designs for Water Cooled Reactors, Brussels, 20-24, October 2003.

17. Julien, B. et al., “Performance of Advanced Fuel Product under PCI Conditions,” Proceedings of the 2004 International Meeting on LWR Fuel Performance, Orlando, 19-22, September 2004.

18. Wright, J. et al., “Fuel Hardware Considerations for BWR PCI Mitigation,” Top Fuel Meeting, Boise Idaho, 2016.

19. Delafoy, C. and Zemek, M., “Washout Behaviour of Chromia-doped UO2 and Gadolinia Fuels in LWR Environments,” Proceeding of a Technical Committee Meeting on Advanced Fuel Pellet Materials and Fuel Rod design for Water Cooled Reactors, Villigen, 23-26 November 2009.

20. Backman, K. et al., “Westinghouse Advanced Doped Pellet – Characteristics and Irradiation Behaviour,” IAEA TechDoc-1654, Villigen, 2009.

21. Coulon-Picard, E. et al., “Assessment of cold composite fuels for PWRs,” Proceeding of Top Fuel 2009, Paris, 6-10 September 2009.

22. Ott, L. J. et al., “Preliminary Assessment of Accident-Tolerant Fuels on LWR Performance during Normal Operation and Under DB and BDB Accident Conditions,” Journal of Nuclear Materials, 448, 520-533, 2014.

23. Kim, H. G. et al., “Development Status of Accident-tolerant Fuel for Light Water Reactors in Korea,” Nuclear Engineering and Technology, 48, 1-15, 2016.

24. Kim, H. G., et al., "Development of surface modified Zr cladding by coating technology for ATF." Top-Fuel, Boise, ID, USA, 2016.

25. Terrani, K. A. et al., “Silicon carbide oxidation in steam up to 2 MPa,” J. Am. Ceram. Soc. 97, 2331-2352. https://doi.org/10.1111/jace.13094, 2014.

26. Hwang, D.H. et al., “Evaluation of physical characteristics of PWR cores with accident tolerant fuels,” Autumn Meeting of the Korean Nuclear Society, Gyeongju, 29-30 October 2015.

27. Hess, S. et al., “Accident-Tolerant Fuel Valuation: Safety and Economic Benefits,” Electric Power Research Institute, Technical Report No. 3002015091, March 2019.

28. Powers, D.A. et al., “What Needs to be done on Design Basis Source Term for ATF Deployment in Operating Reactors?,” Presentation Slides to U.S. Nuclear Regulatory Commission, December 6, 2017.

29. Geelhood, K. G. and Luscher, W. G., “Degradation and Failure Phenomena of Accident Tolerant Fuel Concepts – Chromium Coated Zirconium Alloy Cladding, Revision 1” Pacific Northwest National Laboratory Report, PNNL-28437, June 2019.

30. Oelrick, R. et al., “Update on Westinghouse EnCore® Accident Tolerant Fuel Program.” Transactions of the American Nuclear Society, Vol. 118, 1311. Philadelphia, Pennsylvania: American Nuclear Society, 2018.

31. Karoutas, Z. et al., "Update on Westinghouse Benefits of Encore Fuel," TopFuel conference, Prague, 2018.

32. Shah, H. et al., “Westinghouse-Exelon EnCore® Fuel Lead Test Rod (LTR) Program including Coated Cladding Development and Advanced Pellets,” TopFuel 2018 (p. A0145). Prague, Czech Republic: European Nuclear Society, 2018.

33. Bischoff, J. et al., “AREVA NP's Enhanced Accident-Tolerant Fuel Developments: Focus on Cr-coated M5 Cladding,” Nuclear Engineering and Technology, 50, 223-228, 2018.

34. GNF, “Additive Fuel Pellets for GNF Fuel Designs,” non-proprietary version of NEDO-33406, NRC Adams public documents ML093560118, 2009.

35. Youinou, G. J. and Sen, R. S., “Impact of Accident-Tolerant Fuels and Claddings on the Overall Fuel Cycle: A Preliminary Systems Analysis,” Nuclear technology, 188, 123-138, November 2014.

36. Nelson, A. T. et al., "U_3Si_2 behavior in H_2O environments: Part II, pressurized water with controlled redox chemistry," J. of Nuclear Materials vol. 500, p. 81, 2018.

37. Wood, E. S. et al., "High temperature steam oxidation dynamics of U_3Si_2 with alloying additions: Al, Cr, and Y", J. of Nuclear Materials vol. 533, p. 152072, 2020.

38. KTH and SSM, HRP Member White Paper (DRAFT 2015-10-14), “ATUNE: Accident Tolerant Uranium Nitride Experiment,” supported by NNL (UK), Westinghouse, 2015.

39. Adorno Lopes, D., “Degradation of UN and UN–U3Si2 pellets in steam environment”, Journal of Nuclear Science and Technology, Selim Uygur and Kyle Johnson DOI: 10.1080/00223131.2016.1274689, 2017.

40. Jolkkonen, M. et al., "Uranium nitride fuels in superheated steam," Journal of Nuclear Science and Technology, vol. 54 p. 513, 2017.

41. Zhou, W. and Zhou, W., "Enhanced thermal conductivity accident tolerant fuels for improved reactor safety – A comprehensive review," Annals of Nuclear Energy, vol. 119, p. 66, 2018.

42. Li, B. et al., "High temperature thermal physical performance of SiC/UO2 composites up to 1600 °C," Ceramics International, vol. 44, p. 10069, 2018.

43. Johnson, K. et al., “Oxidation of Accident Tolerant Fuel Candidates,” Journal of Nuclear Science and Technology, 54, 3, 280-286, 2017.

44. Lindley, B. A. et al., “Reactor Physics Modelling of Accident Tolerant Fuel for LWRs Using ANSWERS Codes,” EPJ Nuclear Sciences and Technologies, 2, 14, 2016.

45. Lewis, B.J., “Thermodynamic and kinetic modelling of fuel oxidation behavior in operating defective fuel,” J. Nucl. Mater. 328, 180-196, 2004.

46. Spino, J. and Peerani, P., “Oxygen stoichiometry shift of irradiated LWR-fuels at high burn-ups: review of data and alternative interpretation of recently published results,” J. Nucl. Mater. 375, 8-25, 2008.

47. Yang, J. H. et al., “Thermo-physical Property of Micro-cell UO2 Pellets and High Density Composite Pellets for Accident Tolerant Fuel,” IAEA Technical Meeting on Accident Tolerant Fuel Concepts for LWRs, 13-14, Oak Ridge National Lab, October 2015.

48. Koo, Y. H. et al., “KAERI’S Development of LWR Accident-Tolerant Fuel,” Nuclear technology, 186, 295-304, May 2014.

49. Opila, E.J. and R.E. Hann, “Paralinear oxidation of CVD-SiC in water vapor,” J. Am. Ceram. Soc., Vol. 80, 197-205, 1997.

50. Pint, B. A. et al., “High temperature oxidation of fuel cladding candidate materials in steam-hydrogen environments,” Proc. 8th Int. Symp. High Temp. Corros. Prot. Mater. Les Embiez, 2012.

51. Terrani, K. A. et al., “The effect of fuel thermal conductivity on the behavior of LWR cores during loss-of-coolant accidents,” J. Nucl. Mater. 448 512-519, 2014.

52. Hinoki, T. et al., “Effect of Constituents of Silicon Carbide Composites on Oxidation Behavior,” IAEA-TECDOC, Ser. 314, 2016.

53. Barrachin, M. et al., “Fission-product behaviour in irradiated TRISO-coated particles: Results of the HFR-EU1bis experiment and their interpretation,” Journal of Nuclear Materials, vol. 415, 104-116, 2001.

54. IAEA, “Analysis of Options and Experimental Examination of Fuels for Water Cooled Reactors with Increased Accident Tolerance (ACTOF)” IAEA-TECDOC-1921, International Atomic Energy Agency, Vienna, 2020.

55. Tang, C. et al., “Protective coatings on zirconium-based alloys as accident-tolerant fuel (ATF) claddings,” Corrosion Reviews; 35(3): 141–165, 2017.

56. Idarraga-Trujillo, I. et al., “Assessment at CEA of Coated Nuclear Fuel Cladding for LWRs with Increased Margins in LOCA and Beyond LOCA Conditions,” Conf. Pap. LWR Fuel Perform. Meet. Top Fuel, vol 2013, 860-867, 2013.

57. Kim, H.-G. et al., “Adhesion Property and High-Temperature Oxidation Behavior of Cr-coated Zircaloy-4 Cladding Tube Prepared by 3D Laser Coating,” Journal of Nuclear Materials, 465, 531-539, 2015.

58. Shah, H. et al., “Development of Surface Coatings for Enhanced Accident Tolerant Fuel,” Water React. Fuel Perform. Meet., Jeju Island, Korea, 2017.

59. Kim, H.-G. et al., “Progress of Surface Modified Zr Cladding Development for ATF at KAERI,” Water React. Fuel Perform. Meet., Jeju Island, Korea, 2017.

60. Daub, K. et al., “Investigation of the Impact of Coatings on Corrosion and Hydrogen Uptake of Zircaloy-4,” Journal of Nucl. Materials, Vol. 467, 260-270, 2015.

61. Kuprin, A. S. et al., “Vacuum-arc Chromium-based Coatings for Protection of Zirconium Alloys from the High-temperature Oxidation in Air,” J. Nucl. Mater 465, 400-406, 2015.

62. Bischoff, J. et al., “Development of Cr-coated Zirconium Alloy Cladding for Enhanced Accident Tolerance,” Proceeding of TopFuel Conference, Boise, Idaho, 2016.

63. Brachet, J. C. et al., “Behavior under LOCA conditions of enhanced accident tolerant chromium coated zircaloy-4 claddings”, Top Fuel, Boise, Idaho, 1173-1178, 2016.

64. Kim, H. G. et al., “Application of Coating Technology on Zirconium-Based Alloy to Decrease High-Temperature Oxidation,” Zirconium in the Nuclear Industry: 17th Volume, STP154320120161, B. Comstock and P. Barbéris, Ed., ASTM International, West Conshohocken, PA, 346-369, 2015.

65. Kim, H. G. et al., “High-temperature Oxidation Behavior of Cr-Coated Zirconium Alloy,” Proceeding of LWR Fuel Performance Meeting/Top Fuel, 842-846, 2013.

66. Kim, J. et al., “Microstructure and Oxidation Behavior of CrAl Laser-Coated Zircaloy-4 Alloy,” Metals, Vol. 7(2), 59, 2017.

67. Brachet, J. C. et al., “Early studies on Cr-Coated Zircaloy-4 as Enhanced Accident Tolerant Nuclear Fuel Claddings for Light Water Reactors,” Journal of Nuclear Materials, 517, 15, 268-285, April 2019.

68. Yeom, H. et al., “High Temperature Oxidation and Microstructural Evolution of Cold Spray Chromium Coating on Zircaloy-4 in Steam Environment,” Journal of Nuclear Materials, 526, 2019.

69. Younker, I. and Fratoni, M., “Neutronic Evaluation of Coating and Cladding Materials for Accident Tolerant Fuels,” Progress in Nuclear Energy, 88, 10-18, 2016.

70. Park, J. H. et al., “High Temperature Steam-Oxidation Behavior of Arc Ion Plated Cr Coatings for Accident Tolerant Fuel Claddings,” Surf. Coatings Technol 280, 256-259, 2015.

71. Park, D. J. et al., “Behavior of an Improved Zr Fuel Cladding with Oxidation Resistant Coating under Loss-Of Coolant Accident Conditions,” J. Nucl. Mater 482, 75-82, 2016.

72. Bischoff, J. et al., “Development of Fuels with Enhanced Accident Tolerance,” Proceeding of TopFuel Conference, Zurich, 13-19 September 2015.

73. Zinkle, S.J. and Snead, L.L., “Designing radiation resistance in materials for fusion energy,” Annu. Rev. Mater. Res. 44, 241-267, 2014.

74. Wu, A. et al., “Behavior of Ion Irradiated Chromium Coatings on Zircaloy-4 Substrate”, NuMat, Montpellier, 2016.

75. Alat, E. et al., “Ceramic Coating for Corrosion (C3) Resistance of Nuclear Fuel-Cladding,” Surface and Coatings Technology, Vol. 281, 133-143, 2015.

76. Alat, E. et al., “Multilayer (TiN, TiAlN) Ceramic Coatings for Nuclear Fuel Cladding,” J. Nucl. Mater 478, 236-244, 2016.

77. Van Nieuwenhove, R. et al., “Investigation of the Impact of Coatings on Corrosion and Hydrogen Uptake of Nuclear Components,” Third meeting of the Nuclear Materials Conference, Clearwater, Florida, 2014.

78. Van Nieuwenhove, R., “IFA-774: The First In-pile Test with Coated Fuel Rods,” Enlarged Halden Program Group Meeting, HWR-1106, Røros, 2014.

79. Van Nieuwenhove, R. et al., “In-pile Testing of CrN, TiAlN and AlCrN Coatings on Zircaloy Cladding in the Halden Reactor,” 18th Int. Symp. Zircon. Nucl. Ind., STP1597, Hilton Head, SC, 2017.

80. Maier, B.R. et al., “Cold Spray Deposition of Ti2AlC Coatings for Improved Nuclear Fuel Cladding,” J. Nucl. Mater 466, 712-717, 2015.

81. Yeom, H. et al., “Laser Surface Annealing and Characterization of Ti 2 AiC Plasma Vapor Deposition Coating on Zirconium-Alloy Substrate,” Thin Solid Films 615, 202-209, 2016.

82. Tang, C. et al., “Deposition Characterization and High-Temperature Steam Oxidation Behavior of Single-Phase Ti2AlC-Coated Zircaloy-4,” Corrosion Science, 135, 87-98, 2018.

83. Tang, C. et al., “An overview of high-temperature oxidation behavior of various ATF cladding candidates in steam”, Proceedings of the 24th International QUENCH Workshop, Karlsruhe, 2018.

84. Roberts, D.A., “Magnetron Sputtering and Corrosion of Ti-Al-c and Cr-Al-C Coatings for Zr-alloy Nuclear Fuel Cladding,” University of Tennessee, Knoxville, 2016.

85. Lambrinou, K. et al., “Innovative Accident-tolerant Fuel Cladding Materials: the H2020 IL TROVATORE Perspective,” Water React. Fuel Perform. Meet., Jeju Island, Korea, 2017.

86. Pint, B. A. et al., “Material Selection for Accident Tolerant Fuel Cladding,” Metallurgical and Materials Transactions E, 2E, 190-196, September 2015.

87. Kumar, K.N. et al., “AREVA enhanced accident tolerant fuel program: Current results and future plans,” Proceeding of TopFuel Conference, Boise, Idaho, 2016.

88. Ma, Z. et al., “Evaluation of the Benefits of ATF, FLEX, and Passive Cooling System for an Enhanced Resilient PWR Model,” Prepared for the U.S. Department of Energy, Idaho National Laboratory, INL/EXT-19-56215, October 2019.

89. Parisi, C. et al., “Risk-Informed Safety Analysis for Accident Tolerant Fuels,” Nuclear Science and Engineering, March 2020.

90. Wu, X. and Shirvan, K., “System Code Evaluation of Near-Term Accident Tolerant Claddings During Boiling Water Reactor Short-Term and Long-Term Station Blackout Accidents,” Nuclear Engineering and Design, 356, 2020.

91. Terrani, K. A., “Accident Tolerant Fuel Cladding Development: Promise, Status, and Challenges,” Journal of Nuclear Materials, 501, 13-30, 2018.

92. Brachet, J.C. et al., “Behavior of Chromium Coated M5 Claddings under LOCA Conditions,” Water React. Fuel Perform. Meet., Jeju Island, Korea, 2017.

93. Bischoff, J. et al., “Cr-Coated Cladding Development at Framatome,” TopFuel 2018 (p. A0152). Prague, Czech Republic: European Nuclear Society, 2018.

94. Terrani, K.A. et al., “Protection of zirconium by alumina- and chromia-forming iron alloys under high-temperature steam exposure,” J. Nucl. Mater. submitted 64-71. https://doi.org/10.1016/ j.jnucmat.2013.03.006, 2013.

95. Pint, B.A., “SATS update and community testing,” Advanced Fuels Campaign Meeting, August 2015.

96. Brova, M. J. et al., “Undoped and ytterbium-doped titanium aluminum nitride coatings for improved oxidation behavior of nuclear fuel cladding,” Surf. Coatings Technol 331,163-171, 2017.

97. Ang, C. et al., “Anisotropic swelling and microcracking of neutron irradiated Ti3AlC2 - Ti5 Al2C3 materials,” Scr. Mater 114, 74-78, 2016.

98. Arias, D. and Abriata, J., "The Cr-Zr (Chromium-Zirconium) System," Bulletin of Alloy Phase Diagram, American Society for Metals: 237-244, 1986.

99. Skarohlid, J. and Skoda, R., “High temperature behaviour of CrAlSiN max phase coatings on zirconium alloy,” Water React. Fuel Perform. Meet., Jeju Island, Korea, 2017.

100. Tang, C. et al., “Oxidation and quenching behavior of cold spray Cr-coated Zr alloy fuel cladding”, Proceedings of the 25th International QUENCH Workshop, Karlsruhe, 2019.

101. Pint, B.A. et al.,” High temperature oxidation of fuel cladding candidate materials in steam-hydrogen environments,” https://doi.org/10.1016/j.jnucmat.2013.05.047 , J. Nucl. Mater 440, 420-427, 2013.

102. Pint, B.A. et al., “The effect of steam on the high temperature oxidation behavior of alumina-forming alloys,” Mater. High Temp. 32, 28-35, 2015.

103. Pint, B.A., “Performance of FeCrAl for accident-tolerant fuel cladding in hightemperature steam,” Corros. Rev. 35, 167-175, 2017.

104. Unocic, K.A. et al., “Effect of Al and Cr content on air and steam oxidation of FeCrAl alloys and commercial APMT alloy,” Oxid. Met 87, 431-441, 2017.

105. Robb, K. R., “Analysis of the FeCrAl Accident Tolerant Fuel Concept Benefits During BWR Station Blackout Accidents,” Proc. 16th Int. Top. Meet. Nucl. React. Therm. Hydraul., 1183-1195, Chicago, IL, August 2015.

106. Tang, C. et al., “High-temperature oxidation behavior of Kanthal APM and D alloys in steam,” International Congress on Advances in Nuclear Power Plants, ICAPP 2016, 3, 2112-2119, 2016.

107. Stuckert, J. et al., “Results of the Bundle Test Quench-19 with FeCrAl Claddings,” Proceedings of GLOBAL/TOP FUEL 2019, Seattle, 2019.

108. Field, K.G. et al., “Radiation tolerance of neutron-irradiated model FeeCreAl alloys,” https://doi.org/10.1016/j.jnucmat.2015.06.023, J. Nucl. Mater 465, 746-755, 2015.

109. Field, K.G. et al., “Mechanical properties of neutron-irradiated model and commercial FeCrAl alloys,” J. Nucl. Mater 489, 118-128, 2017.

110. Edmondson, P.D. et al., “Irradiation-enhanced a0 precipitation in model FeCrAl alloys,” Scr. Mater 116, 112-116, 2016.

111. Briggs, S.A. et al., “A combined APT and SANS investigation of a0 phase precipitation in neutron-irradiated model FeCrAl alloys,” Acta Mater 129, 217-228, 2017.

112. Grobner, P.J., “The 885 F (475 C) embrittlement of ferritic stainless steels,” Metall. Trans. 4, 251-260, 1973.

113. Bachhav, M. et al., “A0 precipitation in neutron-irradiated FeeCr alloys,” Scr. Mater 74, 48-51, 2014.

114. Robb, K. R. et al., “Parametric and Experimentally Informed BWR Severe Accident Analysis Using FeCrAl”, Prepared for U.S. Department of Energy, Oak Ridge National Laboratory, M3FT-17OR020205041, ORNL/SPR-2017/373, August 2017.

115. Unocic, K.A. et al., “Microstructure and environmental resistance of low Cr ODS FeCrAl,” Mater, High Temp 32, 123-132, 2015.

116. Sakamoto, K. et al., “Overview of Japanese development of accident tolerant FeCrAl-ODS fuel claddings for BWRs,” Proc. WRFPM2017, 2017.

117. Nagase, F. et al., “Performance degradation of candidate accident-tolerant cladding under corrosive environment,” Corros. Rev. 35, 129-140, 2017.

118. McMurray, J.W. et al., “Solid-liquid phase equilibria of Fe-Cr-Al alloys and spinels,” J. Nucl. Mater 492, 128-133, 2017.

119. Powers, J. J. et al., “Report on Reactor Physics Assessment of Candidate Accident Tolerant Fuel Cladding Materials in LWRs,” Prepared by OAK Ridge National Laboratory, ORNL/TM-2015/415, August 2015.

120. Gamble, K. A., “ATF Material Model Development and Validation for Priority Cladding Concepts, L3:FMC.FUEL.P19.07” Department of Energy Report, CASL-U-2019-1892-000, Rev. 0, August 30, 2019.

121. Field, K.G. et al., “Handbook on the Material Properties of FeCrAl Alloys for Nuclear Power Production Applications,” ORNL/TM-2017/186, 2017.

122. Robb, K. R. et al., “Severe Accident Analysis of BWT Core Fueled with UO2/FeCrAl with Updated Materials and Melt Properties from Experiments,” Oak Ridge National Laboratory Report ORNL/TM-2016/237, Revision 0, June 2016.

123. Robb, K. R. et al., “Design and Analysis of Oxidation Tests to Inform FeCrAl ATF Severe Accident Models,” Oak Ridge National Laboratory, M3NT-18OR020205041/ORNL/SPR-2018/893, 2018.

124. Kim, H. et al., “On the Minimum Thickness of FeCrAl Cladding for Accident-Tolerant Fuel,” Nuclear Technology, 198, 3, 342-346, 2017.

125. Gamble, K. A. et al., “An investigation of FeCrAl cladding behavior under normal operating and loss of coolant Conditions,” J. Nuclear Materials, 491 55-66, April 2017.

126. Yamamoto, Y. et al., “Report on Exploration of New FeCrAl Heat Variants with Improved Properties,” Prepared for U.S. Department of Energy, Oak Ridge National Laboratory, M3FT-19OR020202053, ORNL/TM-2019/1290, August 2019.

127. Kane, K. et al., “Report Summarizing Boiling Transition (Dryout) Testing of FeCrAl Cladding,” M3FT-20OR020206091, Prepared for U.S. Department of Energy, March 13, 2020.

128. Yamamoto, Y. et al., “Development and property evaluation of nuclear grade wrought FeCrAl fuel cladding for light water reactors,” J. Nucl. Mater 467, 703-716, 2015.

129. Yano, Y. et al., “Ultra-high temperature tensile properties of ODS steel claddings under severe accident conditions,” J. Nucl. Mater 487, 229-237, 2017.

130. Cinbiz, M.N. et al., “A pulsecontrolled modified-burst test instrument for accident-tolerant fuel cladding,” Ann. Nucl. Energy 109, 396-404, 2017.

131. Rebak, R.B., “Alloy selection for accident tolerant fuel cladding in commercial LWRs,” Metall. Mater. Trans. E. 2, 197-207, 2015.

132. Sakamoto, K. et al., “Development of Ce-type FeCrAl-ODS ferritic steel to accident tolerant fuel for BWRs,” Proc. TopFuel2016, 673-680, 2016.

133. Terrani, K.A. et al., “Uniform corrosion of FeCrAl alloys in LWR coolant environments,” J. Nucl. Mater 479, 36-47, 2016.

134. Wang, P. and Was, G.S., “In-situ proton irradiation-corrosion study of ATF candidate alloys in simulated PWR primary water,” Proc. 18th Int. Conf. Environ. Degrad. Mater. Nucl. Power Syst. React., Springer, 245-258, 2018.

135. Rebak, R.B. et al., “Characterization of oxides formed on ironchromium- aluminum alloy in simulated light water reactor environments,” Corros. Rev. 35, 177-188, 2017.

136. Liu, M. et al., “Potential impact of accident tolerant fuel cladding critical heat flux characteristics on the high temperature phase of reactivity initiated accidents,” Ann. Nucl. Energy 110, 48-62, 2017.

137. Lee, S. K. et al., “Comparison of Steady and Transient Flow Boiling Critical Heat Flux for FeCrAl Accident Tolerant Fuel Cladding Alloy, Zircaloy, and Inconel,” International Journal of Heat and Mass Transfer, 132, 643–654, 2019.

138. Sweet, R.T. et al., “Fuel performance simulation of iron-chrome-aluminum (FeCrAl) cladding during steady-state LWR operation,” Nucl. Eng. Des. 328, 10-26, 2018.

139. Yamaji, A. et al., “FEMAXI-7 prediction of the behavior of BWR-type accident tolerant fuel rod with FeCrAl-ODS steel cladding in normal condition,” Water React. Fuel Perform. Meet., Jeju Island, Korea, 2017.

140. Massey, C.P. et al., “Cladding burst behavior of Fe-based alloys under LOCA,” J. Nucl. Mater 470, 128-138, 2016.

141. Yan, Y. et al., “Post-quench ductility evaluation of Zircaloy-4 and select iron alloys under design basis and extended LOCA conditions,” J. Nucl. Mater 448, 436-440. https:// doi.org/10.1016/j.jnucmat.2013.05.071, 2014.

142. Dolley, E.J. et al., “Mechanical behavior of FeCrAl and other alloys following exposure to LOCA conditions plus quenching,” Proc. 18th Int. Conf. Environ. Degrad. Mater. Nucl. Power Syst. React., Springer, 185-200, 2018.

143. Pint, B.A. et al., “Development of ODS FeCrAl for compatibility in fusion and fission energy applications,” JOM 66, 2458-2466, 2014.

144. Unocic, K.A. et al., “Advanced TEM characterization of oxide nanoparticles in ODS Fe e 12Cre5Al alloys”, J. Mater. Sci., 9190-9206. https://doi.org/10.1007/s10853-016-0111-5, 2016.

145. Powers, D. A., “Thoughts on the Behavior of Fe-Cr-Al Alloys under Severe Reactor Accident Conditions,” Unpublished, February 17, 2017.

146 Luangdilok, W., “Analysis of FeCrAl Performance in the QUENCH-19 Test,” M4FT-19OR020205041, Prepared for U.S. Department of Energy, September 30, 2019.

147. Wang, J. et al., “Accident Tolerant Clad Material Modeling by MELCOR: Benchmark for Surry Short Term Station Black Out,” Nuclear Engineering Design, 313, 458-469, 2017.

148. Merrill, B. J. et al., “Modification of MELCOR for Severe Accident Analysis of Candidate Accident Tolerant Cladding Materials,” Nuclear Engineering Design, 315, 170-178, 2017.

149. Hollands, T., "Pre- and Post-Test Simulations of the ATF Experiment QUENCH-19 with AC^2," Proceedings of the 24th International QUENCH Workshop, Karlsruhe, 2018.

150. Tiborcz, L. and Hollands, T., "Simulation of recent QUENCH experiments with AC^2," Proceedings of the 25th International QUENCH Workshop, Karlsruhe, 2019.

151. Vasiliev, A., "Post-Test Modelling of the Experiment QUENCH-19 with ATF-Cladding FeCrAl Using SOCRAT Code,” Proceedings of the 25th International QUENCH Workshop, Karlsruhe, 2019.

152. Hales, J. D. and Gamble, K. A., “Modelling Accident Tolerant Fuel Concepts,” Idaho National Laboratory, INL/CON-16-37803, May 2016.

153. Field, K.G. et al., “Heterogeneous dislocation loop formation near grain boundaries in a neutron-irradiated commercial FeCrAl alloy,” J. Nucl. Mater. Vol. 483, 54-61, 2017.

154. APM, “Tube Material Datasheet,” AB Sandvik group, Sandviken, Sweden, undated.

155. Katoh, Y. et al., “Stability of SiC and its composites at high neutron fluence,” J. Nucl. Mater 417, 400-405. https://doi.org/10.1016/j.jnucmat.2010.12.088, 2011

156. Katoh, Y. et al., “Continuous SiC fiber, CVI SiC matrix composites for nuclear applications: properties and irradiation effects,” https://doi.org/10.1016/j.jnucmat.2013.06.040, J. Nucl. Mater 448, 448-476, 2014.

157. Katoh, Y. et al., “Current Status and Recent Research Achievements in SiC/SiC Composites,” Journal of Nuclear Materials, 455, 387-397, 2014.

158. Stempien, J. et al., “Characteristics of Composite Silicon Carbide Fuel Cladding After Irradiation Under Simulated PWR Conditions,” Nuclear Technology, 183, 13-29, July 2013.

159. Kim, D. et al., “Effect of dissolved hydrogen on the corrosion behavior of chemically vapor deposited SiC in a simulated pressurized water reactor environment,” Corrosion Science, Vol. 98, 304-309, 2015.

160. Kim, W.-J. et al., “Development and property evaluation of SiC composite tubes for nuclear fuel cladding application,” ICACC 2016, Daytona Beach, Florida, 2016.

161. Lorrette, C. et al., “Quench behavior of SiC/SiC Cladding after High Temperature Rampe under Steam Conditions,” WRFPM 2017, Jeju Island, 2017.

162. Katoh, Y. and Terrani, K.A., “Systematic Technology Evaluation Program for SiC/SiC Composite-based Accident-tolerant LWR Fuel Cladding and Structures: Revision 2015,” ORNL/TM-2015/454, Oak Ridge National Laboratory, Oak Ridge, 2015.

163. Koyanagi, T. and Katoh, Y., “Mechanical properties of SiC composites neutron irradiated under light water reactor relevant temperature and dose conditions,” J. Nucl. Mater 494, 46-54, 2017.

164. Lorrette, C. et al., “SiC/SiC composite behavior in LWR conditions and under high temperature steam environment,” Top Fuel 2015, Zurich, 2015.

165. Avincola, V. et al., “Thermodynamic modeling of the silica volatilization in steam related to silicon carbide oxidation,” Journal of the European Ceramic Society, Vol. 35 (14), 3809-3818, 2015.

166. Yueh, K. et al., “Clad in clay,” Nuclear Engineering International, Vol. 55, 14-16, 2010.

167. Terrani, K.A et al., “Hydrothermal corrosion of SiC in LWR coolant environments in the absence of irradiation,” Journal of Nuclear Materials, Vol. 465, 488-498, 2015.

168. Park, J.-Y. et al., “Long-term corrosion behavior of CVD-SiC in 360°C water and 400°C steam,” Journal of Nuclear Materials, Vol. 443, 603-607, 2013.

169. Avincola, V.A. et al., “Oxidation at High Temperature in Steam atmosphere and Quench of Silicon carbide Composites for Nuclear Application,” Nuclear Engineering Design, 295, 468-478, 2015.

170. Hayasaka, D. et al., “Oxidation, High Temperature, Resistance of SiC/SiC composites by NITE-method,” Adv. Refract. Ceram. Energy Conserv. Effic. Ceram. Trans. 256, 29, 2016.

171. Shimoda, K. et al., “Development of the tailored SiC/SiC composites by the combined fabrication process of ICVI and NITE methods,” J. Nucl. Mater 384, 103-108, 2009.

172. Braun, J., et al., “Chemical compatibility between UO2 fuel and SiC cladding for LWRs: Application to ATF (Accident-Tolerant Fuels),” Journal of Nuclear Materials, Vol. 487, 380-395, 2017.

173. Deck, C. P. et al., “Characterization of SiC-SiC Composites for Accident Tolerant Fuel,” Journal of Nuclear Materials, 466, 665-681, 2015.

174. Powers, D. A., “Some Initial Thoughts on Silicon Carbide Cladding for Reactor Fuel and Its Behavior under Severe Accident Conditions,” Unpublished, December 2012.

175. Allendorf, M.D. et al., “Theoretical Study of the Thermochemistry of Molecules in the Si-O-H System,” J. Phys. Chem., 99, 15285-15293, 1995.

176. Mondal, B. et al., “Thermochemistry silicic acid formation reaction: Prediction of new reaction pathway,” Chem. Phys. Letters, 478, 115-119, 2009.

177. Jacobson, N.S. et al., “Thermodynamics of gas phase species in the Si-O-H system,” J. Chem. Thermodynamics, 37, 1130-1137, 2005.

178. Lee, Y. et al., “Safety Assessment of SiC Cladding Oxidation Under Loss-of-Coolant Accident Conditions in Light Water Reactors,” Nuclear Technology, 183, 210-227, August 2013.

179. Kazimi, M. et al., "PWR Cores with Silicon Carbide Cladding," Electric Power Research Institute, Technical Report No. 1022908, July 2011.

180. Katoh, Y. et al., “Radiation effects in SiC for nuclear structural applications,” Current Opinion in Solid State and Materials Science, Vol. 16, 143-152, 2012.

181. Bragg-Sitton, S. et al., “Silicon Carbide Gap Analysis and Feasibility Study,” INL/EXT-13-29728, Idaho National Laboratory, Idaho Falls, 2013.

182. Brachet, J. et al., “Evaluation of Equivalent Cladding Reacted parameters of Cr-coated claddings oxidized in steam at 1200 °C in relation with oxygen diffusion/partitioning and post-quench ductility,” Journal of Nuclear Materials vol. 533, p. 152106, 2020.

183. Brachet, J. et al., “High temperature steam oxidation of chromium-coated zirconium-based alloys: Kinetics and process,” Corrosion Science vol. 167, p. 108537, 2020.

184. Cathcart, J. V. et al., “Zirconium Metal-water Oxidation Kinetics, IV: Reaction Rate Studies,” ORNL/NUREG-17, Oak Ridge National Laboratory, 1977.

185. US NRC, “TRACE V5.0 PATCH 5 THEORY MANUAL: Field Equations, Solution Methods and Physical Models,” Division of Safety Analysis. Office of Nuclear Regulatory Research, U.S. Nuclear Regulatory Commission, Washington, DC, USA, 2017.

186. Gurgen, A., Shirvan, K., “Estimation of coping time in pressurized water reactors for near term accident tolerant fuel claddings,” Nucl. Eng. Des. 337, 38–50, 2018.

187. S.R.J. Saunders et al., “Oxidation growth stresses in an alumina-forming ferritic steel measured by creep deflection,” Oxidation of Metals, 48, 189–200, 1997.

188. Leistikow, S. et al., “Comprehensive presentation of extended Zircaloy-4/steam oxidation results 600-1600 c,” In CSNI/IAEA specialists meeting on water reactor fuel safety and fission product release in off-normal and accident conditions, Riso Nat. Lab., Denmark, 1983.

189. Brassfield, H.C. et al., “Recommended Property and Reaction Kinetics Data for Use in Evaluating a Light-Water-Cooled Reactor Loss Of Coolant Incident Involving Zircaloy-4 or 304SS Clad UO2,” GEMP-482, General Electric Co., 1968.

190. Snead, L. et al., “An Overview of SiC-Based Fuel and Cladding Technologies in Support of Accident Tolerant Fuel Development,” Paper 3.5 at Enlarged Halden Program Group Meeting, 2013.

191. Titus, G.W. and Sailing, J.H., “High-temperature irradiation of UO2-BeO bodies,” University of Arizona Library Documents Collection, March 1963.

192. Jenssen, H., “PIE Report on six UO_2 fuel rods Irradiated in IFA-677 High Linear Heat Rating Test,” Halden Reactor Project Report HWR-968, 2010.

193. Arborelius, J. et al., “Advanced Doped UO2 Pellets in LWR Applications”, Journal of Nuclear Science and Technology, Vol. 43, No. 9, p. 967–976, 2006.

194. Barrett, K. E. et al., “Critical processes and parameters in the development of accident tolerant fuels drop-in capsule irradiation tests,” Nuclear Engineering and Design, 294 38, 2015.

195. Li, N. et al., “Oxide Morphologies of FeCrAl Alloys Following Extended Aging,” NTRD-M3FT-17LA020202042, 2017.

196. Luangdilok, W. and Xu, P., "Modeling of SiC Cladding Behavior During Severe Accidents," International Topical Meeting on Probabilistic Safety Assessment and Analysis, Pittsburgh, 2017.

197. Brown, N. et al., “The potential impact of enhanced accident tolerant cladding materials on reactivity initiated accidents in light water reactors,” Annals of Nuclear Energy, v. 99, pp. 353-365, 2017.

198. Irving, J. S., "Environmental Assessment for Use of DOE-Owned High-Assay Low-Enriched Uranium Stored at Idaho National Laboratory," INL/MIS-18-51903-Revision-0, Idaho National Laboratory, 2019.

199. Herczeg, J. W., “High-Assay Low Enriched Uranium (HALEU),” Presentation to the Nuclear Energy Advisory Committee Meeting, 2019.

200. Lightbridge Inc., “Advanced Nuclear Fuel Technology for Current Large Reactors and Coming Small Modular Reactors,” Lightbridge presentation to investors, 2020.

201. Wiss, T. et al., “Properties of the high burnup structure in nuclear light water reactor fuel,” Radiochimica Acta, 105 893, 2017.

202. Rondinella, V. V. et al., “The high burn-up structure in nuclear fuel,” Materials today, Vol 13 (12), 2010.

203. Noirot, J. et al., “High Burnup Changes in UO 2 Fuels Irradiated Up to 83 GWd/T in M5 ®Claddings,” Nuclear Engineering and Technology, Elsevier, 41 (2), 2009.

204. Yan, Y. et al., “LOCA Integral Test Results for High-Burnup BWR Fuel,” ADAMS # ML051920402, 2004.

205. Raynaud, P., "Fuel Fragmentation, Relocation, and Dispersal During the Loss-of-Coolant Accident," NUREG-2121, Nuclear Regulatory Commission, 2012.

206. Flanagan, M. et al., "Research Efforts in the Area of Fuel Fragmentation, Relocation and Dispersal Under LOCA Conditions," Paper 5.4 at Enlarged Halden Program Group Meeting, 2013.

207. Hiernaut, J. P. et al., “Fission product release and microstructure changes during laboratory annealing of a very high burn-up fuel specimen,” Journal of Nuclear Materials, 377, 313-324, 2008.

208. Ronchi, C. et al. “Effect of burn-up on the thermal conductivity of uranium dioxide up to 100.000 MW-d / tn,”J. Nucl. Mater. vol. 327, p. 58, 2004.

209. Beyer, C. E. and Lanning, D. D., "Review of Fuel Thermal Conductivity Data and Models, "Proceedings of Thermal Performance of High Burn-up LWR Fuel Seminar, Cadarache, France, 1998.

210. Barani, T. et al., “Analysis of transient fission gas behaviour in oxide fuel using BISON and TRANSURANUS,” Journal of Nuclear Materials, vol. 486, pp. 96–110, 2017.

211. Brémier, S. et al., “Fission gas release and fuel swelling at burn-ups higher than 50 MW-d/Kg_U”, Fission Gas Behaviour In Water Reactor Fuels, seminar proceedings, pp. 93–106, Cadarache, France, 2000.

212. Noirot, J. et al., “Fission gas release behaviour of a 103 GWd/tHM fuel disc during a 1200 °C annealing tests,” Journal of Nuclear Materials, vol. 446, pp. 163-171, 2014.

213. Alvis, J. M. and Montgomery, R. O., "Licensing Criteria for Fuel Burnup Extension Beyond 62 GWd/tU," Electric Power Research Institute, Technical Report No. 1013278, 2006.

214. IAEA, “Nuclear fuel behavior modelling at high burnup and its experimental support,” Proceedings of a Technical Committee meeting held in Windermere, United Kingdom, IAEA-TECDOC-1233, 19–23 June 2000.

215. Powers, D. A. et al., “Accident Source Terms for Light Water Nuclear Power Plants Using High-Burnup or MOX Fuel,” Sandia National Laboratories, SAND2010-0128, January 2011.

216. Gauntt, R. O., “Synthesis of VERCORS and Phébus Data in Severe Accident Codes and Applications,” Sandia National Laboratories, SAND2010-1633, April 2010.

217. Energy Research, Inc., “Peer Review of Accident Source Terms for Light-Water Nuclear Power Plants Using High-Burnup and Mixed Oxide Fuel,” ERI Report No. ERI/NRC 11-211, ML#12005A043, December 2011.

218. Wiesenack, W., "Extended summary of HPR-380 - Summary of the Halden Reactor Project LOCA Test Series IFA-650," Paper 1.1 at Enlarged Halden Program Group Meeting, 2013.

219. OECD, "Nuclear Fuel Behavior Under Reactivity-initiated Accident Conditions," NEA #6847, 2010.

220. Yakushkin, A. and Vysikaylo P., “Modification of the surface and coating application on fuel cladding tubes for nuclear reactors,” Bulletin of Moscow Region State University. Series: Physics and Mathematics, 2018, no. 4, pp. 92–111. DOI: 10.18384/2310-7251-2018-4-92-111, 2018.

221. Urvanov, S.,“*Modifitsirovanie uglerodnogo volokna uglerodnymi nanostrukturami: dis. ... kand. khim. nauk* [Modification of carbon fiber by carbon nanostructures: PhD thesis in Chemical Sciences],” Troitsk, 2016.

222. Krejci, J. et al., “Chromium and Chromium Nitride Coated Cladding for Nuclear Reactor Fuel,” Proceedings of the 20th International Corrosion Congress, EUROCORR 2017, Prague, Czech Republic (2017).

223. Fejt, F. et al., “Study on neutronics of VVER-1200 with accident tolerant fuel cladding,” Annals of Nuclear Energy 124, 579, 2019.

224. Savchenko, A. et al., “Dispersion type zirconium matrix fuels fabricated by capillary impregnation method,” J. Nucl. Mater. 362, pp. 356-363, 2007.

225. Savchenko, A. et al., “Main results of the development of dispersion type IMF at A. A. Bochvar Institute,” J. Nucl. Mater. 396, 26-31, 2010.

226. Savchenko, A. et al., “Zirconium matrix alloys as innovative material for different types of fuel,” Progress Nucl. Energy 57, 138-144, 2012.

227. Yakushkin A.A. and Vysikaylo P.I., “Modification of the surface and coating application on fuel cladding tubes for nuclear reactors,” Bulletin of Moscow Region State University, Series: Physics and Mathematics, no. 4, pp. 92–111. DOI: 10.18384/2310-7251-2018-4-92-111, 2018.

228. Lipkina, K. et al., “Metallic inert matrix fuel concept for minor actinides incineration to achieve ultra-high burn-up”, Journal of Nuclear Materials, volume 452, issue 1-3, 2014, pp. 378 – 381, 2014.

229. Savchenko, A. and Konovalov, I., “METMET Fuel with Zirconium Matrix Alloys”, Proceedings of the 7th International Conference on WWER Fuel Performance, Modelling and Experimental Support (WWER-2007), 247-258, Albena (Bulgaria), September 2007.

230. Savchenko et al., “CERMET and METMET fuel with zirconium matrix alloys,” Proceedings of the TopFuel-2006 Conference, Salamanca, available through the European Nuclear Society (ENS) website, 2006.

Intentionally left blank

6. BIBLIOGRAPHY

This section provides a list of papers that were reviewed and determined to not contain significant information particularly relevant to the present review scope and objectives.

Ahn, K. et al., (2018), "Safety Evaluation of Silicon Carbide and Zircaloy-4 Cladding during a Large-Break Loss-of-Coolant Accident," Energies, 11, 3324, 1-13.

Ang, C. et al. (2017) "Phase stability, swelling, microstructure and strength of Ti3SiC2 - TiC ceramics after low dose neutron irradiation," J. Nucl. Mater 483, 44-53.

Ashbaugh, S. G. et al., (2010), "Accident Source Terms for Pressurized Water Reactors with High Burnup Cores calculated Using MELCOR 1.8.5," Sandia National Laboratories, SAND2008-6664, April 2010.

Avincola, V.A. et al. (2017), "High-Temperature Tests of Silicon Carbide Composite Cladding under GFR Conditions," Energy Procedia, 127, 320-328.

Boyack, B. E. et al. (2001), "Phenomenon Identification and Ranking Tables (PIRTs) for Loss of Coolant Accidents in Pressurized and Boiling Water Reactors Containing High Burnup Fuel," Los Alamos National Laboratory, NUREG/CR-6744, LA-UR-00-5079, December 2001.

Brachet, J.C. et al. (2015), "On-going Studies at CEA on Chromium Coated Zirconium Based Nuclear Fuel Claddings for Enhanced Accident Tolerant LWRs Fuel," TopFuel 2015, Zurich, Switzerland, 31-38, 2015.

Bragg-Sitton, S. et al. (2014), "Advanced Fuel Campaign: Enhanced LWR Accident Tolerant Fuel Performance Metrics," INLL/EXT-13-29957, FCRD-FUEL-2013-000264, Prepared for U.S. Department of Energy, February 2014.

Bragg-Sitton, S. M. et al. (2016), "Metrics for the Technical Performance Evaluation of Light Water Reactor Accident-Tolerant Fuel," Nuclear Technology, 195, 111-123, August 2016.

Bragg-Sitton, S. M. et al. (2015), "Evaluation of Enhanced Accident Tolerant LWR Fuels," Idaho National Laboratory, INL/CON-15-34936, September 2015.

Carmack, J. et al. (2013), "Overview of the U.S. DOE Accident Tolerant Fuel Development Program," Idaho National Laboratory, INL/CON-13-29288, September 2013.

Charit, I. (2017), "Accident Tolerant Nuclear Fuels and Cladding Materials," The Minerals, Metals & Materials Society, 70, 2, 173-175.

Chen, S. and Yuan, C. (2019), "Minor Actinides Transmutation in Candidate Accident Tolerant Fuel-Claddings U3Si2-FeCrAl and U3Si2-SiC," Annals of Nuclear Energy, 127, 204-214, May 2019.

Cheng, B. et al. (2016), "Improving Accident Tolerance of Nuclear Fuel with Coated Mo-alloy Cladding," Nuclear Engineering and Technology, 48, 16-25.

Core, G. M. et al. (2017), “Accident Tolerant Fuels Series 1 (ATF-1) Irradiation Testing FY 2017 Status Report,” Prepared for U.S. Department of Energy, Idaho National Laboratory, INL/EXT-17-43220, Revision 0, September 2017.

Csontos, A. (2018), “Coated Cladding Gap Analysis”, Electric Power Research Institute, 3002014603, October 2018.

Csontos, A. and Capps, N. (2018), "Accident Tolerant Fuel Technical Update," Electric Power Research Institute, Technical Report No. 3002012250, May 2018.

Dong, S. et al. (2003), “Preparation of SiC/SiC Composites by hot pressing, using tyranno-SA fiber as reinforcement,” J. Am. Ceram. Soc. 86, 26-32.

Galloway, J. and Unal, C. (2016), “Accident-Tolerant-Fuel Performance Analysis of APMT Steel Clad/UO2 Fuel and APMT Steel Clad/UN-U3Si5 Fuel Concepts,” Nuclear Science and Engineering, 182, 523-537.

George, N. M. et al. (2015), “Demonstration of a Full-Core Reactivity Equivalence for FeCrAl Enhanced Accident Tolerant Fuel in BWRs,” ANS 2015, Topical Meeting ANFM.

George, N. M. et al. (2015), “Neutronic Analysis of Candidate Accident-tolerant Cladding Concepts in Light Water Reactors,” Annals of Nuclear Energy, 75, 703-712, January 2015.

Griffith, G. (2011), “U.S. Department of Energy Accident Resistant SiC Clad Nuclear Fuel Development,” U.S. INL/CON-11-23186, Preprint, Enlarged Halden Programme Group Meeting 2011, October 2011.

Hanus, E. et al. (2013), “VERDON program: Performances of Experimental LWR Severe Accident Device Some Results of Fission Products Release and Transport on High Burn-up UO2 and MOX Fuels,” Presentation Slides at the CSARP Meeting, Bethesda, Maryland, September 16-20, 2013.

Hayasaka, D. et al. (2016a), “Gas leak tightness of SiC/SiC composites at elevated temperature,” Fusion Engineering and Design, Vol. 109-111, 1498-1501.

Hayes, S. L. et al. (2016), “Advances in Metallic Fuels for High Burnup and Actinide Transmutation,” 14th Information Exchange Meeting on Actinide and Fission Product Partitioning and Transmutation, INL/CON-16-38752.

IAEA (2014), “Accident Tolerant Fuel Concepts for Light Water Reactors,” Proceedings of a Technical Meeting Held at Oak Ridge National Laboratories, IAEA TECDOC Series, IAEA-TECDOC-1797, October 2014.

IAEA (2011), “Impact of High Burnup Uranium Oxide and Mixed Uranium-Plutonium Oxide Water Reactor Fuel and Spent Fuel Management,” International Atomic Energy Agency, IAEA Nuclear Energy Series, Report No. NF-T-3.8, Vienna, Austria.

Kato, S. et al. (2017), “R&D of ODS ferritic steel cladding for maintaining fuel integrity at accident condition (3) – (2) Mechanical properties of FeCr- and FeCrAl- ODS steels at elevated temperature,” Proc. AESJ 2017 Spring Annu. Meet.

Kim, D.H. et al. (2015b) “Critical heat flux for SiC- and Cr-coated plates under atmospheric condition,” Annals of Nuclear Energy, Vol. 76, 335-342.

Kohyama, A. et al. (2016), “Large scale production of high performance SiC/SiC fuel pins and the behavior under dynamic reactor water in Halden BWR,” 2016 MRS Fall Meeting, Boston, Massachusetts.

Kurata, M. (2016), “Research and Development Methodology for Practical Use of Accident Tolerant Fuel in Light Water Reactors,” Nuclear Engineering and Technology, 48, 26-32.

Leonard, M. T. et al. (2007), “Accident Source Terms for Boiling Water Reactors with High Burnup Cores Calculated Using MELCOR 1.8.5,” Sandia National Laboratories, SAND2007-7697, November 2007.

Lim, K.-Y. et al. (2016), “Effect of additive composition on high temperature oxidation resistance of pressure-less sintered SiC ceramics for particle-based accident tolerance fuel,” KNS Spring Meeting.

Lin, Y. et al. (2018), “Path toward Industrialization of Enhanced Accident Tolernat Fuel,” TopFuel 2018 (p. A0141). Prague, Czech Republic: European Nuclear Society.

Lorson, R. et al. (2018), “Briefing on Accident Tolerant Fuel” Presentation slides to NRC Commission Brief on Accident Tolerant Fuel, U.S. Nuclear Regulatory Commission, April 2018.

Ma, Z. G. et al. (2018), “Plant-Level Scenario-Based Risk Analysis for Enhanced Resilient PWR – SBO and LBLOCA,” U.S. Department of Energy, INL/EXT-18-51436, September 2018.

Miller, T. (2018), “Advanced Modeling and Simulation: Accident Tolerant Fuel Application,” Presentation slides to NRC Commission Brief on Accident Tolerant Fuel, U.S. Department of Energy, April 2018.

Nagase, F. et al. (2009), “Behavior of High Burn-up Fuel Cladding under LOCA Conditions,” Journal of Nuclear Science and Technology, 49, 7, 763-769.

NEI (2019), “The Economic Benefits and Challenges with Utilizing Increased Enrichment and Fuel Burnup for Light Water Reactors,” Prepared by the Nuclear Energy Institute, White Paper, February 2019.

NRC (undated), “Draft Interim Staff Guidance Supplemental Guidance Regarding the Chromium-Coated Zirconium Alloy Fuel Cladding Accident Tolerant Fuel, U.S. Nuclear Regulatory Commission, ATF-ISG-01.

NRC (2018), “Project plan to Prepare the U.S. Nuclear Regulatory Commission for Efficient and Effective Licensing of Accident Tolerant Fuels,” U.S. Nuclear Regulatory Commission Report, September 2018.

Pint, B.A. (2018), “FY18 FCRD Milestone M3NT-18OR020206061: Steam Oxidation, Burst and Critical Heat Flux Testing of FeCrAl Cladding in the Severe Accident Test Station,” Oak Ridge National Laboratory, ORNL/LTR-2018/530, August 2018.

Powers, D. A. (undated), ”Cesium Release Evolution with Increasing Reactor Fuel Burnup,” Sandia National Laboratories.

Powers, D. A. (undated), E-mail to R. Lee, “Views on Uranium Silicide Fuel,”.

Rebak, R. B. (2017b), “Materials for Accident Tolerant Fuels,” Corrosion Reviews, 35, 3, 127.

Robb, K. R. (2015b), “Severe Accident Scoping Simulations of Accident-Tolerant Fuel Concepts for BWRs,” Oak Ridge National Laboratory, ORNL/SPR-2015/347, M3FT-15OR0202333.

Shirvan, K. (2017), “Assessment of the V&V Challenges of Accident Tolerant Fuels,” Presentation Slides to Multiphysics Model Validation Workshop, Department of Nuclear Science and Engineering, MIT, June 2017.

Snead, M. et al. (2015), “Technology Implementation Plan ATF FeCrAl Cladding for LWR Application,” OAK Ridge National Laboratory, ORNL/TM-2014/353, May 2015.

Steinbrück, M. (2009), “Prototypical Experiments Relating to Air Oxidation of Zircaloy- 4 at High Temperatures,” J. Nucl. Mater 392, 531-544.

Wilmshurst, N. (2018), “EPRI R&D Activities: Accident Tolerant Fuel,” Presentation slides to NRC Commission Brief on Accident Tolerant Fuel, Electric Power Research Institute, April 2018.

Yang, J.H. et al. (2014), “Thermo-physical Property of Micro-cell UO2 Pellets and High Density Composite Pellets for Accident Tolerant Fuel,” IAEA Technical Meeting on Accident Tolerant Fuel Concepts for LWRs”, Oak Ridge National Lab, October 2014.

Younan, S. and Novog, D. (2018), “Assessment of Neutronic Characteristics of Accident-Tolerant Fuel and Claddings for CANDU Reactors,” Science and Technology of Nuclear Installations, March 2018.